

Inhibition of Serine and Cysteine Proteases by Peptidomimetic Inhibitors

Submitted in fulfilment of the degree

Master of Philosophy (Chemical Sci)

Nicholas Schumann, *B.Sc. (Adv)*

Supervisor: Andrew Abell



THE UNIVERSITY

of ADELAIDE

School of Physical Sciences

Department of Chemistry

December 2017

Table of Contents

Abstract	VI
Declaration	IX
Acknowledgments	XI
Abbreviations.....	XIV
1 STRUCTURE, FUNCTION AND MECHANISM OF ACTION OF SERINE AND CYSTEINE PROTEASE INHIBITORS	2
1.1 Protein Structure and its Importance in Biology	2
1.2 Overview and Classification of Proteases.....	4
1.2.1 Introduction to proteases.....	4
1.2.2 Protease specificity.....	6
1.3 Proteases as Therapeutic Targets and the Current Design of Protease Inhibitors	9
1.3.1 Serine and cysteine protease inhibitor structural features.....	11
1.3.2 Serine protease inhibitors	12
1.3.3 Cysteine protease inhibitors.....	14
1.4 Overview of the Thesis	16
2 DESIGN AND SYNTHESIS OF B-STRAND CONSTRAINED PEPTIDOMIMETIC INHIBITORS OF CHYMOTRYPSIN AND CATHEPSIN PROTEASES.....	21
2.1 Peptide β -Strand.....	21
2.2 Chymotrypsin and Cathepsin Proteases.....	24
2.2.1 Structural assembly and specificity of Chymotrypsin and Cathepsins	24
2.3 Design of β -strand constrained Chymotrypsin and Cathepsin Inhibitors ..	28
2.3.1 Backbone modified β -strand mimetics.....	28
2.4 Design and Synthesis of N-Terminal Heterocyclic Chymotrypsin Inhibitors	32
2.4.1 Synthesis of heterocycle building blocks.....	34
2.4.2 Synthesis of N-terminal dipeptides	37
2.5 α -Chymotrypsin Inhibition Assay.....	41
2.6 Design and Synthesis of Macrocyclic, N-Terminal Heterocyclic Cathepsin Inhibitors	45
2.6.1 Macrocyclic N-terminal pyrrole-P ₄ ester	47
2.6.2 Macrocyclic N-terminal pyridine-P ₄ amide.....	53
2.7 Conclusions and Future Work	56
3 DESIGN AND SYNTHESIS OF PEPTIDOMIMETIC INHIBITORS OF MYCOBACTERIUM TUBERCULOSIS SERINE PROTEASE HIP1	60

3.1	Mycobacterium tuberculosis	60
3.2	Hip1 Protease.....	60
3.2.1	Structure of Hip1.....	61
3.3	Current Design of Hip1 Substrates and Inhibitors	64
3.3.1	Hip1 substrate probes.....	64
3.3.2	Hip1 irreversible inhibitors	65
3.4	Synthesis of Reversible Hip1 Protease Inhibitors	66
3.4.1	Synthesis of N-terminal Boc inhibitors.....	69
3.4.2	Synthesis of N-terminal Cbz inhibitors.....	71
3.4.3	Synthesis of N-terminal Fmoc inhibitors.....	73
3.5	Tripeptide Boronate Ester Inhibition Assay	76
3.6	Investigation of other Terminal Electrophiles for the Optimised Sequence	80
3.6.1	Synthesis of α -keto heterocycle inhibitor	80
3.6.2	Synthesis of aldehyde inhibitor.....	84
3.6.3	Synthesis of the α -keto ester inhibitor	88
3.7	Extended Series Inhibition Assay	93
3.8	Conclusions and Future Work.....	96
4	EXPERIMENTAL PROCEDURES.....	99
4.1	General Methods	99
4.1.1	General practices	99
4.1.2	Analytical methods	100
4.2	General Procedures	101
4.2.1	In vitro α -Chymotrypsin assay	101
4.2.2	General reaction procedures	102
4.3	Experimental Work Described in Chapter Two.....	104
4.4	Experimental Work Described in Chapter Three	133
4.5	References	162
	Appendix	172
	Appendix 1: Inhibition constants, K_i , of Hip ₁ inhibitors.....	173

Abstract

Proteases are responsible for the hydrolysis of proteins and peptides and have been implicated in the development of various diseases. Herein describes the design and synthesis of reversible peptidomimetic inhibitors of serine and cysteine protease for the control of protease activity. Proteases recognise substrates' secondary peptide structure which conforms to a saw-tooth arrangement of amino acids, known as an extended β -strand geometry. This property has led to the development of potent inhibitors which mimic this conformation.

Chapter two discusses defining β -strand geometry in inhibitors, while maintaining key substituents necessary for recognition by protease hosts, by the replacement of N-terminal residues with heterocyclic constraints. The inclusion of a heterocycle both enforces backbone β -strand conformation while increasing inhibitor bioavailability and metabolic stability. A series of peptidomimetic inhibitors containing heterocycles, including pyrrole, furan, thiophene and pyridine were synthesised, and the associated inhibitory activities against a model serine protease, α -Chymotrypsin, determined in proteolytic assays. Of the series of heterocycles, pyrrole was determined to be the optimum heterocycle for inclusion in inhibitors of this class. Extension of this concept of constraint was investigated in the approach towards heterocycle-containing macrocycles constructed by ring-closing metathesis for the inhibition of cysteine Cathepsin proteases, where the introduction of a macrocyclic

tether couples with the heterocyclic constraint to define the desired backbone β -strand geometry. Pyrrole-containing macrocycle **2.47** was constructed by ring-closing metathesis, but was found to be unstable to hydrogenation conditions. A similar pyridine-containing macrocycle **2.61** was successfully synthesised and hydrogenated, but was unable to be functionalised with appropriate C-terminal residues due to its poor solubility profile.

Chapter three details the design and synthesis of a series of peptidomimetic inhibitors of the serine protease Hip1 which has been implicated with a host innate immune response pathway of *Mycobacterium tuberculosis*. Described is the synthesis of a library of tripeptides containing an electrophilic boronic ester at the C-terminus for reversible covalent attachment to the Hip1 active site and the associated inhibitory assay data. A lead compound, **3.23**, which has exceptional potency of inhibition (low nM activity) was discovered, from which highly potent derivatives featuring a C-terminal aldehyde **3.44**, α -keto heterocycle **3.49**, and α -keto ester **3.58** were established. Further refinement of these inhibitors presents an opportunity for the development of therapeutics for the treatment of tuberculosis.

Declaration

I certify that this work contains no material which has been accepted for the award of any other degree or diploma in my name, in any university or other tertiary institution and, to the best of my knowledge and belief, contains no material previously published or written by another person, except where due reference has been made in the text. In addition, I certify that no part of this work will, in the future, be used in a submission in my name, for any other degree or diploma in any university or other tertiary institution without the prior approval of the University of Adelaide and where applicable, any partner institution responsible for the joint-award of this degree.

I give consent to this copy of my thesis, when deposited in the University Library, being made available for loan and photocopying, subject to the provisions of the Copyright Act 1968.

I also give permission for the digital version of my thesis to be made available on the web, via the University's digital research repository, the Library Search and also through web search engines, unless permission has been granted by the University to restrict access for a period of time.

I acknowledge the support I have received for my research through the provision of an Australian Government Research Training Program Scholarship.

Nicholas Charles Schumann

18-12-17

Acknowledgments

This work was funded with help from an ARC Discovery grant. Acknowledgement must also be given to the Australian Nanoscale Fabrication Facility for the ongoing funding they provide toward our analytical instruments.

First and foremost, I want to thank my supervisor Prof. Andrew Abell for his continuous support and guidance. Thank you for allowing me the freedom to direct my degree and supporting me with the decisions that I made on this journey. Nothing would have gone nearly as smoothly as it did if it weren't for your support.

I would also like to extend my gratitude to Dr. Nathan Goldfarb at California Health Sciences University for his continuous support with the Hip1 project and for assaying all of the compounds I sent to him over the last year.

To my labmates, thanks for keeping me sane. Stephen, thank you for teaching me the ways of the lab, and for all of your little tips and tricks which I would never have thought of. Thank you Borja Pérez for your support. Although we didn't work together for long, you gave me a lot of help, and most importantly, kept encouraging me. To the rest of the lab, Michelle, Victoria, Georgina, Aimee, Pat and Kathryn, thanks for keeping the lab and the office somewhere enjoyable to work. A special shout out to Kathryn for helping me with the Chymotrypsin assays and to Aimee for making the analytical instruments seem less daunting.

To my friends and family who over the last couple of months have insistently asked how my thesis is going, I can safely say that it is done - you can stop asking now lol. Thanks for being understanding when things were going less than ideal and being supportive of me when I couldn't attend things because of my busy schedule.

Mum and Dad, thanks for the endless support through this and for dealing with me through all of the situations the two years threw at me. A special thanks to both of you for listening to me talk about my research, even when you didn't want to (...sorry Mum:)).

Abbreviations

δ	chemical shift (NMR)
Å	angstrom
Ac	acetyl
ACN	acetonitrile
AMC	amino-4-methylcoumarin (Chymotrypsin assay)
aq.	aqueous
Boc	<i>tert</i> -Butyloxycarbonyl
Cbz	carboxybenzyl
COSY	H-H correlated spectroscopy (NMR)
CD ₃ OD	deuterated methanol
CDCl ₃	deuterated chloroform
CH ₂ Cl ₂	dichloromethane
DABCYL	4-((4-(dimethylamino)phenyl)azo)benzoic acid <i>N</i> -succinimidyl ester (Hip1 assay)
DCE	1,2-dichloroethane
DIPEA	<i>N,N</i> -diisopropylethylamine
DMF	<i>N,N</i> -dimethylformamide
DMP	Dess-Martin periodinane
DMSO	dimethyl sulfoxide
EDANS	5-((2-aminoethyl)amino)naphthalene-1-sulfonic acid (Hip1 assay)
EDCI	<i>N</i> -(3-Dimethylaminopropyl)- <i>N'</i> -ethylcarbodiimide hydrochloride
Et ₂ O	diethyl ether
EtOAc	ethyl acetate
EtOH	ethanol
equiv	equivalence
Fmoc	9-fluorenylmethyloxycarbonyl
Grubbs 2 nd Generation Catalyst	Benzylidene-bis(tricyclohexylphosphino)-dichlororuthenium
HATU	1-[Bis(dimethylamino)methylene]-1 <i>H</i> -1,2,3-triazolo[4,5- <i>b</i>]pyridinium 3-oxid hexafluorophosphate
h	hour(s)
HCl	hydrochloric acid
HRMS	high resolution mass spectrometry
HSQC	heteronuclear single quantum coherence spectroscopy (NMR)
Hz	hertz (NMR)
IC ₅₀	half maximal inhibitory constant

<i>J</i>	coupling constant (NMR)
K ₂ CO ₃	potassium carbonate
K _i	inhibitor dissociation constant
KOH	potassium hydroxide
LiCl	lithium chloride
LiOH	lithium hydroxide
LRMS	low resolution mass spectrometry
MeOH	methanol
MgSO ₄	magnesium sulfate
min	minute(s)
Mtb	<i>Mycobacterium tuberculosis</i>
Na ₂ S ₂ O ₃	sodium thiosulfate
NaClO ₂	sodium chlorite
NaH	sodium hydride
NaHCO ₃	sodium bicarbonate
NaH ₂ PO ₄	monosodium phosphate
NaOAc	sodium acetate
NaOH	sodium hydroxide
NH ₄ Cl	ammonium chloride
NMR	nuclear magnetic resonance
Pd/C	palladium on carbon catalyst
POCl ₃	phosphoryl chloride
ppm	parts per million
rcm	ring-closing metathesis
rp-HPLC	reversed phase high performance liquid chromatography
rt	room temperature
sat.	saturated
SOCl ₂	thionyl chloride
TB	tuberculosis
TBAI	tetrabutylammonium iodide
TES	2-[(2-Hydroxy-1,1-bis(hydroxymethyl)ethyl)amino]ethanesulfonic acid (Chymotrypsin assay buffer)
TFA	trifluoroacetic acid
THF	tetrahydrofuran
Ti(O <i>i</i> Pr) ₄	titanium isopropoxide
TLC	thin-layer chromatography

CHAPTER ONE:

Structure, Function and Mechanism of Action of Serine and Cysteine Protease Inhibitors

1 STRUCTURE, FUNCTION AND MECHANISM OF ACTION OF SERINE AND CYSTEINE PROTEASE INHIBITORS

1.1 Protein Structure and its Importance in Biology

Proteins are ubiquitous bioorganic molecules which play vital roles in all aspects of cell structure and function.¹⁻² They are arguably the most versatile class of macromolecules in living systems and perform crucial functions for almost all biological processes, including catalysis, growth and differentiation, as well as serving as the structural components of cells and organisms.³ This function is defined by four levels of structure designated as primary, secondary, tertiary and quaternary, as depicted in Figure 1.01.¹⁻³

Primary structure is defined by the linear sequence of amino acids (known as residues) linked by amide bonds, with a sequence of a small number of amino acids defined as a peptide. Disulfide bridges between cysteine residues are also considered part of the primary structure and these provide conformational constraint and thermodynamic stability to the overall structure.⁴ Secondary structure is predominately dictated by hydrogen bonding between N-H and C=O groups along the peptide backbone, giving rise to two distinct classes of secondary structure: α -helices and β -sheets. Tertiary structure defines the entire structure of a protein and is formed by secondary structures such as α -helices and β -sheets which are linked by loops formed by side chain and backbone interactions or side chain side chain interactions. Quaternary structure refers to the functional unit resulting from the assembly of multiple polypeptide subunits. The work described

herein is concerned with the secondary structure and its role in defining the interaction of an inhibitor with its target enzyme, a protease in this case.

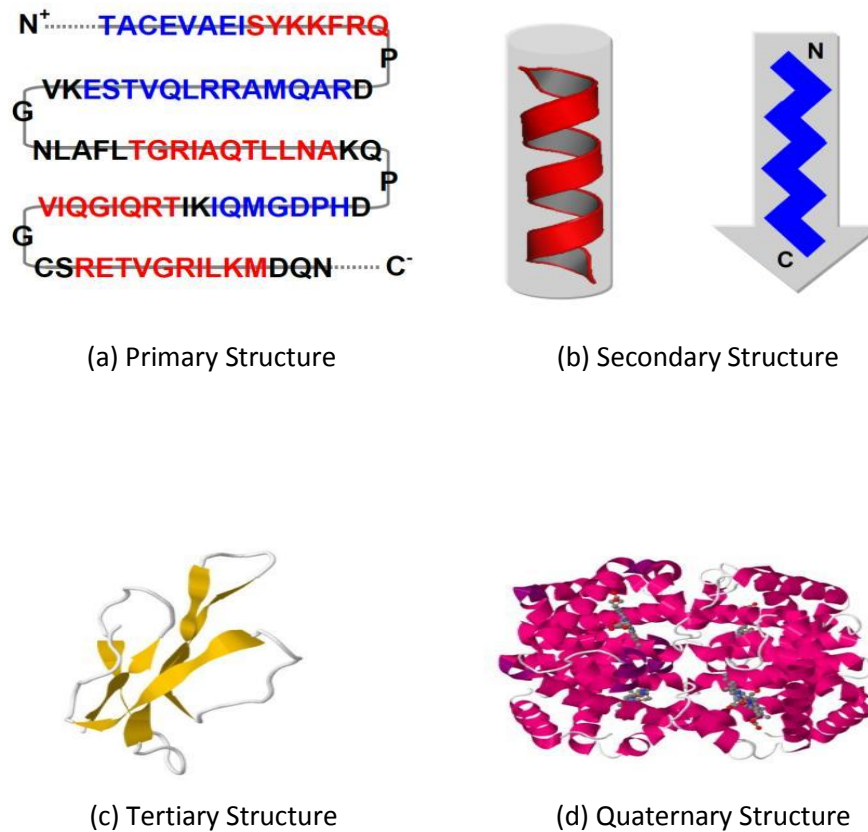


Figure 1.01 Four levels of protein structure. (a) primary structure: amino acid sequence from the N-terminus to the C-terminus. (b) secondary structure: hydrogen bond stabilisation of the primary sequence to form α -helices and β -sheets.² (c) tertiary structure: 3-dimensional structure of a protein (Erabutoxin B, PDB 1ERA).⁵ (d) quaternary structure: multi-polypeptide subunit (human haemoglobin, PDB 1A3N).⁶

1.2 Overview and Classification of Proteases

1.2.1 Introduction to proteases

Proteases are the proteins responsible for proteolysis, the process by which an amino acid or peptide is released from a protein or larger peptide by hydrolysis of amide bonds.⁷ Proteases are involved in numerous physiological processes including DNA replication and transcription, cell differentiation, wound repair, blood coagulation, inflammation, immunity and apoptosis as a few examples.⁸⁻⁹ Almost all organisms require proteases to function, with around 2% of the mammalian genome constituted by proteases, resulting in 600 such enzymes in humans.^{8,10} Organisms which do not encode proteolytic enzymes in their genome, such as some viruses, still require these enzymes for survival and thus manipulate host enzymes to perform proteolysis.

The active site of a protease contains two clefts which are connected through various interactions to form two domains referred to as L (left) and R (right).^{4, 7, 11} Centred between the two clefts is the catalytic dyad or triad (depending on the type of protease) which is responsible for catalytic proteolysis. A typical example is the proteolytic enzyme Chymopapain, whose two clefts are roughly the same size but are of different conformation, with the L domain mainly composed of α -helices, while the R domain is predominately composed of antiparallel β -sheet interactions (Figure 1.02).¹²

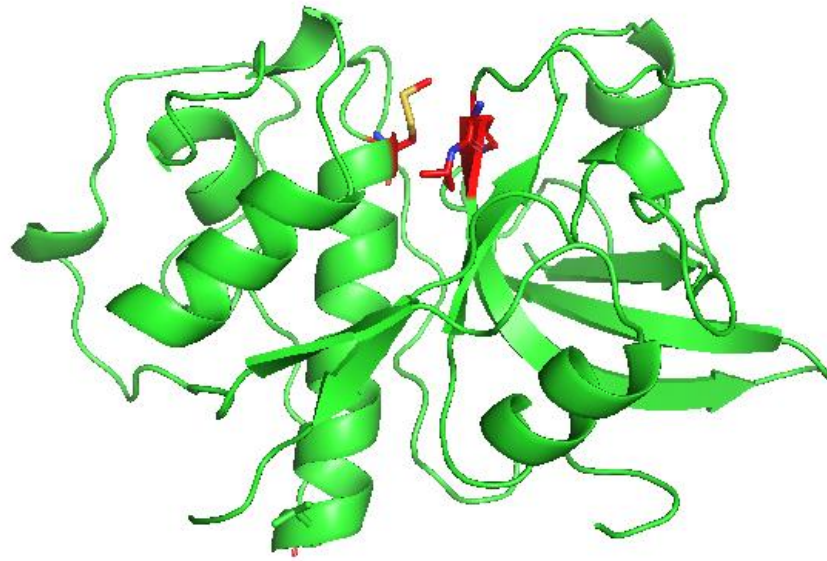
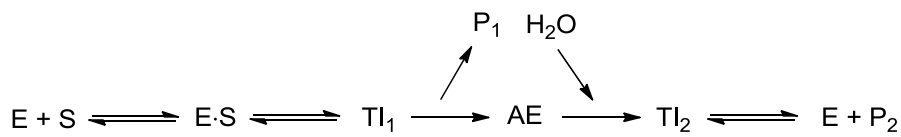


Figure 1.02 X-ray crystal structure of Chymopapain.⁷ The L and R domains flank the catalytic triad Cys₂₅, His₁₅₉, Asp₁₅₈ highlighted in red (PDB 1YAL).¹²

Proteases are classified into six classes: serine, cysteine, threonine, aspartic acid, glutamic acid and metallo proteases; the classification of which is based on the mechanism of peptide bond hydrolysis.¹³ Each protease has its own specificity, localisation and biological function, but all catalyse the cleavage of amide bonds by nucleophilic attack on the carbonyl carbon. Serine, cysteine and threonine proteases contain a catalytic active site nucleophile residue (Ser, Cys and Thr, respectively), while aspartic acid, glutamic acid and metallo proteases activate a water molecule within the active site that then acts as the nucleophile. The pathway for proteolysis for each protease class is summarised in Figure 1.03, where TI indicates the tetrahedral intermediate formed during proteolysis which is held noncovalently within the active site during the noncovalent catalytic pathway.

Covalent catalysis: serine, cysteine and threonine proteases



Noncovalent catalysis: aspartic acid, glutamic acid and metallo proteases

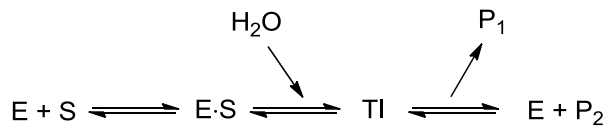


Figure 1.03 Mechanistic pathways for peptide proteolysis. E indicates the enzyme, AE is the activated enzyme formed during the covalent catalytic pathway, S is the substrate, and P₁ and P₂ are product 1 and 2 formed in the hydrolysis reaction, respectively.

1.2.2 Protease specificity

Further classification of these broad classes into subclasses of specific proteases is determined by the specificity of the catalytic active site towards particular amino acids within a substrate. The nature of the amino acids (as defined by their side chains) which make up the groove or pocket into which a substrate or inhibitor binds defines selectivity within a protease family.¹⁴ The manner by which binding occurs is defined by the notation developed by Schechter and Berger based on an early model of a cysteine Cathepsin protease, Papain.¹⁵ Binding pockets or groves known as subsites along the active site of a protease selectively bind amino acids that are complementary in terms of size, shape and hydrophobicity/hydrophilicity. The side chains of the amino acids in a substrate are defined as P_n-P_{n'}, while the corresponding subsites of the enzyme are defined

as S_n - S_n' . Upon binding to the active site, the substrate is cleaved between P_1 and P_1' at the scissile carbonyl bond (Figure 1.04).

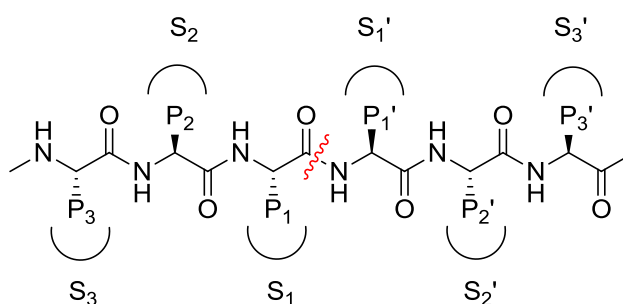
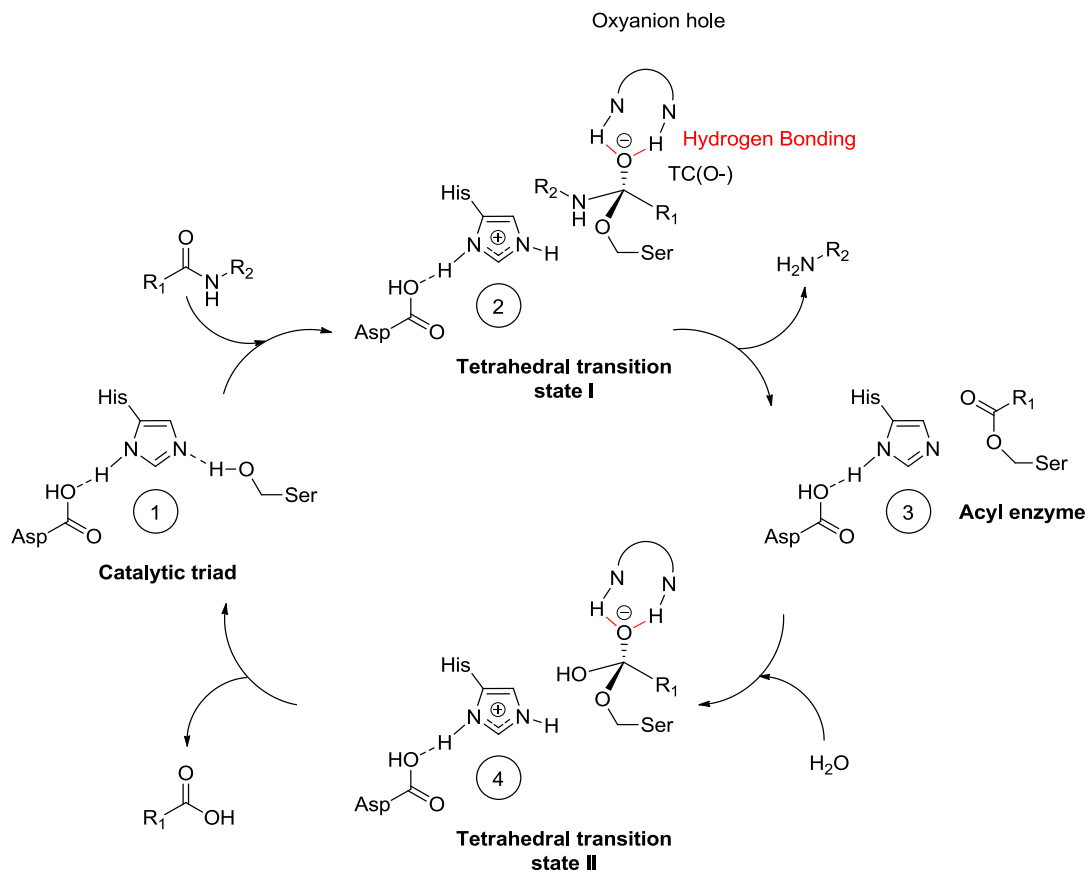


Figure 1.04 Substrate residues (P_n - P_n') and protease binding sites (S_n - S_n') for a general peptide sequence. The cleavage site is denoted by the red line, where P and S sites denoted with a prime indicate the C-terminal side of the cleavage site and non-prime sites indicate the N-terminal side of the cleavage site.

The catalytic triad of serine and cysteine proteases contains an acid-base pair which activates the triad's nucleophilic residue in order to perform covalent catalytic proteolysis of polypeptides. Serine proteases contain a reactive hydroxyl in a Ser residue activated by an Asp and His residue (Figure 1.05 (a)), while cysteine proteases contain a reactive thiol in a Cys residue activated by an Asn and His residue (Figure 1.05 (b)).¹⁶ The active site nucleophile attacks the carbonyl of the scissile amide bond to give a tetrahedral intermediate which is stabilised by an oxyanion hole arising from hydrogen bonding to active site residues (Gly₁₉₃/Ser₁₉₅ for Chymotrypsin – serine protease and Cys₂₅/Gln₁₉ for Papain - cysteine protease). Computational studies suggests that for serine proteases, the formation of the unstable covalent anionic tetrahedral complex, TC(O⁻), is sufficiently thermodynamically stabilised by the energy released in the formation of the new C-O bond that protonation of the anion is not required (Figure 1.05 (a), (2)).¹⁷ The

thiol of cysteine proteases, however, is significantly less able to stabilise the anionic tetrahedral complex and therefore potentially requires further stabilisation by protonation to the neutral TC (OH) complex (Figure 1.05 (b), (2)). Release of the free amine forms an acyl-enzyme (activated enzyme) intermediate which undergoes hydrolysis to liberate the free carboxylic acid and regenerate the catalytic triad.

(a) Serine protease catalytic cycle



(b) Cysteine protease catalytic cycle

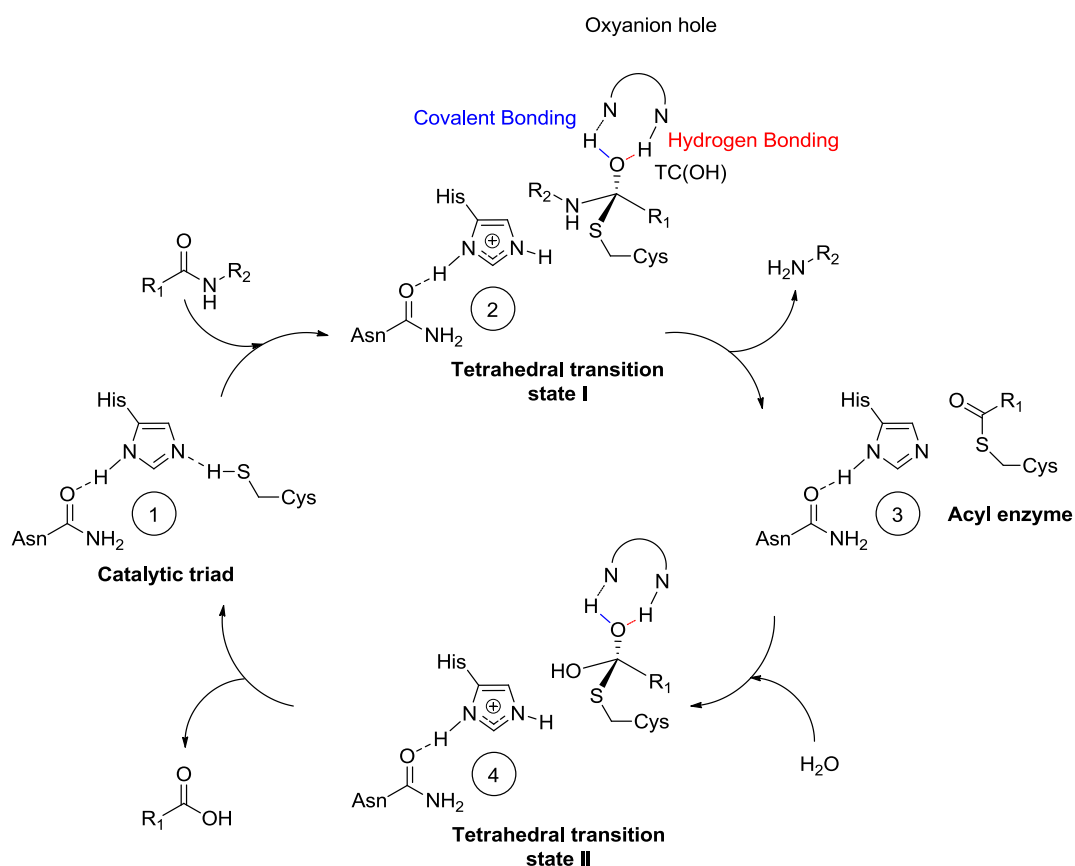


Figure 1.05 Mechanistic pathways for proteolysis catalysed by (a) serine and (b) cysteine proteases.

The nature and details of proteases belonging to the serine and cysteine families is discussed further in chapter two.

1.3 Proteases as Therapeutic Targets and the Current Design of Protease Inhibitors

Proteases play a key role in a diverse range of biological processes, including, for example, the cell cycle,¹⁸ cell motility,¹⁹ and cell fate determination.²⁰ As a consequence, abnormally high activity in proteases is associated with a range of important diseases including osteoarthritis,²¹ inflammatory lung diseases,

Alzheimer's²² and cancer.²³ One way to reduce the number of undesired proteolytic events is by protease inhibition using small molecule protease inhibitors.

Enzymatic inhibitors are broadly classified by their mode of action. Four of these classes include "active-site directed", "mechanism based", "tight-binding" and "slow-binding" inhibitors. An initial classification is based upon whether inhibitors interact with the active site directly (active-site directed) or whether they interact at another site of the enzyme (allosteric effectors), with the number of active-site directed inhibitors currently far outweighing the number of allosteric effector inhibitors. The S₁-S₃ subsites are the most significant in defining which groups bind in the corresponding substrate.¹⁶ Active-site directed inhibitors are further classified as reversible or irreversible. Reversible inhibitors typically bind non-covalently, though covalent binding is sometimes evident as is the case for peptidic aldehydes and nitriles, as discussed in more detail in chapter two.²⁴ A covalent tetrahedral adduct forms between the protease and a reversible inhibitor which is usually in equilibrium with the free enzyme and inhibitor.²⁵ In contrast, irreversible inhibitors are not in equilibrium with their unbound state and invariably react covalently. Reversible inhibition is typically distinguished from irreversible inhibition by systematically treating the enzymes with decreasing concentrations of inhibitor which will result in an increase in enzyme activity in the case of reversible inhibitors. While this distinction between inhibitor types may appear to be simple, it is often quite difficult to differentiate them. For example, reversible inhibitors which bind to the enzymes with a very high affinity and thus have a very slow rate of reversibility can appear as irreversible inhibitors.

1.3.1 Serine and cysteine protease inhibitor structural features

Protease inhibitors generally have the same core structure as a natural protein or peptide substrate as is required for recognition by the protease host. Such inhibitors are as such termed as “peptidomimetic” inhibitors. A high level of affinity for a given protease generally requires the inhibitor to contain at least two amino acid residues. Furthermore, substrate sequences (P_n - P_n' , see Figure 1.04 for a definition) known to bind at active site binding sites (S_n - S_n') of the target protease must be incorporated into the inhibitor design.²⁶ In addition, the hydrolytically labile amide bond on the P_1 residue is typically replaced with an electrophilic group, commonly referred to as “warhead”, which acts as the substitute reactive group and forms the covalent linkage to the protease on binding. If this covalent linkage can be reversibly broken to release the two free species, the inhibitor is reversible.

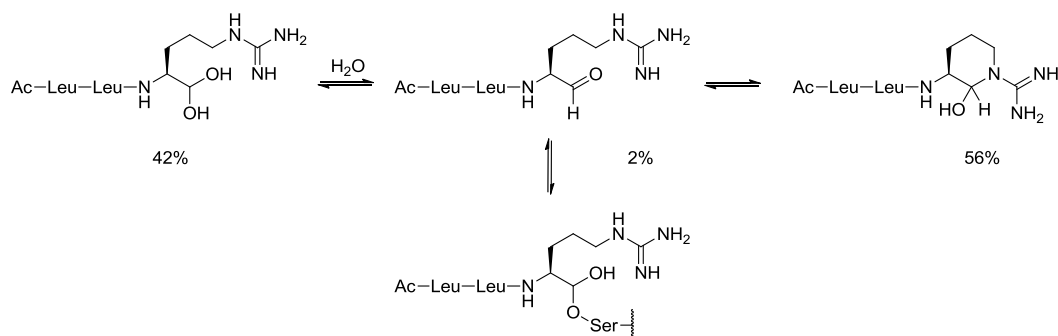
Reversible inhibitors are generally more desirable than irreversible inhibitors in therapeutic applications due to decreased toxicity and associated side effects.²⁷ The current approach to the development of new cysteine and serine protease inhibitors is therefore primarily focused on peptidomimetic inhibitors containing electrophiles whose electronic properties can be tuned for selective reversible inhibition. The geometry or conformation of the peptidic backbone of inhibitors, as defined by its β -strand character (chapter two), is also known to be critical for binding to a protease. The introduction of a planar heterocyclic constraint into the peptidic backbone has been demonstrated to both assist in defining this geometry while reducing peptide character to improve biostability.²⁸ Introducing a

macrocyclic link between the P₁ and P₃ residues has also been shown to define this geometry.²⁹ These ideas are developed further in chapter two.

1.3.2 Serine protease inhibitors

In order to inhibit proteases, inhibitors must have both an appropriate amino acid sequence which is complementary to the binding sites and a suitable C-terminal electrophile. A broad range of electrophilic warheads have been reported for serine protease inhibitors.³⁰ Leupeptin, a naturally occurring peptidic aldehyde with the sequence Ac-Leu-Leu-Arg-CHO, was found to reversibly inhibit the mammalian serine protease Trypsin (IC₅₀ = 5.0 μM) (Figure 1.06, (a)).³¹ The critical P₁ Arg of Leupeptin is known to interact favourably with the corresponding Asp₁₈₉ S₁ pocket via a salt bridge interaction, while the amide bonds of the P₂ and P₃ residues (Leu-Leu) interact with the corresponding amides in the S₂ Ser₂₁₄ and S₃ Gly₂₁₆ residues respectively.³¹ Leupeptin demonstrates “slow binding”, that is, a slow attainment of a steady state when introduced to serine proteases. Leupeptin is not a slow binder in the classical sense of only binding following a conformational change in the enzyme, but rather binds slowly because the concentration of the free reactive aldehyde in aqueous solution which is able to act as an inhibitor at any given time is low. This is largely due to the formation of hydrates, a common feature of all peptidic aldehyde inhibitors which are likely to exist a concentration of less than 10% free aldehyde at any given time in aqueous environments (Figure 1.06, (b)).³² Leupeptin exists at a lower concentration than most peptidic aldehydes in aqueous solutions due to a unique intramolecular cyclisation between the P₁ Arg and terminal aldehyde which forms a stable 6-membered hemiaminal ring system; Figure 1.06, (a).

(a)



(b)

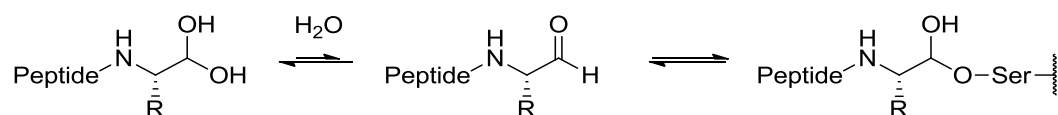
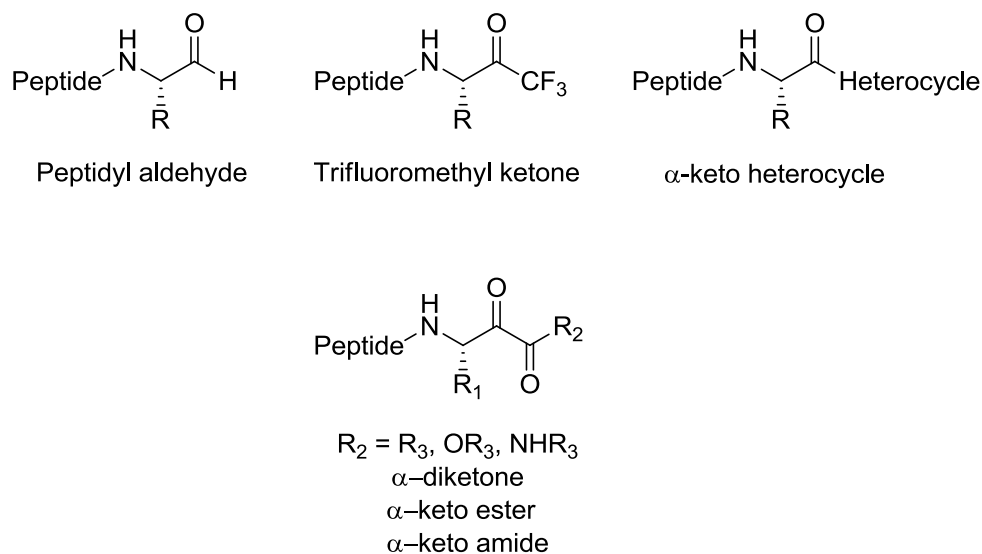


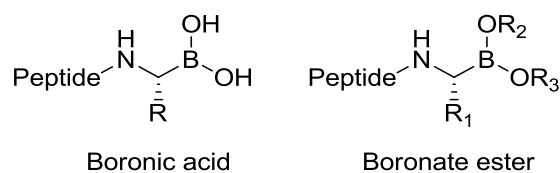
Figure 1.06 (a) Inhibition of serine proteases by Leupeptin. (b) General inhibition of serine proteases by peptidic aldehydes.

A significant drawback of such peptidic aldehydes is that they are often limited by chemical and metabolic instability, in addition to being prone to epimerisation at the P₁ position. In response to this, other electrophilic terminal carbonyl groups have been designed to provide reversible inhibition while minimising these problems. Inhibitors containing trifluoromethyl ketones, α -keto heterocycles, α -diketones and α -keto esters and amides have been developed (Figure 1.07, (a)).³³⁻
³⁷ Reversible inhibitors containing non-carbonyl electrophiles have also been shown to be potent serine protease inhibitors, with organoboronic acids and boronate esters having also demonstrated increased metabolic and chemical stability (Figure 1.07, (b)).^{33, 38}

(a) Reversible serine protease inhibitors



(b) Organoboronic acid and boronate ester serine protease inhibitors

**Figure 1.07** Design of reversible serine protease inhibitors.**1.3.3 Cysteine protease inhibitors**

Cysteine proteases are also inhibited by peptidic aldehydes,³⁹ trifluoromethyl ketones,⁴⁰ and α -dicarbonyls.⁴¹ However, in this case it is not the electrophilicity of the reactive terminal group that defines binding efficacy, but rather the non-covalent interactions (e.g., hydrogen bonding) that the reactive group intermediate can make with the active site on binding to the protease (Figure 1.05). A computational study comparing the transition states of serine and cysteine proteases with various inhibitors revealed that changing the electrophilicity of the reactive terminal group greatly affected the thermodynamic

stability of the serine-inhibitor transition state, but had a minimal effect on the stability of the cysteine-inhibitor transition state.¹⁷ Contributions from hydrogen bonding stabilisation to the newly formed oxyanion hole complex from active site residues (Figure 1.05), however, significantly affects the efficacy of binding to cysteine proteases, while playing a minor role in the binding stability of serine proteases. This selectivity is directly related to nature of cysteine proteases which bind a substrate in a groove located on the surface of the enzyme, which is relatively polar and contains many interacting hydrogen bonding donor and acceptor groups.⁴² This is exemplified for vinyl sulfone inhibitors which are relatively unreactive towards nucleophiles compared to the analogous vinyl ketones or esters, but are capable of forming reversible transition state complexes with protonated histidine residues in the active site of cysteine proteases (pH range of 4.5-6.5) (Figure 1.08).⁴³ This is also apparent for nitriles, a class of inhibitors which are weakly electrophilic but are sufficiently reactive with cysteine residues due to the secondary interactions which can be formed on binding. For example, in a crystal structure of a nitrile inhibitor bound to the cysteine protease Cathepsin K, the inhibitor-thiol adduct was found to be within hydrogen bonding distance of the residue His₁₆₂ (Figure 1.09).⁴⁴⁻⁴⁵

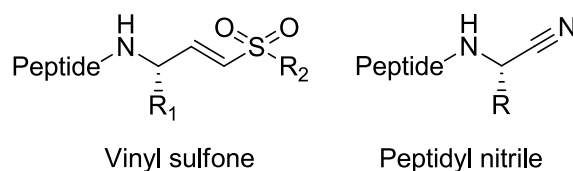


Figure 1.08 Design of reversible cysteine protease inhibitors.

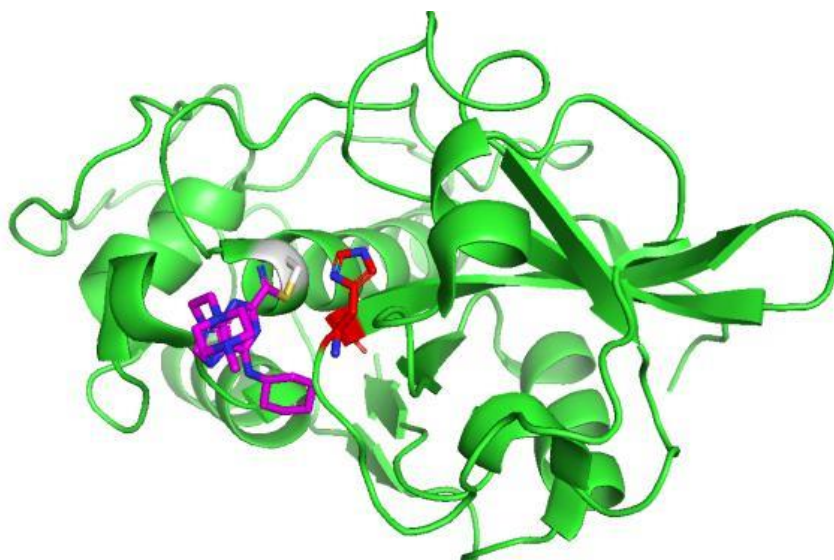


Figure 1.09 Protein-ligand crystal structure of a nitrile inhibitor (coloured purple) covalently bound by Cys₂₅ (coloured white) to Cathepsin K which is within hydrogen bonding distance of His₁₆₂ (coloured red) (PDB 1U9V).⁴⁴

1.4 Overview of the Thesis

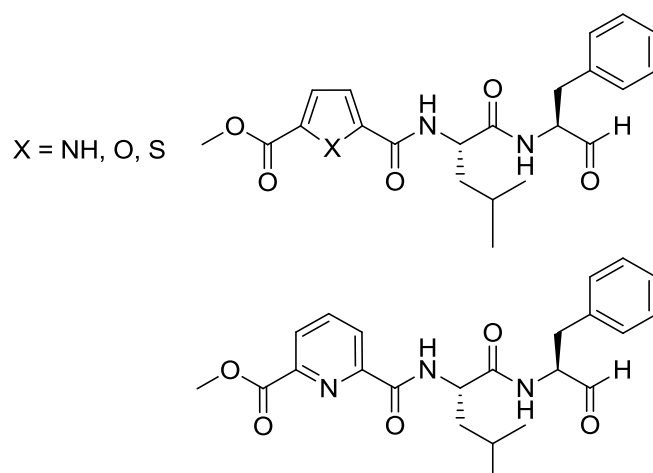
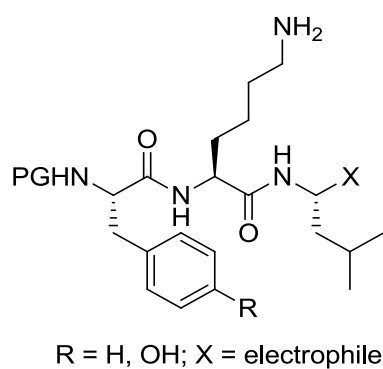
Reversible peptidomimetic protease inhibitors present an opportunity for the treatment of diseases associated with the overactivity of proteolytic enzymes. Systematic modification of peptidic structure and the nature of the P₁ electrophile of such compounds allows for screening of potent inhibitors which may be of therapeutic interest.

The aim of the first project (chapter two) was to synthesise constrained peptidomimetic inhibitors which have reduced peptidic character by the insertion of a heterocycle into the inhibitor backbone to effectively remove an amino acid from the binding sequence. Replacement of amino acid residues in peptidomimetic protease inhibitors with planar heterocycles has been demonstrated to both improve binding affinity (as mentioned above and

discussed in detail in chapter two) and biostability.⁴⁶⁻⁴⁷ While examples of such inhibitors have been previously investigated, the optimum heterocyclic constraint has not yet been determined. A series of N-terminal heterocyclic inhibitors of the model serine protease α -Chymotrypsin were synthesised (Figure 1.10, (a)) and inhibitory potencies determined in a proteolytic assay. Drawing on findings from the assay, macrocyclic inhibitors of cysteine Cathepsins containing optimised heterocycles were investigated and their attempted syntheses are discussed.

The second project (chapter three) describes the preparation of peptidomimetic inhibitors of a newly identified *Mycobacterium tuberculosis* serine protease, Hip1, which has been implicated in one of the organism's pathways for evasion of innate immunity response of a host organism. A series of tripeptide inhibitors containing a reactive boronate ester at P₁ were synthesised (Figure 1.10, (b)) and an optimised peptidic sequence was determined. Modifying the terminal electrophile in the optimised sequence with an α -keto heterocycle and α -keto ester gave rise to highly potent inhibitors which have picomolar range inhibition constants, K_i.

(a) Heterocyclic Chymotrypsin protease inhibitors

(b) Tripeptide inhibitors of the *Mycobacterium tuberculosis* serine protease Hip1**Figure 1.10** Target inhibitors for inhibition of (a) Chymotrypsin and (b) Hip1

CHAPTER TWO:
Design and Synthesis of β -
Strand Constrained
Peptidomimetic Inhibitors of
Chymotrypsin and Cathepsin
Proteases

2 DESIGN AND SYNTHESIS OF B-STRAND CONSTRAINED PEPTIDOMIMETIC INHIBITORS OF CHYMOTRYPSIN AND CATHEPSIN PROTEASES

2.1 Peptide β -Strand

A β -sheet is a distinct secondary structure, formed by the pairing of discrete structural elements known as β -strands through hydrogen bonding. The component β -strands are themselves defined as segments of polypeptide chains which are typically 3 to 10 residues long, which, unlike tightly coiled α -helices, are almost fully extended.² These strands consist of alternating amino acid residues which are: orthogonal to the extended peptide backbone, coplanar as dictated by the amide bonds, and contain no intramolecular hydrogen bonds between amino acid residues. The classic β -strand structure has torsional angles of $\phi = \psi = 120^\circ$ and is depicted as a “saw-tooth” arrangement of amino acids in a linear sequence (Figure 2.01).⁴⁸ The dihedral angles found in parallel ($\phi = -119^\circ$, $\psi = 113^\circ$) and antiparallel ($\phi = -139^\circ$, $\psi = 135^\circ$) β -sheets are the closest values to those of fully extended strand structures ($\phi = \psi = 180^\circ$) (Figure 2.02).

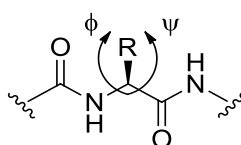


Figure 2.01 Dihedral angles, ϕ and ψ , for the peptide β -strand.

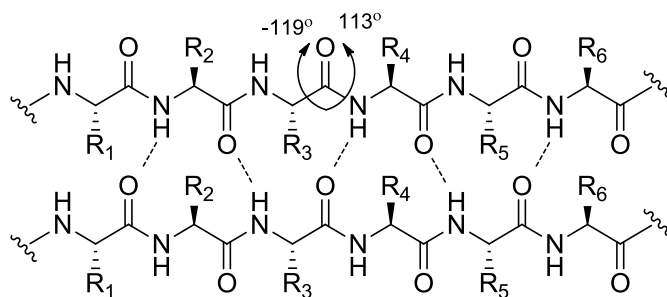
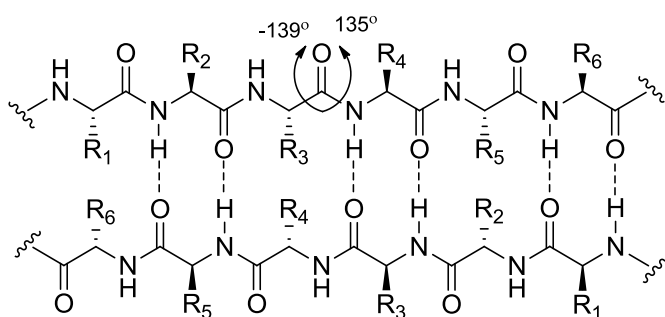
(a) Parallel β -sheet(b) Anti-parallel β -sheet

Figure 2.02 Schematic representation of (a) parallel β -sheets and (b) anti-parallel β -sheets. Hydrogen bonding is denoted with dashed lines.

The β -strand motif plays a central role in the interaction and binding of a number of important biological substrates with a corresponding protein host. Here, the substrate is only recognised by the host, a protease in this case, upon forming a β -strand geometry.⁴⁹⁻⁵¹ A review of over 1500 three dimensional (X-ray) and solution (NMR) structures from the protein data bank of substrates and inhibitors bound to the six classes of proteases, reveals that in almost all instances the active site recognises a substrate in an extended β -strand conformation.⁵²⁻⁵³ This interaction is dictated by the tertiary structure of the protease, which defines an active site geometry with pockets appropriately positioned to bind the extended

amino acid side chains of the substrate in a β -strand. The evolution of this conformational selection arises from a number of different factors. Firstly, helices, turns, loops and sheets which contribute to tertiary structure are collectively required to impart function to a protein unit. These structures need to be resistant to proteolysis as it would be illogical for cellular machinery to expend energy in folding polypeptides into such structural elements and yet the structures remain susceptible to cleavage and degradation by proteases. Consequently, proteases do not recognise folded helices, turns or loops, and instead selectively bind β -strand structures.⁵⁴ Interestingly, β -sheets also tend to be resistant to proteolysis, as unlike isolated β -strands, β -sheets utilise most of their backbone amides in inter-strand hydrogen bonded networks and are therefore not available for interactions with a protease.⁵⁵ Secondly, 'stretching' of the substrate amide bonds towards the transition state required for binding is most efficient when the forces are directionally opposed, with *trans* amide bonds and L-conformations of each amino acid in the β -strand structure enforcing this. Thirdly, maximum exposure of the peptide main-chain amide bond atoms to solvent and host residues, which would otherwise be shielded by hydrogen-bonding helices, turns and or sheet structures, occurs when there is an extension of the peptide in a β -strand geometry. Because of this high degree of exposure, extensive hydrogen bonding between the amide backbone and the host can occur, promoting facile dissociation of substrate and products. Finally, large helical/turn/sheet substructures are not accommodated by the relatively extended and narrow geometry of protease active sites.

2.2 Chymotrypsin and Cathepsin Proteases

2.2.1 *Structural assembly and specificity of Chymotrypsin and Cathepsins*

The six classes of proteases: serine, cysteine, threonine, aspartic acid, glutamic acid and metallo proteases have unique mechanisms of action. Within a given class, protease families are broadly defined by the folded structure of their polypeptide backbones.^{25, 52} Here the focus is on serine proteases and particularly Chymotrypsin, a well-studied model system of serine proteases, and also cysteine proteases typified by the Cathepsins which are known to be associated with various pathologies, osteoporosis, rheumatoid arthritis, osteoarthritis, and bronchial asthma.⁵⁶ Selective inhibition of Cathepsin L is of particular interest due to its association with tumour metastasis.⁵⁷

Chymotrypsin

Serine proteases primarily adopt trypsin-like and subtilisin-like structural folds, with most examples formed from the trypsin-like or Chymotrypsin-like structural folds.⁴⁵ The trypsin-like structure consists of two β -barrels (a beta sheet which coils to a closed structure by inter-strand hydrogen bonding), with the catalytic triad (Asp₁₀₂, His₅₇ and Ser₁₉₅, α -Chymotrypsin numbering) coming together at the interface of the two domains (Figure 2.03). Proteases of the Chymotrypsin family consist of two perpendicular β -barrel domains formed by six antiparallel β -strands.⁵⁸ The key catalytic and substrate binding sites lie in a cleft between the β -barrels, with substrate-enzyme interactions bridging the domains. The oxyanion binding site of Chymotrypsin (Gly₁₉₃ and Ser₁₉₅) belongs to the C-terminal β -barrel. In the ground state, these residues form long-range hydrogen bonds with the amide backbone and the scissile carbonyl of the binding substrate, with the length

of the hydrogen bonds becoming significantly shortened in the anionic transition state.

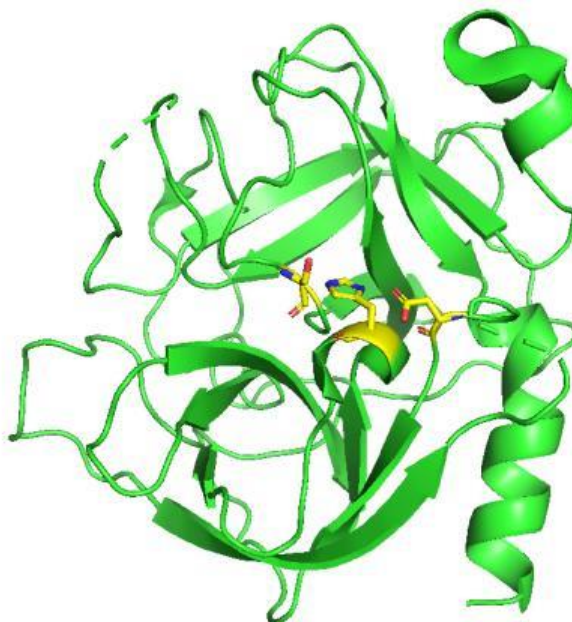


Figure 2.03 X-ray crystal structure of bovine α -Chymotrypsin. The catalytic residues coloured yellow from left to right are Ser₁₉₅, His₅₇ and Asp₁₀₂, as depicted by stick representation (PDB 4Q2K).²⁹

The active site of Chymotrypsin is defined by three β -strand motifs (residues 189-192, 214-216 and 226-228) that defines the specificity profile of the enzyme. Specificity of binding within the wider class of serine proteases is dominated by the S_1 - P_1 interaction, while binding interactions more removed (S_2 - S_4) have significantly reduced influence, the magnitude of which dramatically decreases with separation from S_1 .⁵⁹ Chymotrypsin exhibits a clear preference for hydrophobic residues at S_1 , with P_1 residues defining the orientation of the substrate in the active site. An increase in the volume of the P_1 residue also improves catalytic activity, with a strong preference for aromatic side chains.

These cumulative effects result in highly preferential binding of Phe, Tyr and, to a lesser degree, Leu at P₁.⁶⁰ The effect on specificity dramatically decreases with separation from S₁, with S₂ and S₃ demonstrating little specificity towards residue side chains. In fact, D-amino acids at P₂-P₄ provide somewhat comparable specificity to L-amino acids. S₄ and S₅ sites, in addition to S' sites, have negligible influence on specificity and all residues are essentially accepted at these positions. Despite a low specificity for residues at binding sites beyond S₁, enzyme-substrate interactions with amino acids at these positions are still important for catalytic activity since interaction with corresponding amino acid side chains helps define a β -strand geometry required for substrate binding. As an example, the N-H of Trp₂₁₅ and the carbonyl of P₃ are known to form a hydrogen bond interaction which is critical for efficient substrate binding.⁶¹ Consequently, substrates lacking residues beyond P₁ have a reduced rate of proteolysis.⁶⁰⁻⁶¹

Cathepsins

The human cysteine Cathepsin family is comprised of 11 different types: Cathepsin B, C, F, H, K, L, O, S, V, X and W.¹¹ The Papain model (chapter one) which is constituted by a L domain consisting of three α -helices and a R domain constructed from a β barrel and two α -helices, is representative of cysteine Cathepsins.¹² Overall, the structural assembly of the Cathepsins within the family is highly conserved, with L and R domains across the family maintaining a similar size.⁶² The substrate binding cleft containing the site of catalysis is located at the junction of these two domains. The key active site residues, Cys₂₅ and His₁₆₃ (Cathepsin L numbering) are essentially conserved across the nine Cathepsins (Figure 2.04). Active site residues Gln₁₉, Gly₆₈ and Trp₁₈₃ and the N-terminus Pro₂,

which form interaction with the main chain of the binding substrate are also conserved.

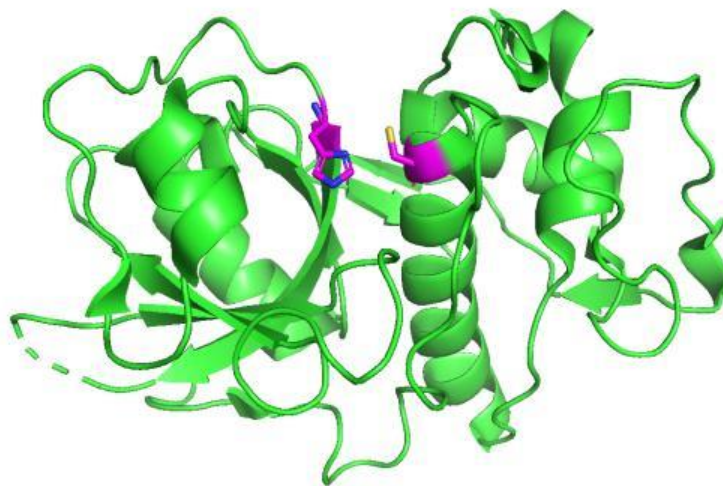


Figure 2.04 X-ray crystal structure of Cathepsin L. The catalytic residues coloured purple from left to right are His₁₆₃ and Cys₂₅₅, as depicted by stick representation (PDB 2XU1).⁶³

Unlike serine proteases, substrate binding specificity for the cysteine Cathepsins is dominated by the P₂ site, with a large preference for hydrophobic residues at the complementary S₂ site.⁶⁴ Furthermore, S₂-P₂ interactions are the primary determinant of differences in specificity between Cathepsins. For example, the S₂ subsite in Cathepsin S consists of Gly₁₃₇/Gly₁₆₅, Cathepsin K consists of Ala₁₃₄/Ala₁₆₃, and Cathepsin L consists of Ala₁₃₅/Gly₁₆₄.⁶⁵ The S₂ subsite of Cathepsin S favours slightly bulky aliphatic side chains (preference for Val, Met, Phe and Nle, a straight chain isomer of Leu) while Cathepsin K favours smaller aliphatic groups (Leu) in addition to a preference for Pro, a specificity unique to mammalian Cathepsins.¹¹ Cathepsin L, however, favours aromatic residues (Phe, Trp, Tyr) at S₂.⁶⁶ Substrate specificity is much less defined beyond these interactions, though all human

Cathepsins generally prefer charged side groups (Arg and Lys) at P₁, S₃ and S₄ demonstrate very little specificity and can accept a range of residues.

2.3 Design of β -strand constrained Chymotrypsin and Cathepsin Inhibitors

Substrate preferences must be incorporated into peptide-based inhibitors (peptidomimetics), especially those that contribute significantly to binding as discussed above. Affinity can be significantly enhanced by defining the backbone of the inhibitor into a β -strand, a geometry that defines binding. An important approach towards inhibitors of this type involves introducing a carefully designed conformational constraint to pre-organise the otherwise flexible backbones into a β -strand conformation.

2.3.1 *Backbone modified β -strand mimetics*

Planar aromatic rings have been introduced into a peptide backbone to define the required geometry, e.g. the biphenyl scaffold of the Trypsin inhibitor **2.00** shown in Figure 2.05. A crystal structure of this inhibitor bound to Trypsin revealed that it binds in an extended conformation, with the two predominant interactions arising from ionic interactions with the S₁ pocket and hydrophobic interactions with the S₄ pocket.⁶⁷

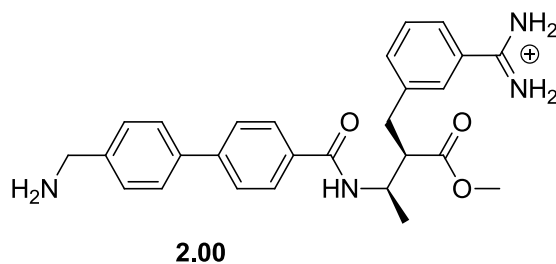


Figure 2.05 Trypsin inhibitor constrained into an extended conformation by a biphenyl spacer.

Pyrrolinone based scaffolds have also been used to define an extended binding geometry in protease inhibitors, including HIV-1 protease inhibitor **2.01**, as shown in Figure 2.06.⁶⁸ Replacement of amide bonds in this way has a two-fold implication. Firstly, as with the biphenyl system, pyrrolinone linkers pre-organise the inhibitor into a β -strand conformation for improved binding efficacy. This was demonstrated in the X-ray crystal structure of the free inhibitor which revealed that its backbone is constrained into the desired β -strand geometry. Secondly, amide bond replacement improves bioavailability and proteolytic stability of the inhibitors.^{46-47, 69} More traditional short peptide-based inhibitors are conformationally flexible, often existing as random structures in aqueous solutions,⁷⁰ while also being susceptible to degradation by proteolytic enzymes and exhibiting low bioavailability and poor membrane permeability. This results in a poor pharmacological profile.⁷¹ Replacing amide bonds in these inhibitors in this way reduces their peptidic character, resulting in an improvement in bioavailability and proteolytic stability. Importantly, key interactions with active site residues achieved with amide bonds in peptidic inhibitors are maintained by pyrrolinone-based inhibitors. Indeed, the pyrrolinone-based inhibitor **2.01** shown

in Figure 2.06 has significantly improved cell transport capability compared to the peptidic analogue. Furthermore, **2.01** ($IC_{50} = 1.6$ nM) retains the high potency of the parent peptidic inhibitor ($IC_{50} = 0.6$ nM).

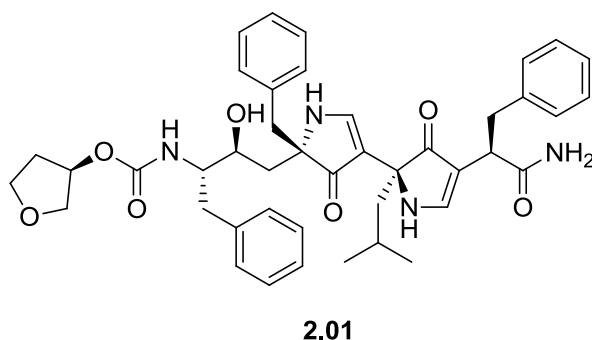


Figure 2.06 β -strand constrained pyrrolinone-based HIV-1 protease inhibitor.

Peptidomimetic aldehydes with an N-terminal heterocycle have also been reported to both define a β -strand geometry and to improve metabolic stability.⁷² For example, dipeptides containing an N-terminal pyrrole as shown in Figure 2.07 have been reported as potent inhibitors of Calpain, a calcium dependent cysteine protease associated with the development of cortical cataracts.⁷² The component heterocycle provides favourable interactions with the hydrophobic S_3 pocket of the protease, with the pyrrole N-H also interacting with the amide carbonyl of Gly₁₉₈ within the S_3 pocket. The dipeptide (Leu-Val) backbone sequence interacts with S_1 and S_2 subsites, respectively. Docking of these inhibitors to Calpain 1 and Calpain 2 shows that the backbone binds in a β -strand geometry. These pyrrole containing inhibitors are highly potent against Calpain 2, with the most potent inhibitor (R = CHO) having an $IC_{50} = 25$ nM.

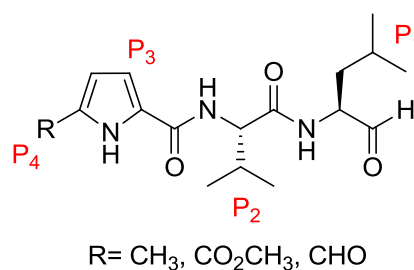


Figure 2.07 Pyrrole-containing Calpain inhibitors.

An alternative approach to achieving pre-organised inhibitors is by the chemical linkage of either P₁ and P₃ or P₁' and P₃'. The conformers of the backbone of macrocyclic Calpain inhibitor **2.02** (IC₅₀(Calpain 1) = 400 nM and IC₅₀(Calpain 2) = 850 nM) depicted in Figure 2.08 were all found to have the requisite extended β-strand conformation, as determined by computational conformational searches.²⁸ Further reduction of the peptidic character of this class of macrocyclic inhibitor has been achieved by replacing two amino acids of the macrocyclic backbone with a substituted pyrrole (e.g., Figure 2.09), where the pyrrole is expected to maintain the planar geometry required for an extended β-strand conformation.²⁹ Aliphatic macrocycle **2.03** is a potent inhibitor of Cathepsin L (Inhibition constant, K_i = 0.44 nM) and Cathepsin S (K_i = 0.92 nM). Introduction of aromatic groups into the macrocyclic linker and replacement of Leu with Phe at P₁ afforded a selective inhibitor of α-Chymotrypsin (**2.04**, K_i = 33 nM). A crystal structure of **2.04** covalently bound to Ser₁₉₅ of α-Chymotrypsin confirmed binding of the backbone in an extended β-strand conformation, as defined by the pyrrole and macrocyclic linker. An overlay of the backbone of **2.04** with the P₁-P₄ region of an extended peptide-based inhibitor of α-Chymotrypsin (PMP-C, PDB 1GL1)⁷³ shows the β-

strand backbones of the two inhibitors nicely superimpose, as per the design of the macrocyclic inhibitor.

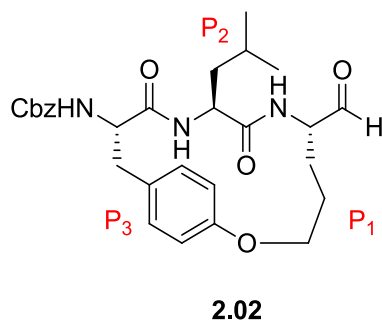


Figure 2.08 Preorganised macrocyclic inhibitor of Calpain.

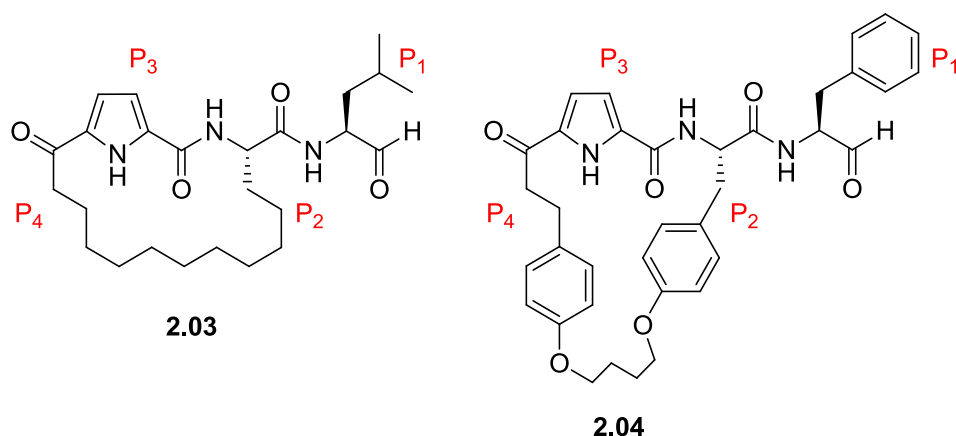


Figure 2.09 Macrocyclic inhibitor of Cathepsins L and S (**2.03**) and α -Chymotrypsin (**2.04**).

2.4 Design and Synthesis of N-Terminal Heterocyclic Chymotrypsin Inhibitors

As discussed, macrocyclic inhibitors containing a backbone pyrrole constraint are highly potent inhibitors of Cathepsins and Chymotrypsin and are therefore of interest regarding further development of inhibitors of these proteases, in addition to other relevant cysteine and serine proteases. While only pyrrole has been investigated in this context, other heterocycles have been used to reduce

peptidic character and enhance binding affinity of peptidomimetic protease inhibitors, as has been demonstrated with non-aromatic morpholines⁷⁴ and aromatic quinolines⁷⁵ and tetrazoles.⁷⁶ Despite the prevalence of heterocycles in the wider area of peptidomimetics, the optimum heterocycle for use as a constraint in protease inhibitors has not been investigated.

What follows is a discussion on the synthesis of a series of model dipeptide substrates containing N-terminal heterocycles aimed at binding to Chymotrypsin, a well-characterised protease for studying relative inhibitor potencies, with the goal of expanding the scope of heterocyclic constraints (pyrrole **2.30**, furan **2.31**, thiophene **2.32** and pyridine **2.33**, Figure 2.10) and determining the ideal heterocycle that gives a combination of reduced backbone peptidic character and an extended backbone geometry to facilitate active site binding. Pyrrole, furan and thiophene were investigated as examples of π -excessive heterocycles and to determine their relative abilities to facilitate binding. The hydrogen bond donor N-H of pyrrole is also of interest regarding binding affinity. The properties of a π -deficient heterocycle were also investigated with pyridine. The relationship of the target peptidomimetics to a natural substrate is depicted in Figure 2.10. An electrophilic aldehyde was incorporated at the C-terminus as this group is known to covalently and reversibly bind to Ser₁₉₅, as per naturally occurring serine protease inhibitors detailed in chapter one. Phe was incorporated at P₁ since Chymotrypsin has a clear preference for hydrophobic aromatic side chains at this site, while Leu was incorporated P₂ due to a slight preference for aliphatic side chains at S₂, as discussed above.⁶⁰ Finally, a methyl ester was appended to the

heterocycles (potential P₄ site) as this site is not considered important for binding. This group provides a reference with **2.34**, a purely peptidic substrate which features an *N*-acetyl alanine residue (closest amino acid mimic to the heterocyclic constraints) to probe the effect of heterocycles on binding.

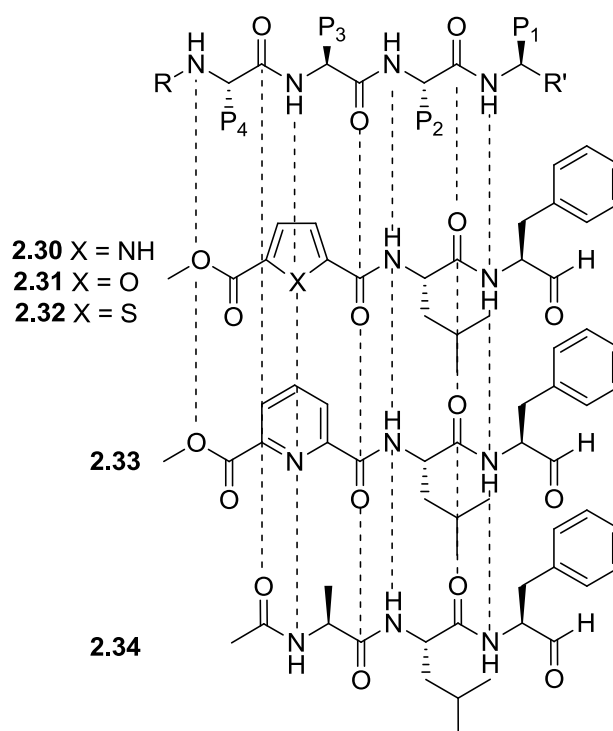
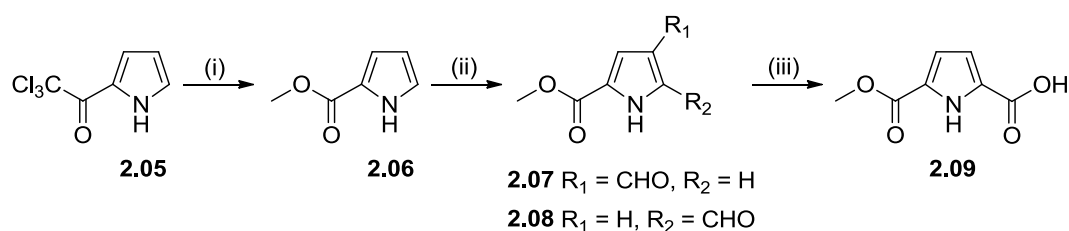


Figure 2.10 Design of N-terminal heterocyclic peptidomimetic substrates of Chymotrypsin. The dashed lines between the natural substrate and heterocyclic substrates indicate their mimetic nature.

2.4.1 Synthesis of heterocycle building blocks

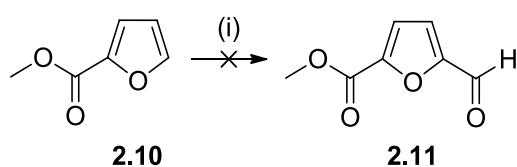
The key heterocycle building blocks **2.09**, **2.14** and **2.17** were first synthesised for use in the synthesis of the targets **2.30**, **2.31** and **2.32**. Pyrrole **2.09** was prepared in three steps from 2-trichloroacetyl pyrrole **2.05**. Treatment of **2.05** with sodium methoxide in MeOH gave the corresponding methyl ester **2.06**.⁷⁷ Formylation of this ester under Vilsmeier-Haack⁷⁸ conditions gave a mixture of 4- (**2.07**) and 5-

formyl (**2.08**) substituted products in a 3:7 ratio, as determined by ^1H NMR, which were separable by flash chromatography. Pinnick oxidation⁷⁹ of the desired aldehyde **2.08** with sodium chlorite in phosphate buffer gave carboxylic acid **2.09** in a 65% yield (Scheme 2.4.1).



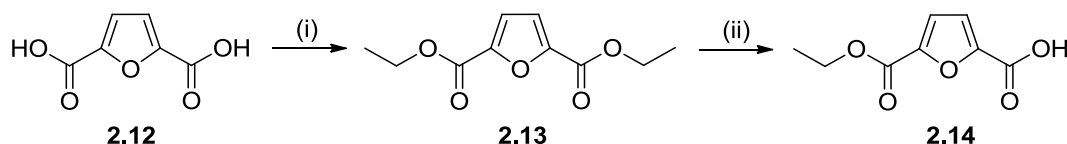
Scheme 2.4.1 Reagents and Conditions: i) NaH, MeOH, THF, 0°C , 0.75 h \rightarrow rt, 18 h (71%), ii) POCl_3 , DMF, DCE, reflux, 0.25 h, then H_2O , $\text{NaOAc}\cdot 3\text{H}_2\text{O}$, reflux, 0.25 h (68%), iii) NaClO_2 , NaH_2PO_4 , H_2O , DMSO, rt, 3h (65%).

The synthesis of the corresponding furan **2.11** was initially attempted using an analogous synthetic approach. Attempted formylation of commercially available methyl 2-furoate **2.10** under the same Vilsmeier-Haack conditions used in the preparation of pyrrole **2.08** failed to give the desired formylated furan **2.11**, with only starting material recovered (Scheme 2.4.2). This may potentially be due to the less electron excessive nature of furan compared to pyrrole which prevents electrophilic aromatic substitution.⁸⁰



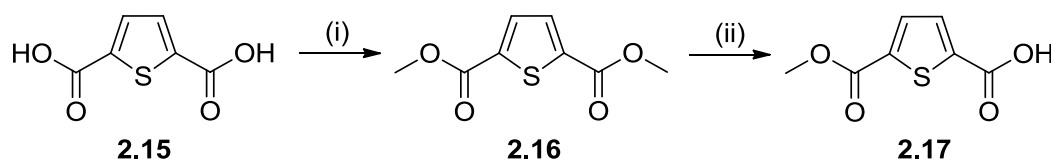
Scheme 2.4.2 Reagents and Conditions: i) POCl_3 , DMF, DCE, reflux, 0.25 h, then H_2O , $\text{NaOAc}\cdot 3\text{H}_2\text{O}$, reflux, 0.25 h.

An alternative approach for the preparation of **2.11** was therefore investigated. 2,5-Furandicarboxylic acid **2.12** was reacted with EtOH under Fischer esterification conditions⁸¹ to give the diester **2.13** and this was subsequently hydrolysed using a stoichiometric quantity of anhydrous NaOH in anhydrous EtOH to give the monoester **2.14** (Scheme 2.4.3).^a Attempted preparation of the corresponding methyl ester was successful, as confirmed by NMR and mass spectrometry, but surprisingly the product could not be purified due to poor solubility in common organic solvents, making this approach unviable.



Scheme 2.4.3 Reagents and Conditions: i) H₂SO₄, EtOH, reflux, 18 h (98%), ii) NaOH, EtOH, 0°C, 2h (95%).

The thiophene unit being sufficiently soluble in most organic solvents was prepared as the desired methyl ester **2.17**. Diesterification of 2,5-thiophenedicarboxylic acid **2.15** with thionyl chloride in MeOH afforded diester **2.16**, which was subsequently selectively mono-deprotected using anhydrous NaOH to afford monoacid **2.17** (Scheme 2.4.4).

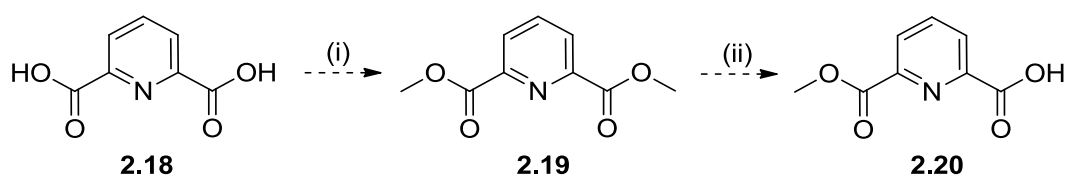


Scheme 2.4.4 Reagents and Conditions: i) SOCl₂, MeOH, reflux, 18 h (88%), ii)

NaOH, MeOH, Acetone, rt, 18 h (70%).

^aEthyl ester **2.14** was prepared from diacid **2.12** by Stephen Kirby at The University of Adelaide.

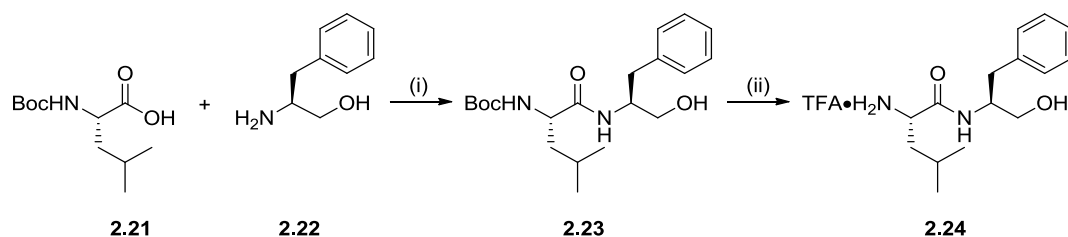
Pyridine **2.20** was commercially available and therefore did not need to be prepared, but can be readily synthesised by diesterification of 2,6-pyridinedicarboxylic acid **2.18** with thionyl chloride in MeOH to diester **2.19**,⁸² followed by selective deprotection with potassium hydroxide to yield monoester **2.20** (Scheme 2.4.5).⁸³



Scheme 2.4.5 Reagents and Conditions: i) SOCl₂, MeOH, reflux, ii) KOH, MeOH, rt.

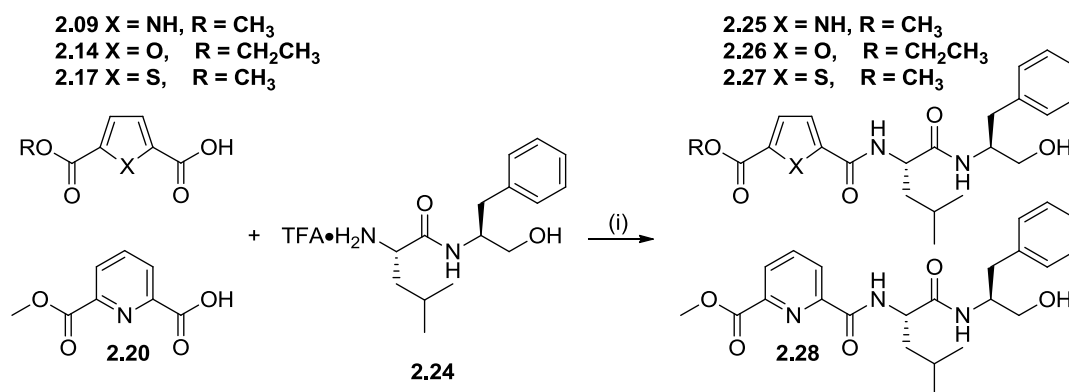
2.4.2 Synthesis of N-terminal dipeptides

The dipeptide intermediate **2.24** used in the preparation of alcohols **2.25-2.29** was prepared over two steps from Boc-leucine **2.21** and phenylalaninol **2.22**. Amidation of **2.21** and **2.22** gave the dipeptide **2.23** in a quantitative yield using the amide coupling reagent HATU. HATU is a uronium/aminium salt which contains a 1-hydroxy-7-azabenzotriazole (HOAt) moiety which forms OAt active esters on reaction with carboxylic acids. OAt esters subsequently react with amines to form amide linkages. HATU mediated amidations are desirable as it has been demonstrated that coupling reagents based on HOAt give faster, more efficient couplings, and most significantly, with no appreciable levels of epimerisation.⁸⁴ Subsequent deprotection of the acid labile Boc protecting group of **2.23** with TFA gave the TFA salt of amine **2.24** in a quantitative yield (Scheme 2.4.6).



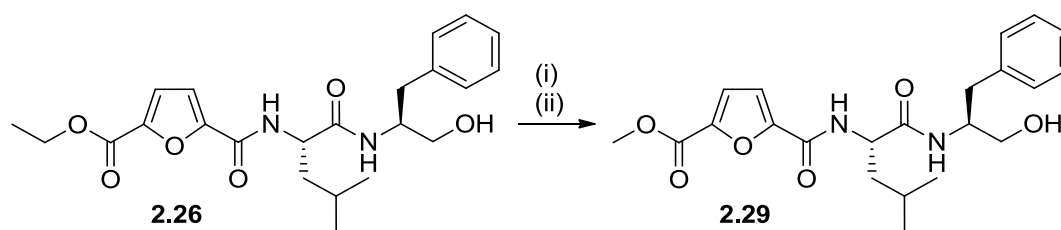
Scheme 2.4.6 *Reagents and Conditions:* i) HATU, DIPEA, DMF, rt, 18 h (99%), ii) TFA, CH₂Cl₂, rt, 5h (100%).

With dipeptide **2.24** in hand, alcohols **2.25-2.28** were prepared in moderate yields by separate amide coupling reactions between heterocyclic carboxylic acids **2.09**, **2.14**, **2.17** and **2.20** and amine salt **2.24** (Scheme 2.4.7).



Scheme 2.4.7 *Reagents and Conditions:* i) HATU, DIPEA, DMF, rt, 18 h (43-62%).

Ethyl ester **2.26** was subsequently converted to the desired methyl ester **2.29** over two steps. Firstly, saponification of **2.26** with aqueous LiOH afforded the intermediate carboxylic acid (not shown). Esterification was initially attempted using Fischer esterification conditions, but this led to degraded material. Alkylation with methyl iodide, however, led to the desired methyl ester **2.29** in a good yield (Scheme 2.4.8).

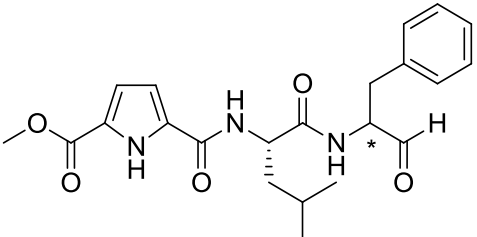
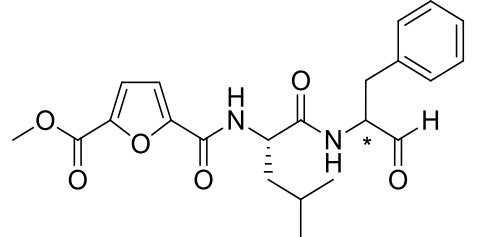
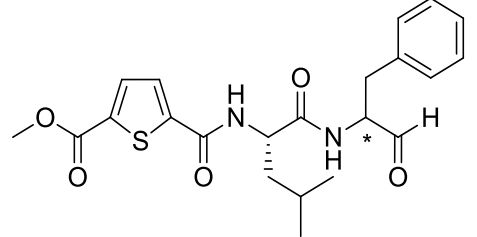
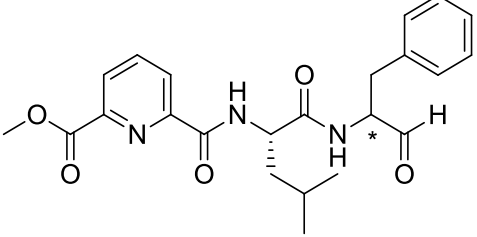


Scheme 2.4.8 *Reagents and Conditions:* i) LiOH, H₂O, THF, rt, 2 h (79%), ii) MeI, K₂CO₃, DMF, rt, 24 h (71%).

With the alcohols **2.25-2.29** prepared, a final oxidation step was required to provide the desired aldehydes **2.30-2.33**. Dess-Martin Periodinane (DMP) was the oxidant used for this transformation as it can chemoselectively transform primary alcohols to aldehydes under mild conditions.⁸⁵ Importantly, DMP does not cause oxidative ring opening of sensitive heterocycles such as furans in instances where other oxidants might.⁸⁶ Additionally, DMP generally has a low tendency to induce α -epimerisation; however peptidic aldehydes are known to be prone to α -epimerisation.⁸⁷⁻⁸⁸ Indeed, while oxidation with DMP in CH₂Cl₂ (THF was used as the solvent for the oxidation of thiophene **2.27** as it is insoluble in chlorinated solvents) at rt did furnish the desired aldehydes **2.30-2.33**, varying levels of α -epimerisation at P₁ was observed, ranging from 6 to 26% R isomer. This result is likely due to activation of the α -position by the Phe benzyl substituent, making this position more prone to stereomutation. Attempted purification of **2.30** by flash chromatography induced higher levels of α -epimerisation.⁸⁸ Therefore, the aldehydes were purified by reversed-phase high pressure liquid chromatography (rp-HPLC). The diastereomeric aldehydes were not separable by HPLC and their ratios, as determined by ¹H NMR (where S is the natural configuration and R is the

unnatural configuration), in the mixtures isolated following purification are reported in Table 2.4.1.

Table 2.4.1 Ratio of diastereomers obtained from DMP oxidation. The asterisks indicate the epimerised centres.

Entry	Structure	Diastereomer Ratio (S:R)
2.30		94:6
2.31		79:21
2.32		74:26
2.33		87:13

The peptidic backbones of the alcohols **2.25**, **2.27**, **2.28** and **2.29** and aldehydes **2.30-2.33** were defined as β -strand by ^1H NMR. An indicative indicator of

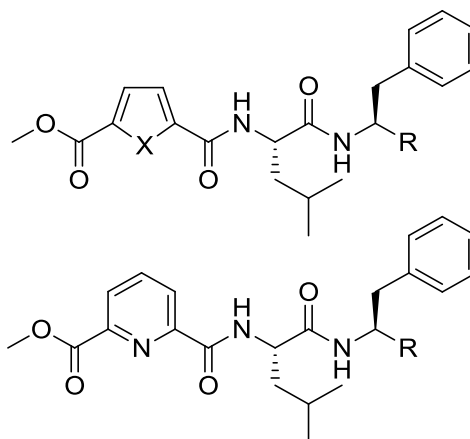
backbone β -strand geometry in peptide sequences is a string of consecutive coupling constants ≥ 8 Hz for couplings between α -hydrogens and their adjacent amide hydrogens, $^3J_{\text{H}\alpha\text{-HN}}$.⁸⁹ All $^3J_{\text{H}\alpha\text{-HN}}$ for alcohols **2.25**, **2.27**, **2.28** and **2.29** and aldehydes **2.30-2.33** were found to range from 8.0 to 8.7 Hz, suggesting that the model substrates' backbones do indeed form the desired β -strand geometry.

2.5 α -Chymotrypsin Inhibition Assay

The inhibitory potencies of the alcohols **2.25-2.29** and aldehydes **2.30-2.33** were determined by measuring their inhibition constants, IC_{50} , using an *in vitro* assay as discussed below. IC_{50} , in this instance, indicates the concentration of a given compound required to decrease activity of a target protease by 50% and is a relative value, the magnitude of which is dependent on the concentration of substrate used in the assay. The activity of α -Chymotrypsin was assayed spectrophotometrically on a 96-well plate using a microplate reader. Ala-Ala-Phe-7-AMC was used as the substrate which upon hydrolysis by α -Chymotrypsin releases the AMC (7-Amino-4-Methylcoumarin) fluorophore with excitation = 380 nm and emission = 460 nm. By measuring the change in fluorescence over time, the capacity of a given compound to compete with the substrate for binding to the target protease can be measured and its inhibitory activity determined quantitatively. The following was added to each well: TES buffer (pH = 8.0, adjusted with NaOH), substrate in DMSO, an alcohol or aldehyde at seven different concentrations in DMSO and α -Chymotrypsin in 1 mM aqueous HCl. In addition to measuring the change in fluorescence, two controls were also used during the assay: (1) Negative control (background fluorescence subtracted from

the measured fluorescence changes): a non-enzymatic hydrolysis of the blank to verify that the substrate is not degraded over time; and (2): Positive control: fluorescence reading due to complete hydrolysis of the substrate by the enzyme to which the measurements are normalised. Progress curves were monitored over 10 min for each concentration of every compound and each measurement was made in triplicate. The IC_{50} values were determined graphically for both the alcohols and aldehydes and are given in Table 2.5.1.

Table 2.5.1 Potencies of alcohols and aldehydes against α -Chymotrypsin as determined by the fluorogenic assay.



Compound	Substituents	IC ₅₀ (μ M)
2.25	X = NH, R = CH ₂ OH	> 500
2.29	X = O, R = CH ₂ OH	> 500
2.27	X = S, R = CH ₂ OH	> 500
2.28	Pyridine, R = CH ₂ OH	> 500
2.30	X = NH, R = CHO	0.54
2.31	X = O, R = CHO	34.5
2.32	X = S, R = CHO	70.0
2.33	Pyridine, R = CHO	33.1

Alcohols **2.25-2.29** did not inhibit at the highest concentration tested (500 μ M) and are therefore not considered to be inhibitors of α -Chymotrypsin. This is expected as they lack the reactive C-terminal aldehyde and are thus only able to act as non-covalent binders. The corresponding aldehydes, however, were found

to inhibit with differing potencies. Pyrrole **2.30** was found to be the most potent inhibitor with an IC_{50} of 0.54 μM , over 50-fold more activity than the π -excessive furan **2.31** and π -deficient pyridine **2.33**. This significant difference in activity is likely due to the pyrrole providing a hydrogen bond donor, which is unique amongst the heterocyclic series studied. As shown in Figure 2.10, the mimetic nature of the heterocyclic inhibitors is such that the heteroatom replaces the amide N-H at the P_3 position in the natural peptidic substrate. This amide N-H is known to form a hydrogen bond with the Gly₂₁₆ amide carbonyl in α -Chymotrypsin, an interaction which contributes to the orientation of Gly₂₁₆ at S_3 .⁹⁰⁻⁹¹ Upon attaining an appropriate orientation, Gly₂₁₆ both assists in orienting the scissile bond at P_1 in the protease complex for cleavage and in improving the protease's discrimination of residues at P_1 .^{60, 92-93} Indeed, this interaction is apparent in the crystal structure of macrocycle **2.04** (Figure 2.09) bound to α -Chymotrypsin which reveals a 3 Å separation between the pyrrole nitrogen and the Gly₂₁₆ carbonyl oxygen.²⁹ This strongly suggests that maintaining a hydrogen-bond donor at this position is important for achieving maximal inhibitory potency. As pyrrole **2.30** is the only aldehyde to contain this hydrogen bond donor at P_3 , this likely accounts for its improved activity over the other heterocyclic aldehydes. Following on, furan **2.31** and pyridine **2.33** possessed very similar potencies despite having different electronic properties and ring sizes. Despite its similar properties to furan **2.31**, thiophene **2.32** is less active still, with half the potency of both the furan and pyridine aldehydes. This suggests that binding is not significantly affected by the electronics or size of a binding heterocycle, but rather is dependent on hydrogen bond donor capabilities, as exemplified by the most potent aldehyde, pyrrole **2.30**.

While tripeptide **2.34** has not been discussed, synthesis and subsequent characterisation of its inhibitory potency against α -Chymotrypsin will be valuable for understanding the importance of backbone heterocyclic constraints for tight binding.

2.6 Design and Synthesis of Macrocyclic, N-Terminal Heterocyclic Cathepsin Inhibitors

As previously discussed, macrocyclisation can be used to preorganise the backbone of peptidomimetic protease inhibitors into the β -strand geometry required for binding. Macrocycles have been inserted into inhibitors of a number of proteases beyond the examples already given. As demonstrated in Figure 2.11, macrocyclisation of the linear hexapeptide HIV-1 protease inhibitor **2.35** resulted in dimacrocycle **2.36** which is 75-fold more potent than the linear peptide.⁹⁴

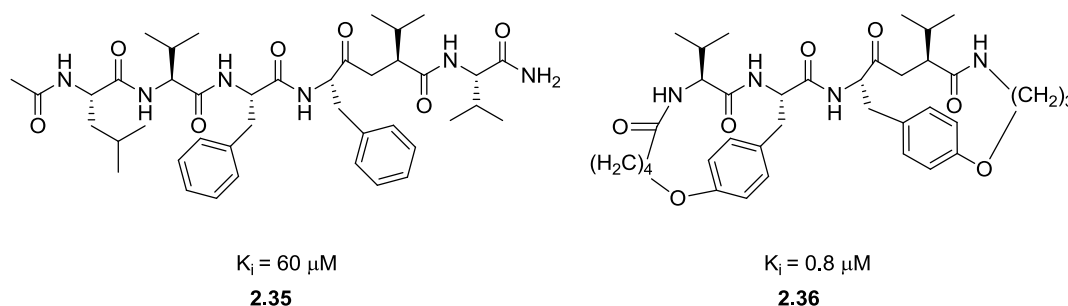


Figure 2.11 Linear and corresponding macrocyclic derivative of a HIV-1 protease inhibitor.

Similar to macrocycle **2.02**, linear peptide **2.37** had its inhibitory potency improved by more than four-fold by macrocyclisation between P₁ and P₃, giving rise to CAT811, **2.38**, a potent inhibitor of Calpain 2 (Figure 2.12).²⁸

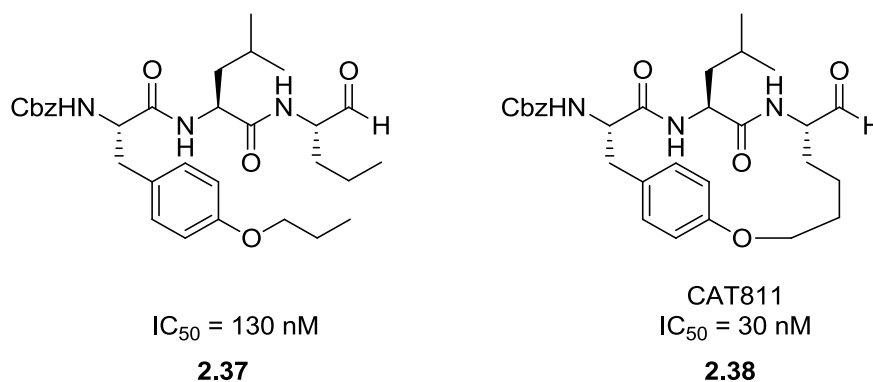


Figure 2.12 Inhibitory potencies for the Calpain 2 inhibitors, CAT811, and its acyclic equivalent.

A number of approaches have been developed for side chain cyclisation of peptidomimetics, including lactamisation, Click chemistry,⁹⁵ and disulfide bridge formation by oxidation of cysteine residues within close spatial proximity.⁹⁶ These macrocyclic linkers, while versatile, require functionality in the linker units (e.g., dimacrocycle **2.36**) for cyclisation. With the development of ruthenium based Grubbs catalysts, however, synthesis of macrocycles from dienes (e.g., macrocycle **2.38**) has become possible. Macrocyclisation by ring-closing metathesis (RCM) is typically performed using Grubbs 2nd Generation catalyst (Grubbs 2nd Gen.), with ring-closure generally being achieved under relatively mild conditions to afford E and Z macrocycles. When performing RCM, careful consideration of reaction time, temperature and concentration must be made to reduce ring-opening metathesis (ROMP) events and oligomerisation (Figure 2.13).⁹⁷

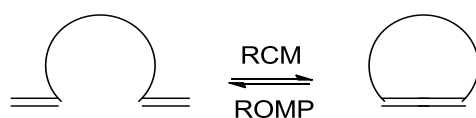


Figure 2.13 Equilibrium formed during RCM reactions

2.6.1 *Macrocyclic N-terminal pyrrole-P4 ester*

As demonstrated earlier, pyrrole is the optimal N-terminal heterocycle for reducing peptidic character and improving the β -strand geometry of the backbone of peptidomimetic protease inhibitors of Chymotrypsin. It was therefore envisaged that pyrrole would also be a suitable constraint for incorporation into inhibitors of cysteine Cathepsins. Similar to Chymotrypsin, hydrogen bond interactions with the P₃ backbone amide (or pyrrole N-H in the case of heterocyclic inhibitors) are important for achieving maximal binding to the active site. In the case of Cathepsin L, hydrogen bonding exists between the amide carbonyl of Gly₆₈ and the P₃ amide N-H of binding substrates.⁹⁸ The importance of a pyrrole constraint in macrocyclic Cathepsin inhibitors has already been discussed, with macrocycles **2.03** and **2.04** being potent inhibitors of Cathepsins L and S. A drawback of these inhibitors is that the acyl substituent linking P₄ and P₂ needs to be introduced by Friedel-Crafts acylation, which is often very low yielding. Additionally, the natural substrate features an amide bond at P₄ (Figure 2.10) which presumably imparts hydrogen bonding interactions with the S₄ site to improve binding efficacy; an interaction not possible for these acyl inhibitors. Ideally, these interactions could be attained simply by substituting an amide linkage at P₄ in place of the acyl linkage. Unfortunately, this is synthetically challenging, with previous attempts to cyclise dienes with P₄ amide linkages being unsuccessful.^b It is postulated that cyclisation is not possible due to an internal hydrogen bond between the pyrrole N-H and the P₄ amide, forcing the amide bond into a trans configuration. As a consequence, the terminal alkenes are too spatially separated to participate in RCM, preventing cyclisation (Figure 2.14).

^bAbell personal communication.

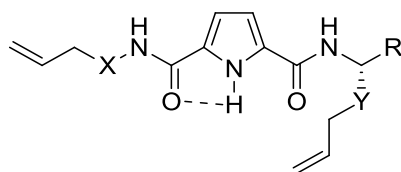


Figure 2.14 Proposed conformation of pyrrole-P₄ amide cycles which prevents cyclisation.

To circumvent this, it was anticipated that replacement of the amide linker with a more conformationally flexible ester linker would allow for RCM, as proposed for macrocycles **2.49** (Figure 2.15). Macrocyclic lactones would be expected to have similar metabolic stabilities to the amide analogues, with a rate of hydrolysis insignificant at physiological pH.⁹⁹⁻¹⁰⁰ The macrocycles are designed for selective inhibition of Cathepsin L, as defined by the aromatic substituent at P₂.⁶⁶ The linear nature of the syntheses of these macrocycles, as demonstrated in Figure 2.15, allows for various residues with different terminal warheads to be incorporated at P₁. In designing a Cathepsin L selective inhibitor, incorporation of Leu at P₁ is favoured, as demonstrated for similar macrocyclic Cathepsin inhibitors such as **2.03**.²⁹ Appending a suitable electrophile at P₁ such as a nitrile will improve selectivity over other protease classes such as serine proteases, as discussed in chapter one.

It was envisaged that the macrocycles **2.49** (where R is an aliphatic amino acid side chain and X is a terminal electrophile) could be prepared as outlined in Figure 2.15. Amidation of carboxylic acid **2.41** and TFA salt of amine **2.45** gives diene **2.46** which can be cyclised by RCM to give macrocycles **2.47**. It is then imagined that

hydrogenation would afford carboxylic acid **2.48** which can undergo a final amidation step with an appropriate terminal residue to give **2.49**

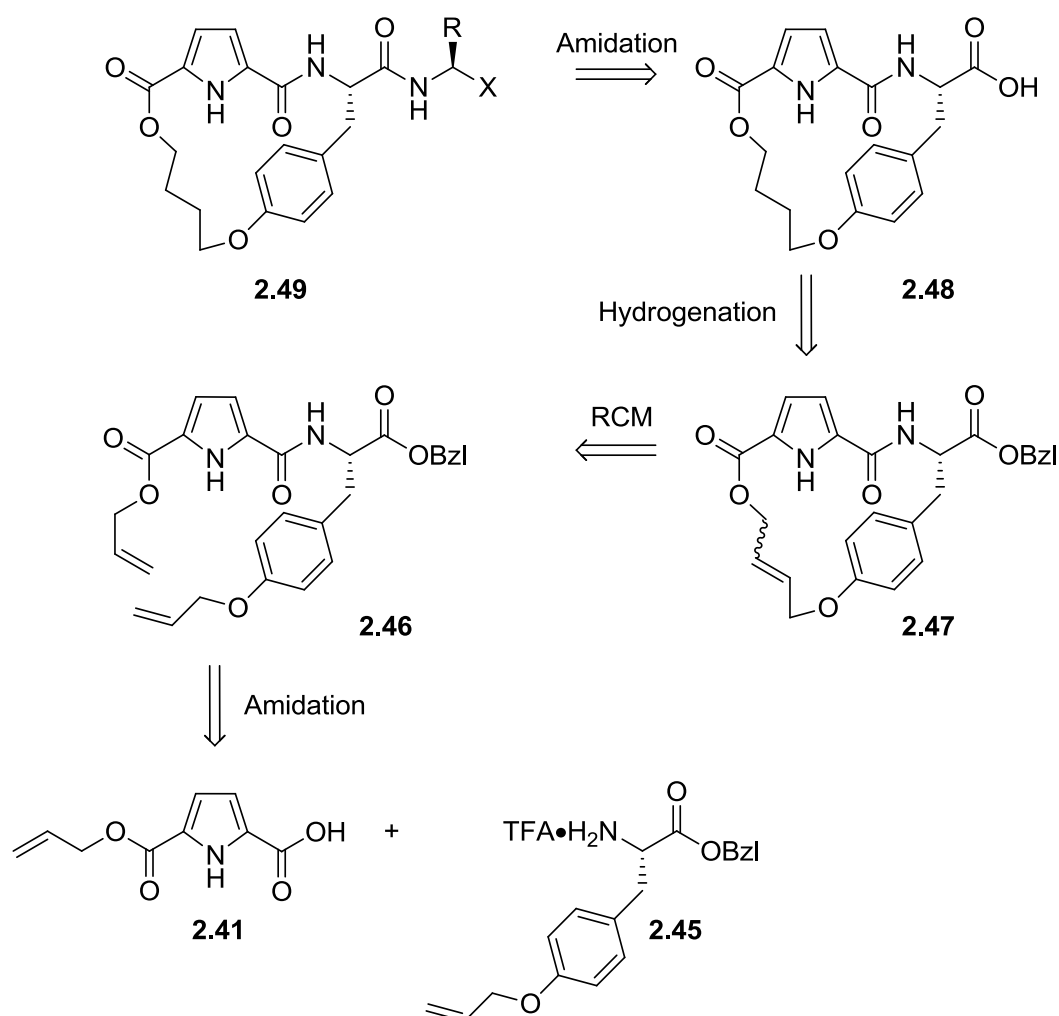
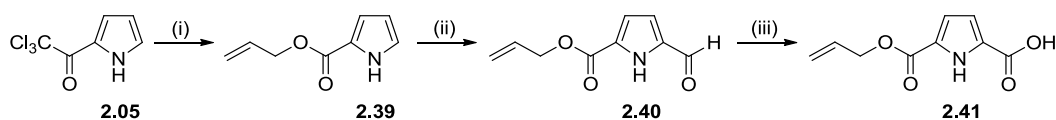


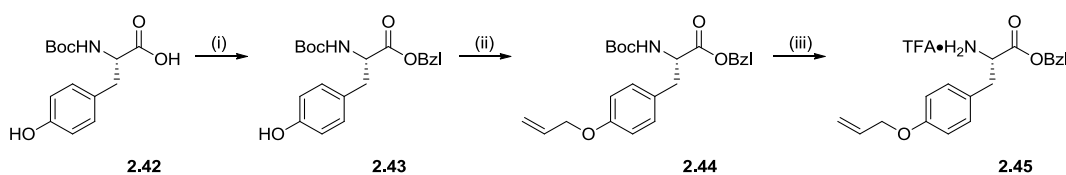
Figure 2.15 Retrosynthetic analysis of macrocyclic Cathepsin L inhibitors **2.49**. Bzl = Benzyl.

Synthesis of pyrrole **2.41** followed the same general approach as used for pyrrole **2.09**: esterification of 2-trichloroacetyl pyrrole **2.05** with allyl alcohol gave allyl ester **2.39** that was formylated under Vilsmeier-Haack conditions to give **2.40**. Final Pinnick oxidation provided carboxylic acid **2.41** (Scheme 2.6.1).



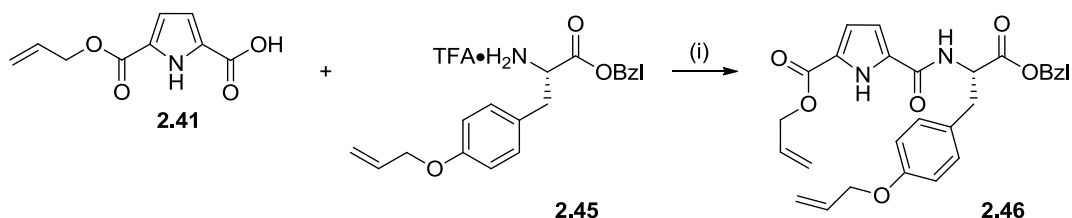
Scheme 2.6.1 *Reagents and Conditions:* i) NaH, allyl alcohol, THF, 0°C, 0.75 h → rt, 18 h (100%), ii) POCl₃, DMF, DCE, reflux, 0.25 h, then H₂O, NaOAc·3H₂O, reflux, 0.25 h (22%), iii) NaClO₂, NaH₂PO₄, H₂O, DMSO, rt, 3h (94%).

Construction of the TFA salt of amine **2.45** began with esterification of Boc-L-tyrosine **2.42** using benzyl bromide to form benzyl ester **2.43**. Allylation of the phenol with allyl bromide under Finkelstein conditions gave allyl ether **2.44** in near quantitative yields, which was subsequently Boc-protected using TFA to quantitatively afford **2.45** (Scheme 2.6.2).



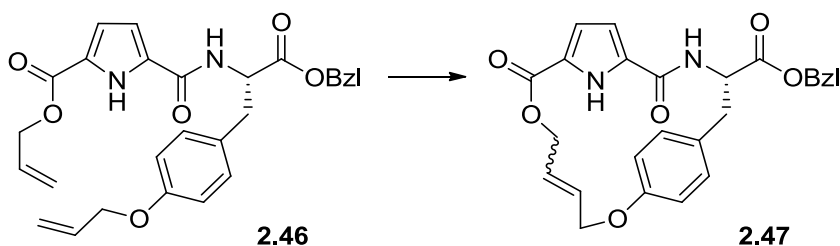
Scheme 2.6.2 *Reagents and Conditions:* i) Benzyl bromide, DIPEA, THF, rt, 18 h (55%), ii) Allyl bromide, K₂CO₃, TBAI, DMF, 40 °C, 18 h (92%), iii) TFA, CH₂Cl₂, rt, 3 h (100%).

With the required amine and carboxylic acid in hand, amidation was performed to give diene **2.46** in a 76% yield (Scheme 2.6.3).



Scheme 2.6.3 *Reagents and Conditions:* i) HATU, DIPEA, DMF, rt, 18 h (76%).

Attempted macrocyclisation of diene **2.46** proved challenging, with the macrocycles **2.47** only being produced in low yields (Table 2.6.1). RCM was initially attempted with Grubbs 2nd Gen. in EtOAc to give a mixture of the desired E and Z macrocycles **2.47**, but only in a yield of 19%. This low yield may reflect a low conformational flexibility of the diene due to internal hydrogen bonding, similar to the proposed conformation for a P₄ amide depicted in Figure 2.14. LiCl was therefore used as an additive in an attempt to disrupt potential hydrogen bonding interactions between the P₄ ester and pyrrole N-H to improve peptide flexibility and hence RCM.¹⁰¹ The reaction in the presence of LiCl however gave similar yields to the conditions without additive. The use of the alternative Lewis acid catalyst titanium isopropoxide, Ti(O*i*Pr)₄, gave a significantly improved yield of 50%. Grubbs 2nd Gen. and related ruthenium RCM catalysts have been shown to chelate to dienes, preventing the ruthenium centre from forming a covalent bond with alkenes, as required for the reaction to proceed and thereby deactivating the catalyst. Ti(O*i*Pr)₄ has been demonstrated to preferentially chelate to dienes, preventing deactivation of the ruthenium catalyst by chelation to the alkene. Furthermore, chelation of Ti(O*i*Pr)₄ to dienes organises the substrate into a conformation that promotes RCM.¹⁰²

Table 2.6.1 Optimisation of RCM of diene **2.46**.

Entry	Grubbs 2 nd Gen. (mol %)	Solvent	Temperature (°C)	Reaction Time (h)	Additive	2.47 Yield (%)
1	10	EtOAc	55	3	-	19
2	10	EtOAc	55	3	LiCl (1.5 equiv)	17
3	10	CH ₂ Cl ₂	40	3	LiCl (1.5 equiv)	15
4	10	EtOAc	45	3	Ti(O <i>i</i> Pr) ₄ (4.0 equiv)	50

Macrocycles **2.47** were obtained as 2:1 mixture of Z:E isomers, as determined by ¹H NMR, but this was of no consequence as subsequent reductive cleavage of the benzyl ester to the corresponding carboxylic acid and reduction of the alkenes by hydrogenation would give rise to a single common alkane. However, hydrogenation of **2.47** with Pd/C in EtOAc returned only starting material, even after increasing the reaction time from 4 h to 72 h. EtOAc was substituted for MeOH, but this reaction only gave degraded material which was proposed to be due to transesterification of the P₄ ester with MeOH. Performing the reaction in a

mixed EtOAc and MeOH solvent system with varying concentrations of MeOH also resulted in degraded material. Due to the labile nature of the P₄ ester under the reductive conditions used, a more chemically stable macrocycle was pursued.

2.6.2 Macrocyclic N-terminal pyridine-P₄ amide

To improve the chemical stability of the macrocyclic Cathepsin L inhibitor, the P₄ ester of the previous target macrocycle **2.49** was replaced with the optimum amide linkage. The backbone pyrrole was also replaced with a pyridine to avoid issues during RCM, as discussed earlier (Figure 2.14). Additionally, P₄ was substituted with an aromatic substituent in order to further enforce rigidity into the macrocyclic tether and consequently the desired β -strand geometry of the peptidic backbone. These modifications give rise to target macrocycle **2.50**, as depicted in Figure 2.16.

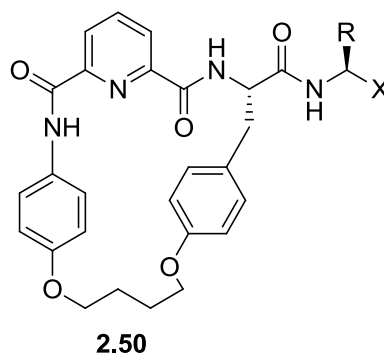
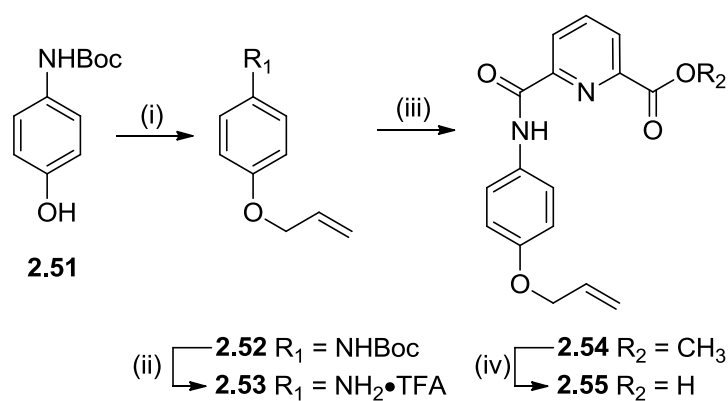


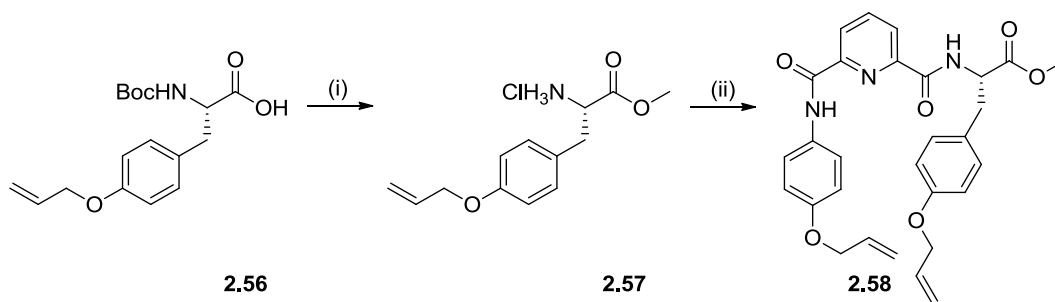
Figure 2.16 Target pyridine-P₄ amide macrocycle **2.50**.

Allylation of commercially available 4-*N*-Boc-aminophenol **2.51** with allyl bromide gave allyl ether **2.52**, which was treated with TFA to afford the TFA salt of amine **2.53**. Amidation with pyridine **2.20** gave methyl ester **2.54** which was saponified with LiOH to afford carboxylic acid **2.55** in an overall yield of 89% (Scheme 2.6.4).



Scheme 2.6.4 *Reagents and Conditions:* i) Allyl bromide, K_2CO_3 , ACN, reflux, 3 h \rightarrow rt, 18 h (76%), ii) TFA, CH_2Cl_2 , rt, 0.5 h (100%), iii) **2.20**, HATU, DIPEA, DMF, rt, 18 h (87%), iv) LiOH, H_2O , THF, rt, 2 h (94%).

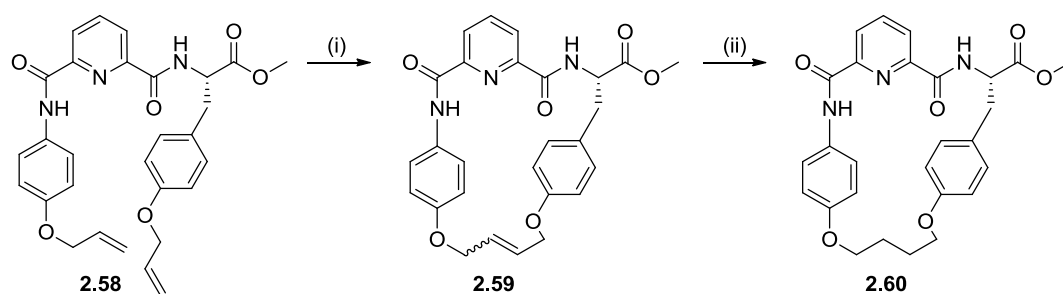
HCl salt of amine **2.57**, prepared by concurrent Boc-deprotection and methyl esterification of commercially available Boc-Tyr(Allyl)-OH **2.56** with thionyl chloride in MeOH, was coupled to carboxylic acid **2.55** to give diene **2.58** in a quantitative yield (Scheme 2.6.5).



Scheme 2.6.5 *Reagents and Conditions:* i) SOCl_2 , MeOH, 0°C , 1 h \rightarrow rt, 18 h (100%), ii) **2.55**, HATU, DIPEA, DMF, rt, 18 h (100%).

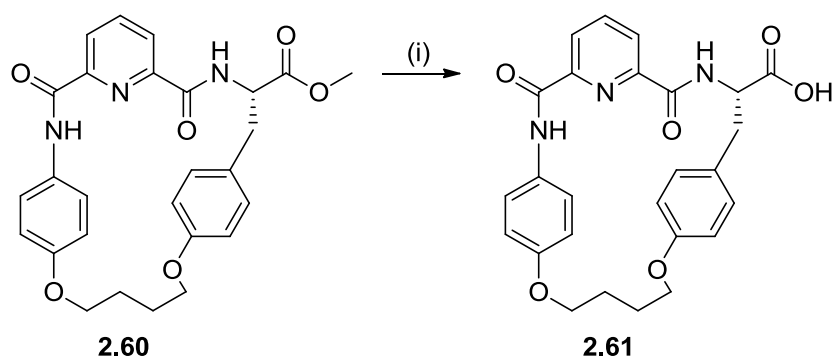
RCM of diene **2.58** with Grubbs 2nd Gen. gave macrocycles **2.59** as a 1.7:1 mixture of E:Z isomers, as determined by ^1H NMR. The macrocycles are poorly soluble in most solvents, but are partially soluble in chlorinated solvents. Subsequent

hydrogenation was therefore performed using a 1.5:1:1 CH₂Cl₂: EtOAc: MeOH solvent system, affording the corresponding saturated macrocycle **2.60** (Scheme 2.6.6). The C-terminal carboxylic acid was originally protected with a benzyl ester, with the intention of removing it during the hydrogenation reaction. Surprisingly, all attempts to perform a global hydrogenation on the equivalent benzyl ester of **2.59**, including high pressure conditions (3 atm. H₂), failed to give the desired product and starting material was only ever recovered.



Scheme 2.6.6 Reagents and Conditions: i) Grubbs 2nd Gen., CH₂Cl₂, reflux, 24 h (30%), ii) H₂, Pd/C, CH₂Cl₂, EtOAc, MeOH, rt, 18 h (90%).

Similar to **2.59**, the saturated macrocycle **2.60** is also poorly soluble in most solvents and could not be hydrolysed under standard conditions. Saponification with NaOH in 9:1 CH₂Cl₂:MeOH¹⁰³ successfully converted methyl ester **2.60** to the desired carboxylic acid **2.61** (Scheme 2.6.7). **2.61** is insoluble in all solvents investigated except for DMSO, preventing further purification or amidation reactions to form the target macrocycles **2.50**. Further functionalisation of **2.61** was consequently abandoned due to solubility issues.



Scheme 2.6.7 Reagents and Conditions: i) NaOH, CH₂Cl₂, MeOH, rt, 2 h.

2.7 Conclusions and Future Work

In summary, a series of N-terminal heterocyclic constrained peptidomimetics as inhibitors of α -Chymotrypsin were prepared and the associated inhibitory potencies determined. Aldehydes **2.30-2.33** inhibit α -Chymotrypsin, with pyrrole **2.30** being the most potent of the series ($IC_{50} = 0.54 \mu\text{M}$), while furan **2.31**, thiophene **2.32** and pyridine **2.33** are significantly less potent inhibitors. This significant reduction in potency is likely as a result of **2.31-2.33** lacking a P₃ hydrogen bond donor. Further investigation into disubstituted heterocycles such as imidazole is of interest to determine if heteroatoms at different ring positions can improve binding efficacy. Future testing of tripeptide **2.34** against α -Chymotrypsin is also of interest for understanding the effect of backbone heterocyclic constraints on binding efficacy.

Macrocyclic intermediates **2.47** of macrocyclic inhibitors of Cathepsin L, **2.49**, were successfully prepared, but were found to be unstable to hydrogenation conditions due to the labile nature of the P₄ ester. Preparation of P₄ ester macrocycles functionalised with P₁ residues will consequently require either retaining or functionalising the intermediate alkenes, as in **2.47**. Carboxylic acid

intermediate **2.61** was also successfully synthesised, but was unable to be purified or further reacted due to its poor solubility profile. Investigations into similar pyridine macrocycles with improved solubilities provides an opportunity to investigate the effect of P₄ amide linkages on binding efficacy to Cathepsin L and other suitable Cathepsin proteases.

CHAPTER THREE:

Design and Synthesis of Peptidomimetic Inhibitors of *Mycobacterium tuberculosis* Serine Protease Hip1

3 DESIGN AND SYNTHESIS OF PEPTIDOMIMETIC INHIBITORS OF *MYCOBACTERIUM TUBERCULOSIS* SERINE PROTEASE HIP1

3.1 *Mycobacterium tuberculosis*

Mycobacterium tuberculosis (Mtb), the bacterium that causes tuberculosis (TB), evades host innate immunity and causes disease by replication within macrophages.¹⁰⁴ Once assimilated into macrophages, Mtb can modulate macrophage responses and interfere with dendritic cells (immune response cells), enabling the pathogen to escape early detection of an immunity response.¹⁰⁵⁻¹⁰⁶ The factors by which Mtb modulates host immunity are still currently under investigation and are important for the development of new therapeutics for treatment of TB.

3.2 Hip1 Protease

The cell-wall associated Mtb serine protease Hip1 (hydrolase important for pathogenesis; previously Rv2224c) has recently been implicated in modulating interactions between Mtb and dendritic cells which results in dampened (regulate a reduced response) macrophage proinflammatory responses. Importantly, Hip1 has been shown to inhibit maturation of dendritic cells and impair antigen presentation and T cell responses.¹⁰⁷⁻¹⁰⁸

Hip1 performs proteolysis on a specific protein substrate, GroEL2, a cell wall-associated heat-shock protein.¹⁰⁹ GroEL2 is a stress-induced secreted protein, the release of which is induced by, for example, heat, nutrient starvation and hypoxia, and has been shown to modulate macrophage cytokine responses.¹¹⁰⁻¹¹¹ The function of Hip1 in GroEL2 cleavage was studied by measuring the rate of

proteolysis of the protein in the presence of wild type Hip1 and a mutant strain whose catalytic active site had been mutated. Wild type and mutated versions of Hip1 were introduced into a transposon mutant disrupted in Hip1, and their effects tested on GroEL2 processing. Expression of wild type Hip1 gave increased amounts of processed forms of GroEL2, while expression of mutant Hip1 failed to give processed GroEL2, indicating that Hip1 is associated with the cleavage of GroEL2. It is presumed that the proteolytically cleaved form of GroEL2 is responsible for the dampening of host innate immune responses required to drive disease propagation and pathology. Indeed, it has been demonstrated that Hip1 is required for optimal growth both *in vivo* and *in vitro*. Furthermore, studies of mice infected with Mtb containing mutant Hip1 showed they had significantly increased rates of survival and reduced lung pathology compared to wild type Mtb.¹⁰⁹ As such, Hip1 is a valuable target for adjunctive therapeutic treatment against Mtb.

3.2.1 Structure of Hip1

Purified Hip1 protease has been crystallised and its X-ray structure solved.¹¹² This reveals Hip1 to be a 520 residue protein that forms a kidney-shaped monomer unit with dimensions of 68 Å x 48 Å x 42 Å. The primary sequence contains eleven cysteine residues that form 5 disulfide bonds. The two structural domains which form the clefts between the active sites are characteristic of serine proteases. One domain is a mixed α/β domain, while the other is an α only domain (Figure 3.01). The catalytic active site formed at the centre of the clefts contains the classical catalytic triad, as discussed in chapter one, comprising of Ser₂₂₈, Asp₄₆₃ and His₄₉₀. The protease was confirmed to be from the serine family by single point mutations

of these residues to alanine, which resulted in abolition of catalytic activity.¹¹³ The catalytic residues form a characteristic hydrogen bonding network prevalent in serine proteases which then facilitates nucleophilic attack on hydrolytically labile amide bonds at P₁. Gly₁₁₀ and Tyr₂₂₉ stabilise the oxyanion hole formed during proteolysis, as determined by their positioning in the S₁ subsite.

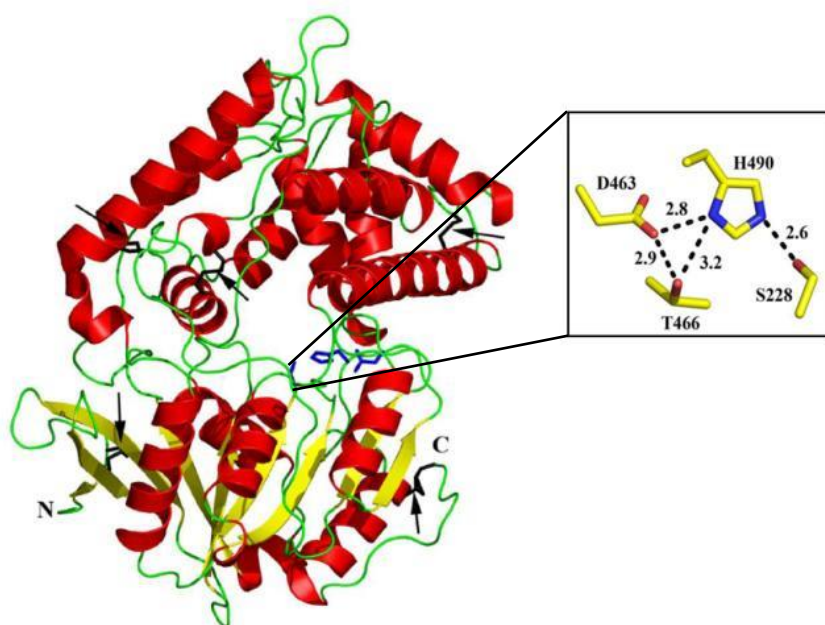


Figure 3.01 Structure of Hip1 monomer. The catalytic residues are enlarged for clarity.¹¹²

3.2.1 Hip1 active site

The substrate specificity of Hip1 has been determined by position scanning-synthetic combinatorial libraries.¹¹⁴ Synthetic libraries were constructed which have the general formula: Ac-X-X-X-P₁-ACC, Ac-X-X-P₂-X-ACC, etc., where Ac = acetyl, X is a mixture of all natural amino acids (excluding Cys and Nle), P₁-P₄ are fixed single amino acids, and ACC is a fluorogenic tag used for the quantitation of

cleaved substrate in fluorogenic assays. The substrate specificity determined is shown schematically in Figure 3.02

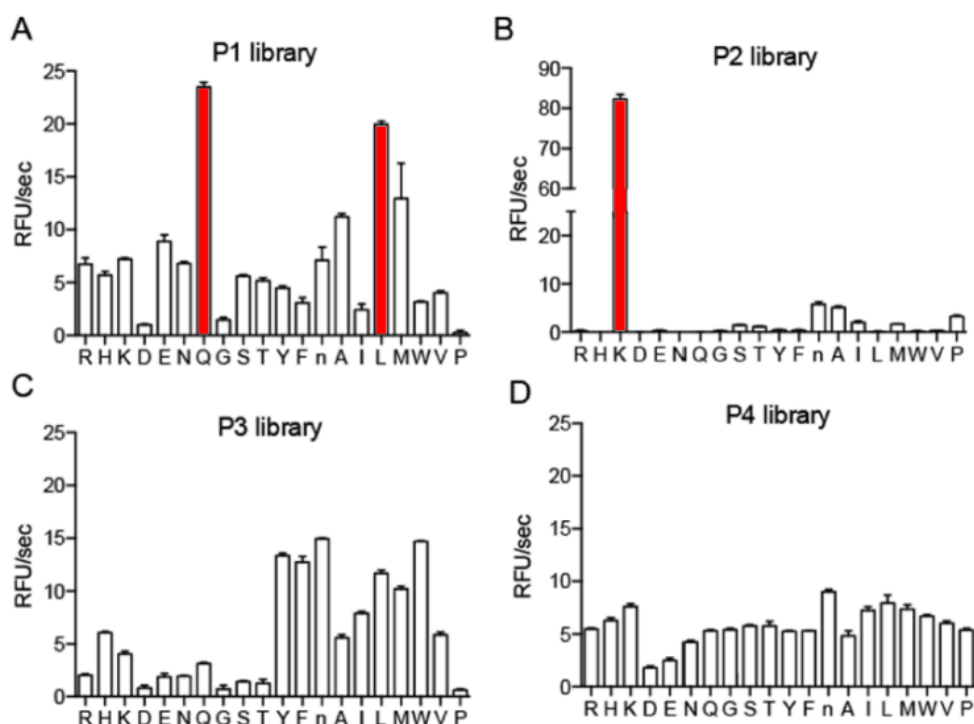


Figure 3.02 Hip1 protease P₁-P₄ substrate specificity as determined by position scanning-synthetic combinatorial libraries. Bars coloured red indicate preferred residues for binding at the defined site.¹¹⁴

The P₂ residue of Hip1 has the most pronounced effect on substrate selectivity, with an almost exclusive preference for Lys (K) at S₂. Other binding sites have a much-reduced effect on substrate specificity. There is no apparent preference for a particular type of side chain at S₁, although Gln (Q) and Leu (L) are slightly favoured at this position. A slight preference for aromatic residues (Tyr, Y; Phe, F; Trp, W) is apparent at S₃, though aliphatic residues (Nle, n; Ile, I; Leu, L; Met, M; Val, V) are still accepted at this position. S₄ is comparatively unselective, but negatively charged Asp (D) and Glu (E) residues are disfavoured. This data is in

good agreement with multiplex substrate profiling by mass spectrometry which was used to determine the cleavage of 228 defined 14-mer peptides by Hip1 in an MS/MS-based readout. Mass spectrometry was also utilised to determine preferences at S_n' binding sites. There appears to be a preference for Gly, Phe, Arg and Ser, at S_1' , while a variety of aliphatic and aromatic residues are accommodated at $S_2'-S_4'$. This combined specificity data is in good agreement with the cleavage profile for Hip1's proteolytic substrate, GroEL2, which is cleaved at two sites in its N-terminal region (AKT-IAYDEEARR-GLERGLN, dashes indicate cleavage sites). The first cleavage site contains the optimal P_2 Lys, while the second cleavage site contains many suboptimal residues at P_4-P_4' , suggesting that cleavage at the first site is faster compared to the second cleavage site. In summary, Lys is an obligatory residue at P_2 for binding substrates and inhibitors, while there is reduced specificity at S_1 , S_3 and S_4 .

3.3 Current Design of Hip1 Substrates and Inhibitors

3.3.1 Hip1 substrate probes

Selective fluorogenic probes of Hip1 were developed in order to visualise Hip1 activity *in vivo*.¹¹⁴ Optimised selective fluorogenic Hip1 substrates **3.00** and **3.01** (Figure 3.03) were developed based on the previously discussed profiling data. These probes have been used to determine whether Hip1 activity can be monitored selectively by fluorescence based assays relative to the background fluorescence of all total extracts derived from macrophage cell lines. Macrophage cell lysates were spiked with a range of concentrations of Hip1 and treated with the substrates. While both probes showed a strong signal-to-noise ratio upon addition of small amounts of Hip1 (as low as 270 pg), **3.01** demonstrated a lower

background signal than **3.00**, showing essentially no activity in macrophages infected with mutant Mtb lacking Hip1, making it an ideal candidate for *in vivo* imaging of Mtb.

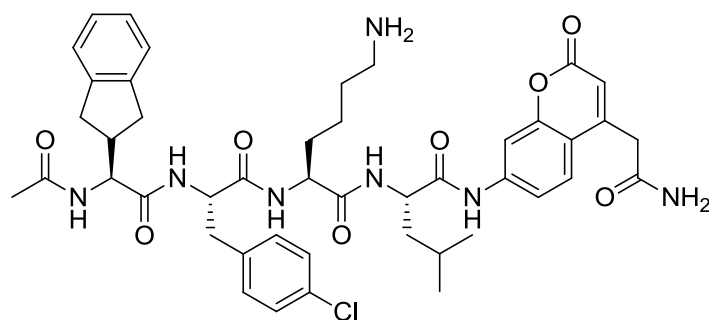
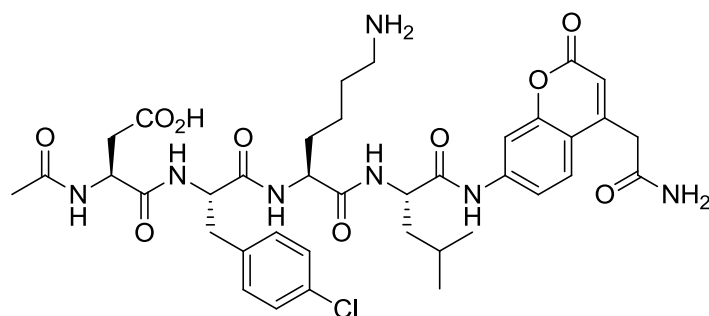
**3.00****3.01**

Figure 3.03 Selective fluorogenic substrates for visualising Hip1 activity *in vivo*.

3.3.2 Hip1 irreversible inhibitors

Irreversible inhibitors have been developed for activity-based relationship studies based on the fluorogenic substrates discussed above. Approximately 500 small molecules containing serine-reactive electrophiles were screened against Hip1 using a fluorogenic substrate readout in order to identify possible potent pharmacophores.¹¹⁴ Of the compounds assayed against Hip1, a series of isocoumarins were identified with nM activity. Optimisation of these isocoumarins lead to the development of a series of potent irreversible inhibitors

(Figure 3.04). Various Fmoc protected residues with different side chain functionalities were substituted at P₂ (R₁). Substitution of the L-Lys side chain with different chain lengths (i.e., hLys, Orn) or substituents (i.e., D-Lys, PhNCS, Leu and Lys(biotin)) reduced the potency of inhibition, indicating that maintaining L-Lys at P₂ is essential for activity. Indeed, the inhibitor featuring Fmoc-L-Lys at P₂ was found to be the most potent of the series, with an IC₅₀ = ~34 nM.

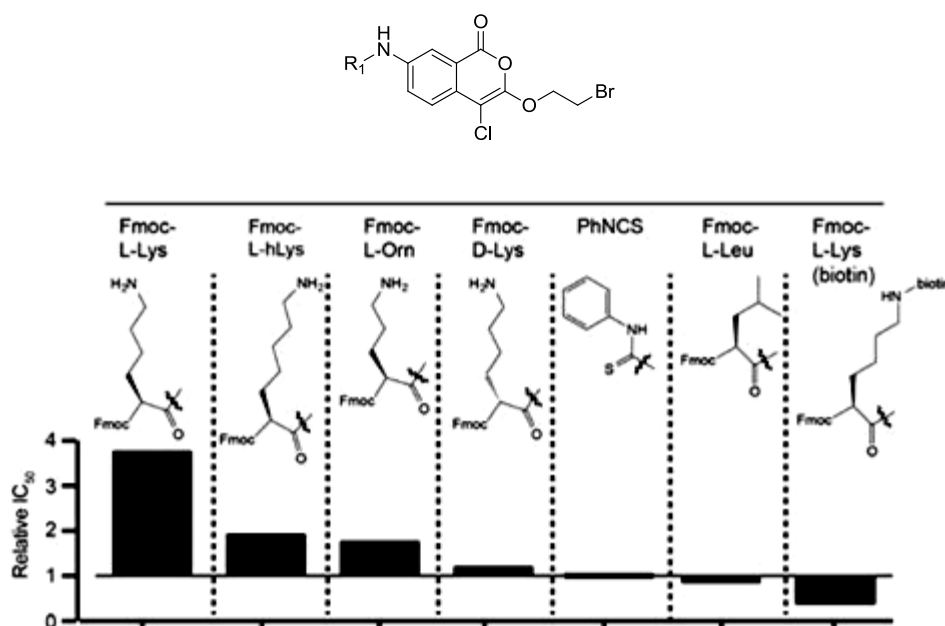


Figure 3.04 Top: structure of the optimised terminal electrophile for irreversible binding to Hip1. Bottom: Comparison of relative IC₅₀ values of inhibitors with various side chains at P₂.

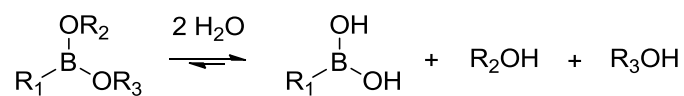
3.4 Synthesis of Reversible Hip1 Protease Inhibitors

The inhibitors discussed above have a number of disadvantages. Firstly, P₁ is entirely occupied by an electrophilic warhead, preventing functionalisation with an amino acid residue (e.g., Glu or Leu). Furthermore, these inhibitors lack P₃ and P₄ functionality which presumably provide important interactions with the active

site. Finally, these inhibitors are irreversible, owing to the nature of the warhead (e.g., isocoumarin irreversible inhibition by lactone ring opening upon nucleophilic attack by Ser₂₂₈). Irreversible inhibitors are generally less favoured as therapeutic agents due to their toxicity and associated side effects.²⁷ Addressing these issues with reversible inhibitors featuring residues at P₁-P₄ is therefore of interest towards the development of potential immunodulatory therapeutics against Mtb.

Work described in this chapter is concerned with the design, synthesis and evaluation of N-terminal protected tripeptides as reversible Hip1 protease inhibitors, as depicted in Figure 3.06. A pinanediol boronate ester was selected as the C-terminal warhead, a common electrophile featured in serine protease inhibitors which acts as a prodrug of the active boronic acid.^{38, 115} Boronic acids are strong Lewis acids whose reactivity is due to a vacant p orbital centred on the boron atom. Under physiological conditions boronate esters are hydrolysed to the corresponding boronic acids (Figure 3.05, (a)).¹¹⁵ The unmasked boronic acid is then able to readily react with serine proteases to form a reversible tetrahedral adduct, with one of the OH groups positioned in the oxyanion hole to stabilise the protease-inhibitor complex (Figure 3.05, (b)).³⁸

(a) Boronate ester hydrolysis under physiological conditions



(b) Reversible inhibition of serine proteases by boronic acids

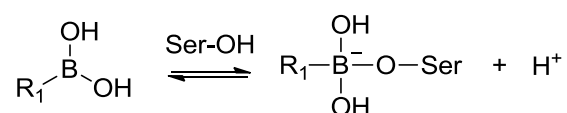


Figure 3.05 Overall mode of reversible inhibition of serine proteases by boronate esters.

Lys was incorporated at P₂ given that the S₂ site displays an almost exclusive preference for this amino acid. Leu was introduced at P₁ as it is somewhat preferred at S₁, as discussed earlier. As demonstrated in Figure 3.02, there appears to be some specificity for aromatic residues at S₃, providing an opportunity to investigate the optimised residue at this position. In this study, Phe and Tyr were investigated at P₃. Finally, given the low specificity at S₄, P₄ residues were substituted with the N-terminal protecting groups Boc (tert-Butyloxycarbonyl), Cbz (Carboxybenzyl) and Fmoc (Fluorenylmethyloxycarbonyl) (Figure 3.06) and the optimum protecting group at this site investigated.

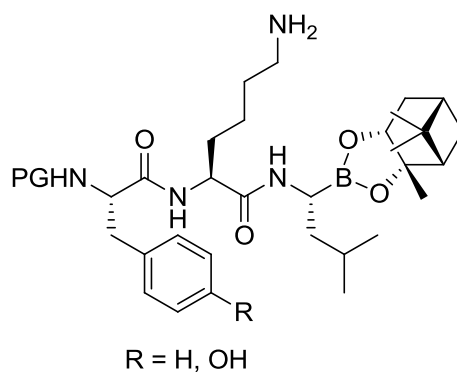


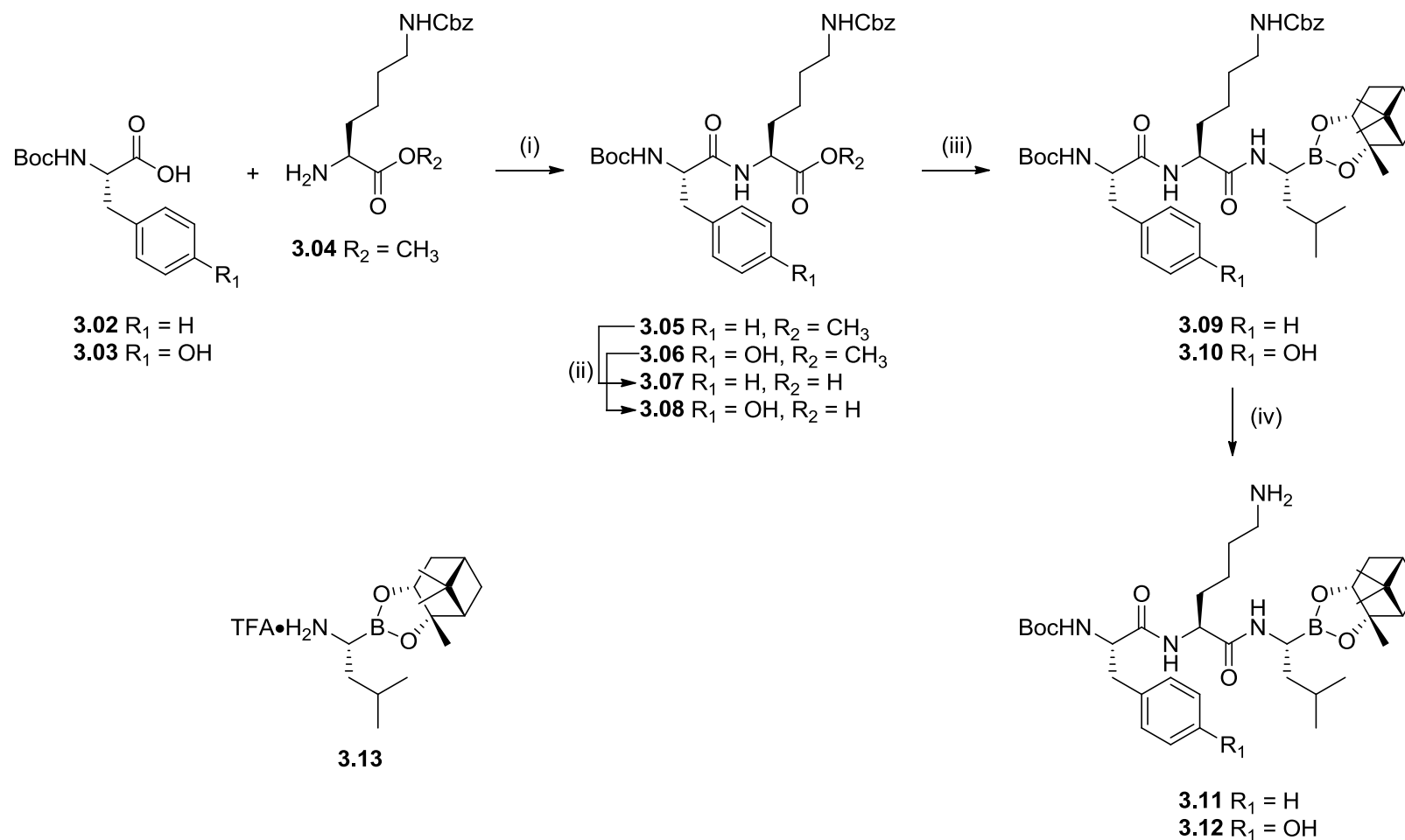
Figure 3.06 General structure of reversible tripeptide Hip1 protease inhibitors (PG = protecting group).

The synthesis of the P₃ Phe and Tyr inhibitors featuring N-terminal Boc protecting groups **3.11** and **3.12**, N-terminal Cbz protecting groups **3.23** and **3.24**, and N-terminal Fmoc protecting groups **3.35** and **3.36**, respectively, proceeded via a similar approach. Inhibitors **3.12** and **3.35** were prepared by the methods described below.^a

3.4.1 Synthesis of N-terminal Boc inhibitors

N-terminal Boc inhibitors **3.11** and **3.12** were prepared over four steps from Boc-L-phenylalanine **3.02** and Boc-L-tyrosine **3.03**. Amidation of **3.02** and **3.03** with L-lysine(Cbz)-methyl ester **3.04** under standard HATU mediated amide coupling conditions gave dipeptide esters **3.05** and **3.06** in excellent yields. Alkaline hydrolysis of these esters with aqueous LiOH afforded carboxylic acids **3.07** and **3.08** respectively, which were subsequently coupled to the commercially available leucine pinanediol boronate ester **3.13** to give tripeptides **3.09** and **3.10** in excellent yields. Deprotection of the Cbz-protected side chains under standard hydrogenation conditions gave the desired inhibitors **3.11** and **3.12** in near quantitative yields (Scheme 3.4.1).

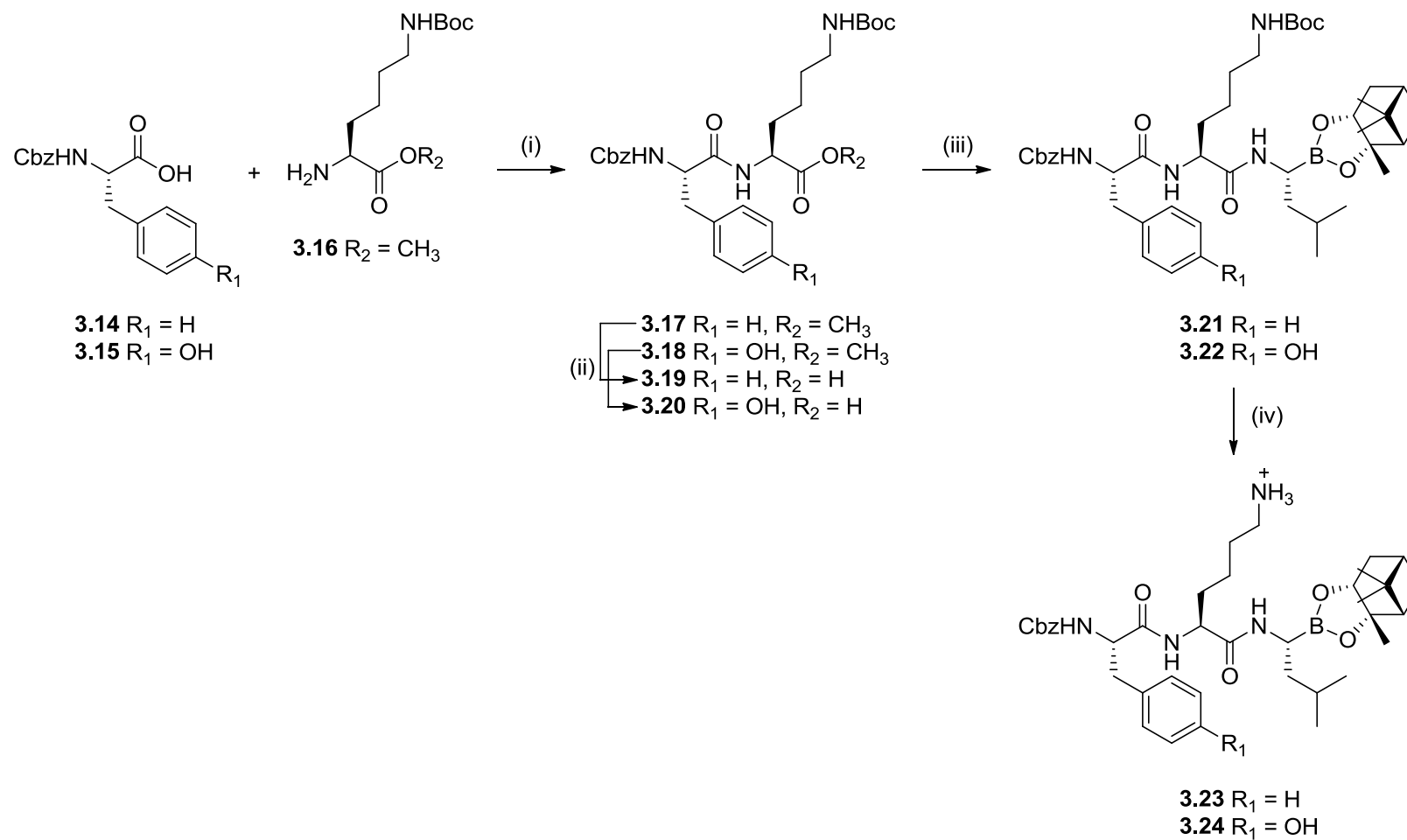
^a**3.12** and **3.35** were prepared by Dr Borja López Pérez at The University of Adelaide.



Scheme 3.4.1 *Reagents and Conditions:* i) HATU, DIPEA, DMF, rt, 18 h (93% $R_1 = \text{H}$, 88% $R_1 = \text{OH}$), ii) LiOH, H_2O , THF, rt, 2 h (100% $R_1 = \text{H}$, 98% $R_1 = \text{OH}$), iii) **3.13**, HATU, DIPEA, DMF, rt, 18 h (92% $R_1 = \text{H}$, 70% $R_1 = \text{OH}$), iv) H_2 , Pd/C, MeOH, EtOAc, rt, 5 h (98% $R_1 = \text{H}$, 100% $R_1 = \text{OH}$).

3.4.2 Synthesis of N-terminal Cbz inhibitors

The synthesis of the N-terminal Cbz inhibitors **3.23** and **3.24** proceeds via a similar sequence to the Boc-protected inhibitors described above. HATU-mediated amidation of Cbz-L-phenylalanine **3.14** and Cbz-L-tyrosine **3.15** with L-lysine(Boc)-methyl ester **3.16** gave the dipeptide methyl esters **3.17** and **3.18** respectively, which were saponified to give carboxylic acids **3.19** and **3.20**. These acids were then coupled to boronate ester **3.13** to give tripeptides **3.21** and **3.22**. Boc-deprotection of **3.21** was achieved using anhydrous HCl to give the HCl salt of amine **3.23** in a quantitative yield. Attempted deprotection of **3.22** under the same conditions, however, failed to furnish the desired product **3.24**. Repeating the reaction using TFA in place of HCl gave rise to rapid Boc-deprotection to give the desired deprotected amine **3.24** in a near quantitative yield (Scheme 3.4.2).



Scheme 3.4.2 *Reagents and Conditions:* i) HATU, DIPEA, DMF, rt, 18 h (95% $R_1 = \text{H}$, 60% $R_1 = \text{OH}$), ii) LiOH, H_2O , THF, rt, 2 h (99% $R_1 = \text{H}$, 98% $R_1 = \text{OH}$), iii) **3.13**, HATU, DIPEA, DMF, rt, 18 h (50% $R_1 = \text{H}$, 67% $R_1 = \text{OH}$), iv) HCl, Et_2O , rt, 18 h (99% $R_1 = \text{H}$); TFA, CH_2Cl_2 , rt, 2 h (95% $R_1 = \text{OH}$).

3.4.3 Synthesis of N-terminal Fmoc inhibitors

Synthesis of Fmoc-protected inhibitors was initially attempted using an analogous approach to that used for the Boc- and Cbz-protected inhibitors, see Scheme 3.4.1 and 3.4.2. However, this approach was found to be unviable for Fmoc inhibitors, with exposure of Fmoc-protected dipeptides **3.25** to alkaline ester hydrolysis conditions resulting in partial or complete cleavage of the base-labile Fmoc-protecting group, affording dideprotected dipeptides **3.26**. A number of conditions were trialled for hydrolysis of **3.25** in order to minimise or prevent Fmoc cleavage, including low molar equivalence of hydroxide or reactions at 0 °C and -25 °C. In all instances, ester hydrolysis was incomplete and partial cleavage of the Fmoc group still occurred (Figure 3.07).

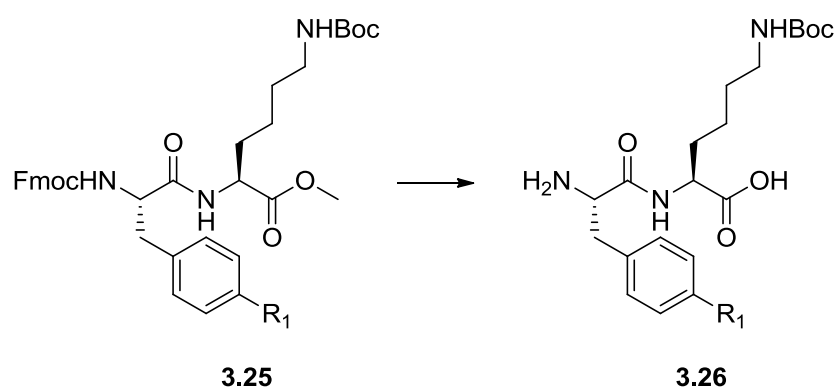


Figure 3.07 Resulting dideprotected dipeptides under ester hydrolysis conditions.

It was envisaged that this issue could be circumvented by reversing the order of the synthesis, i.e. initially coupling boronate ester **3.13** to Boc-L-lysine(Cbz)-OH **3.27** to afford dipeptide **3.29**, which upon Boc-deprotection would afford a common dipeptide intermediate **3.31** (Scheme 3.4.3). Coupling of this intermediate to Fmoc-L-phenylalanine or Fmoc-L-tyrosine would then afford the

Fmoc-protected tripeptides. Formation of the desired inhibitors would then be achieved by Cbz-deprotection at the lysine side chain under hydrogenation conditions. This route was applicable for the synthesis of phenylalanine inhibitor **3.35** (Scheme 3.4.3), but failed to give the desired tyrosine inhibitor due to both cleavage of the Cbz- and Fmoc-protecting groups of tripeptide **3.37** in the final hydrogenation reaction to give the undesired dideprotected tripeptide **3.38** (Figure 3.08).

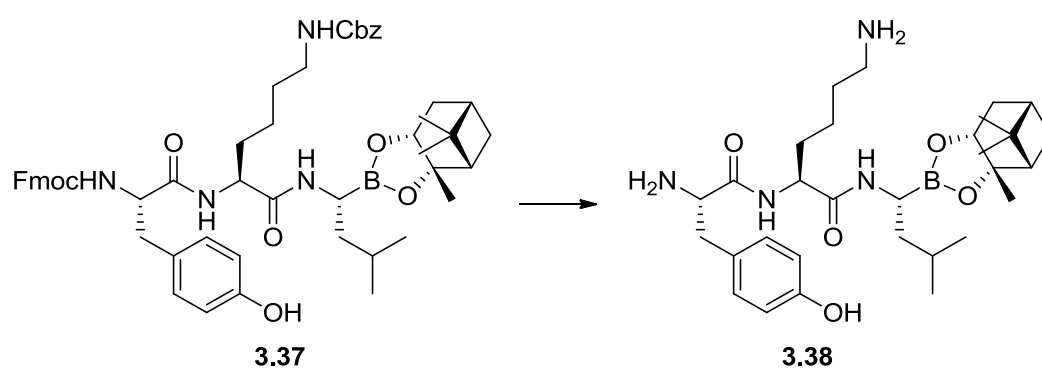
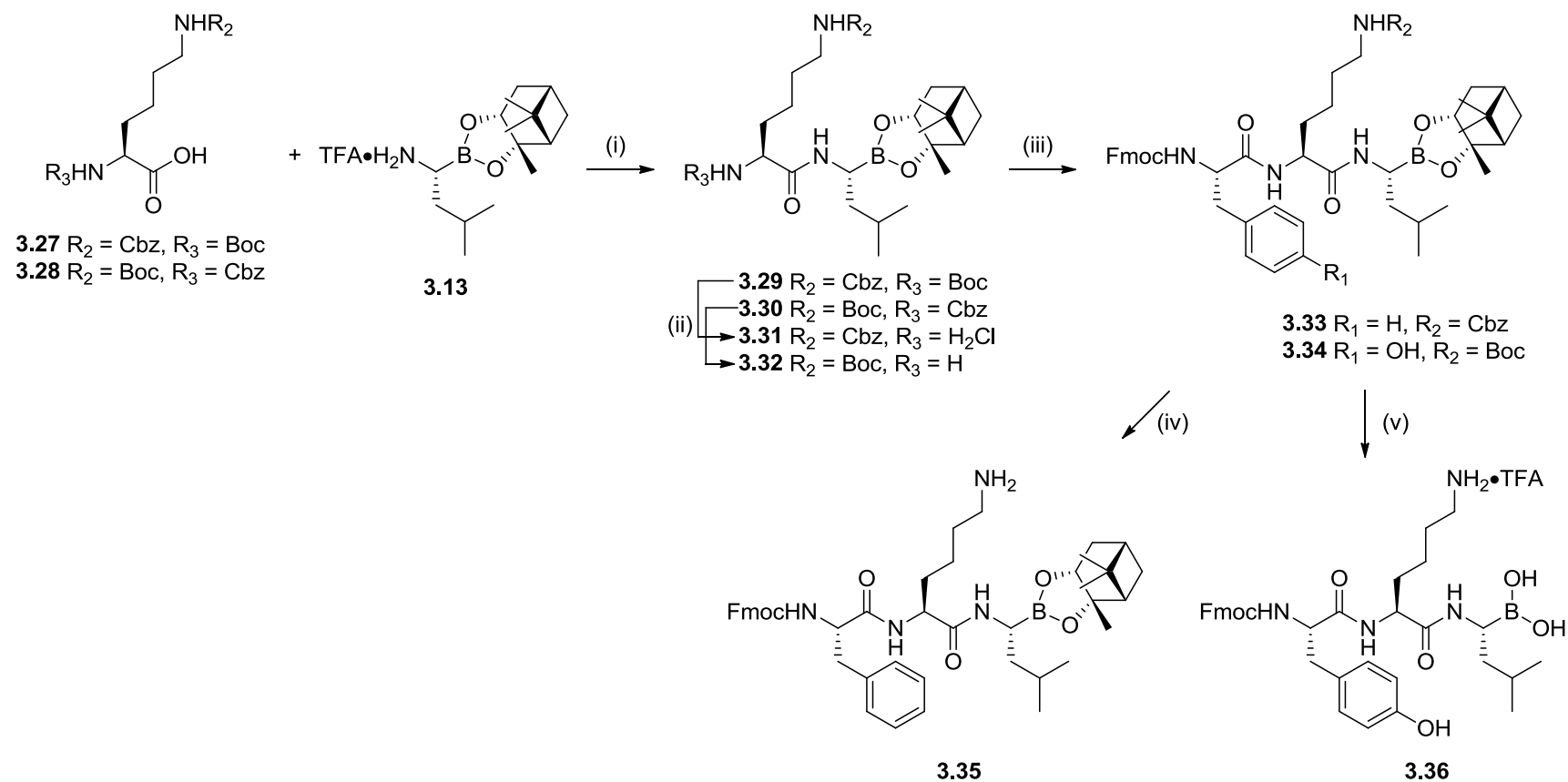


Figure 3.08 Cleavage of **3.37** Cbz- and Fmoc-protecting groups under hydrogenation conditions (H_2 , Pd/C, rt, 18 h).

It was thought that substituting the Cbz protecting group at the lysine side chain with the acid-labile Boc group would avoid cleavage of Fmoc as it is stable under the acidic conditions required for Boc-deprotection. Synthesis of Boc-protected tripeptide **3.34** was performed over three steps from Cbz-L-Lysine(Boc)-OH **3.28**, which was Boc-deprotected with anhydrous HCl. Surprisingly, cleavage of the boronic ester of **3.34** to the boronic acid **3.36** was also observed under acidic conditions, despite Cbz-protected inhibitors **3.23** and **3.24** being stable under such condition



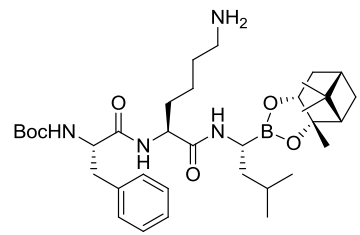
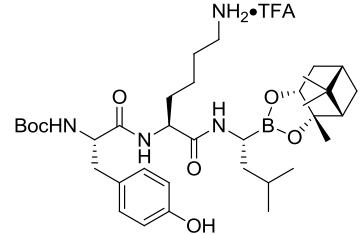
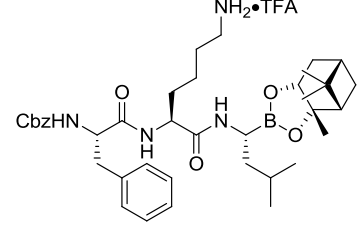
Scheme 3.4.3 *Reagents and Conditions:* i) HATU, DIPEA, DMF, rt, 4 h (92% $R_2 = \text{Cbz}$, $R_3 = \text{Boc}$; 92% $R_2 = \text{Boc}$, $R_3 = \text{Cbz}$), ii) HCl, 1,4-dioxane, rt, 18 h (100% $R_2 = \text{Cbz}$, $R_3 = \text{Boc}$); H_2 , Pd/C, MeOH, EtOAc, rt, 3 h (100% $R_2 = \text{Boc}$, $R_3 = \text{Cbz}$), iii) Fmoc-Phe-OH, HATU, DIPEA, DMF, rt, 4 h (51% $R_2 = \text{Cbz}$, $R_3 = \text{H}_2\text{Cl}$); Fmoc-Tyr-OH, HATU, DIPEA, DMF, rt, 4 h (58% $R_2 = \text{Boc}$, $R_3 = \text{H}$), iv) H_2 , Pd/C, MeOH, rt, 18 h (99%, $R_1 = \text{H}$, $R_2 = \text{Cbz}$), v) HCl, THF, 1,4-dioxane, rt, 18 h (47% $R_1 = \text{OH}$, $R_2 = \text{Boc}$).

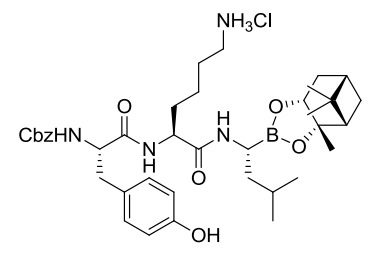
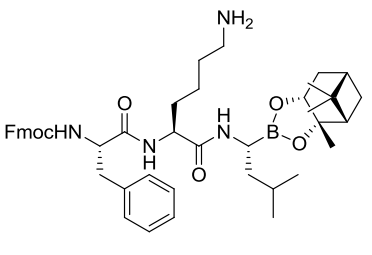
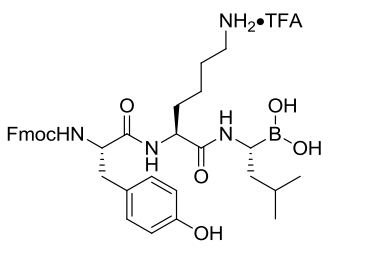
3.5 Tripeptide Boronate Ester Inhibition Assay

Inhibition of Hip1 by the tripeptide inhibitors **3.11**, **3.12**, **3.23**, **3.24**, **3.35** and **3.36** was determined by a fluorometric assay using a microplate reader by our collaborator Nathan Goldfarb.^b All inhibitors were tested for their ability to inhibit Hip1-dependent hydrolysis of the substrate, Dabcyl-Glu-Ala-Arg-Arg-Gly-Leu-Glu(EDANS)-Arg-OH, a novel FRET-based substrate (EDANS is a naphthalenesulfonic acid fluorophore moiety and Dabcyl is an azobenzoic acid quenching group) based on a previously discussed natural cleavage site at the N-terminus of GroEL2. Inhibitors **3.11**, **3.12**, **3.24** and **3.35** were screened against Hip1 at two different concentrations, 1000 and 500 nM, while **3.23** and **3.36** were tested at three additional concentrations of 100, 10 and 1 nM given that they exhibited complete inhibition of Hip1 at 500 nM. Approximately 75 nM purified Hip1 was preincubated with each concentration of inhibitor for 50 min at 25 °C and pH = 8.5 in Tris buffer. A control reaction containing 2% DMSO instead of inhibitor was included for each inhibitor tested. Reactions were initiated by the addition of substrate. Percent inhibition values were calculated by: $100 - [\text{initial rate of inhibited reaction} / \text{initial rate of control reaction} * 100]$ and the results from the screening are given in Table 3.5.1.

^bProteolytic assays performed at the California Health Sciences University.

Table 3.5.1 % inhibition of Hip1 by tripeptide inhibitors and associated K_i values as determined by fluorometric assays.

Compound	Structure	% inhibition of Hip1 proteolytic activity					K_i (nM)
		1000 nM	500nM	100 nM	10 nM	1 nM	
3.24		45	53	- ^c	-	-	-
3.35		100	67	-	-	-	-
3.36		100	100	86	90	39±15	16

Compound	Structure	% inhibition of Hip1 proteolytic activity					K _i (nM)
		1000 nM	500nM	100 nM	10 nM	1 nM	
3.24		45	27	-	-	-	-
3.35		68	-	-	-	-	-
3.36		100	100	79	96	70±15	7

^cNo data available.

No clear preference is apparent for the P₃ and P₄ residues investigated, as demonstrated by the lack of a trend in potencies between inhibitors. However, inhibitor **3.23** was particularly potent, inhibiting Hip1 by 39% at a 1 nM concentration which was determined to be an inhibition constant, K_i = 16 nM (Appendix 1). This is an improvement on the most potent inhibitor of Hip1 reported thus far: the Fmoc-Lys reversible inhibitor depicted in Figure 3.04 which is significantly less active with an IC₅₀ of ~34 nM. There appears to be a preference for Phe at P₃ and Cbz as an N-terminal protecting group (P₄ group) given that **3.23** is significantly more potent than the other boronate esters assayed. Interestingly, boronic acid **3.36** has comparable activity (K_i = 7 nM, Appendix 1) to **3.23** despite featuring a presumably less favoured Tyr at P₃ and Fmoc N-terminal protecting group. This unprecedented activity is likely as a result of **3.36** not needing to be hydrolysed in order to act as a reversible inhibitor. As described earlier, a boronate ester acts as a masking group which is hydrolysed to the active boronic acid and then interacts with the active site nucleophile (Ser₂₂₈ for Hip1). While boronate esters are typically labile under aqueous conditions in a mild pH range, pinanediol boronate esters have been reported to be highly robust towards hydrolysis, even under extreme pH conditions.¹¹⁶ As a consequence, the enhanced activity of the boronic acid **3.36** is likely as a result of it not requiring hydrolysis prior to reaction with the active site nucleophile, while boronate esters **3.11**, **3.12**, **3.24** and **3.35**, and to a lesser degree, **3.23**, are likely weaker inhibitors due to possessing hydrolytically stable pinanediol protecting groups.

3.6 Investigation of other Terminal Electrophiles for the Optimised Sequence

As discussed, C-terminal pinanediol boronate esters appear somewhat hydrolytically stable and are therefore not ideal masked warheads for achieving reversible inhibition of Hip1. Nevertheless, **3.23** is an exceptional inhibitor which indicates that Phe and Cbz are optimal P₃ and P₄ substituents. To further improve upon this potency, other C-terminal electrophiles which are common to serine protease inhibitors and which do not require activation (e.g., hydrolysis) to inhibit Hip1 were investigated for the optimised sequence, namely α -keto heterocycle, aldehyde and α -keto ester warheads (Figure 3.09).

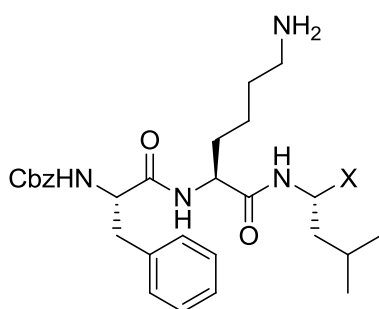


Figure 3.09 Sequence of the optimised tripeptide Hip1 protease inhibitor derived from **3.23**. X indicates the reactive terminal electrophile to be investigated.

3.6.1 Synthesis of α -keto heterocycle inhibitor

A key premise of designing reversible serine protease inhibitors is the inclusion of a suitably electrophilic C-terminal warhead. The ketone of α -keto heterocycles is activated for reaction with serine due to the electron-withdrawing properties of the adjacent heterocycle. This group has been used to generate potent α -keto heterocyclic inhibitors of other serine proteases such as Human neutrophil elastase,¹¹⁷ thrombin,¹¹⁸ and trypsin.¹¹⁹ In most instances, an sp^2 donor nitrogen

in the heterocycle provides key interactions with the active site. Additionally, ring oxygen and sulfur atoms have been shown to be beneficial for improving binding affinity.³⁶ α -keto benzothiazole was therefore selected as the C-terminal electrophile as it features both ring nitrogen and sulfur atoms, i.e., **3.44**.

A retrosynthetic analysis of the target α -keto heterocycle **3.44** gives rise to two independent fragments **3.19** and **3.41**, which upon amidation, oxidation, and Boc-deprotection would afford the target inhibitor (Figure 3.10). Formation of the benzothiazole fragment **3.41** proceeds via a Weinreb ketone synthesis to form α -keto heterocycle **3.39**, reduction to the secondary alcohol **3.40**, and finally Boc-deprotection to give the TFA salt of amine **3.41**. Synthesis of dipeptide **3.19** is depicted in Scheme 3.4.2.

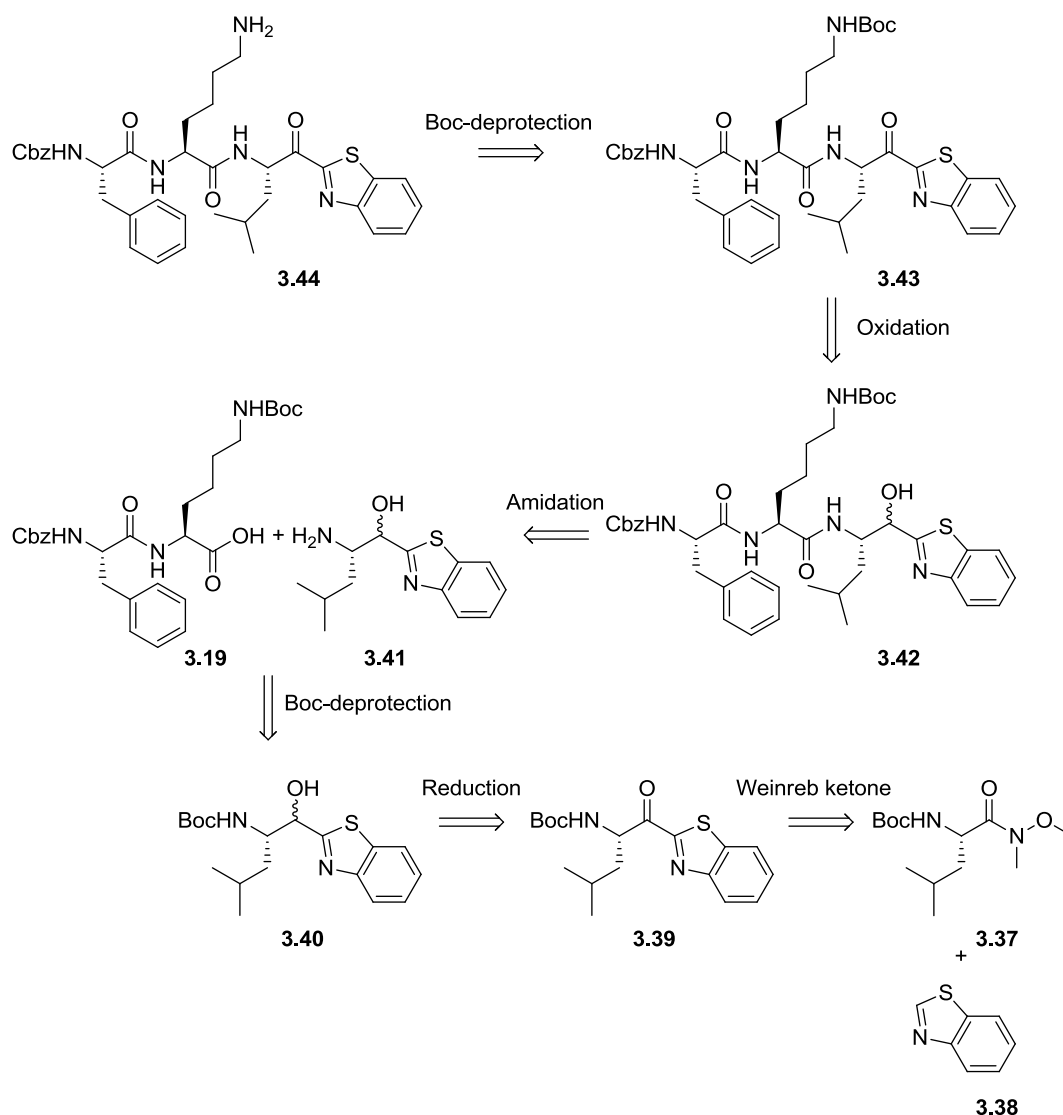
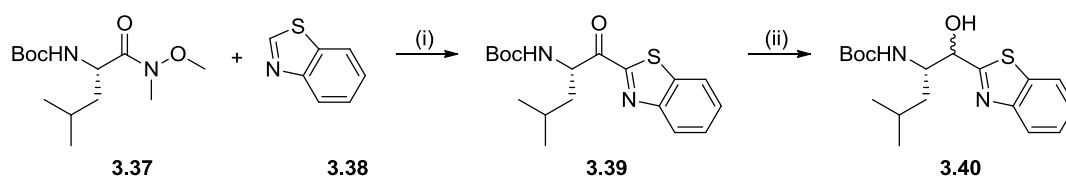


Figure 3.10 Retrosynthetic analysis of α -keto heterocycle **3.44**.

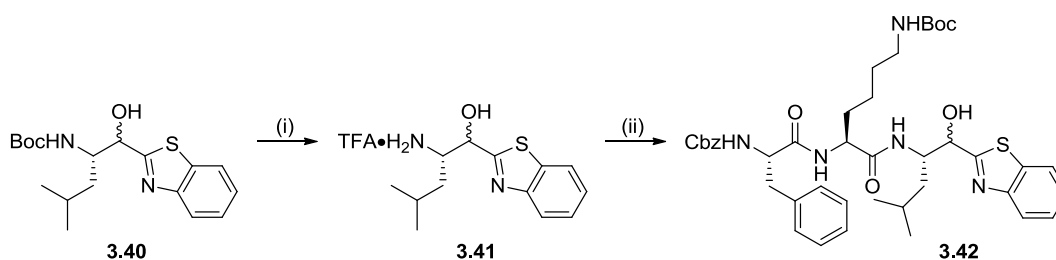
Synthesis of benzothiazole fragment **3.41** began with a Weinreb ketone synthesis between commercially available Weinreb amide Boc-L-Leucine *N,O*-dimethylhydroxamide **3.37** and benzothiazole **3.38**. Weinreb ketone synthesis is a highly versatile method for the formation of ketones.¹²⁰ The reaction proceeds via addition of an organometallic species to the Weinreb amide, which upon quenching at low temperatures by addition of aqueous acid, forms the desired ketone. Unlike many other organometallic addition reactions, Weinreb amides

avoid formation of over-addition products due to an assumed metal-chelate intermediate.¹²¹ Low temperature addition of Weinreb amide **3.37** to lithiated benzothiazole **3.38** afforded α -keto heterocycle **3.39**. Despite having the desired oxidation state, **3.39** was reduced with sodium borohydride to the secondary alcohol **3.40** as a 3:1 mixture of diastereomers, as determined by ^1H NMR (Scheme 3.6.1). This then deactivates the amino acid α -carbon and prevents epimerisation in the amidation step which is performed under alkaline conditions (Scheme 3.6.2). Related C-terminal 2-ketothiazoles have been demonstrated to readily undergo α -epimerisation under enzymatic assay conditions of pH 7.4, but were found to be stereochemically stable at pH 3-4.¹²²



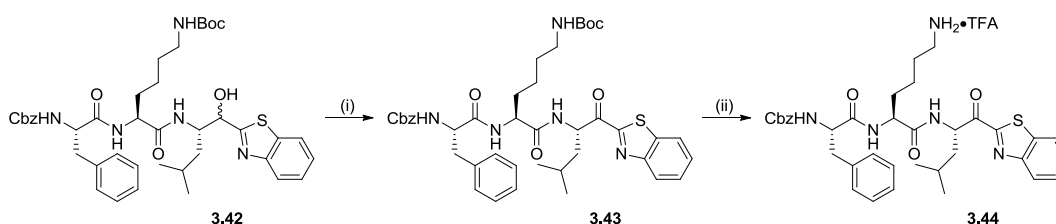
Scheme 3.6.1 Reagents and Conditions: i) *n*-BuLi, THF, $-78\text{ }^\circ\text{C}$, 1.75 h, then sat. aq. NH_4Cl , $-78\text{ }^\circ\text{C}$, ii) NaBH_4 , MeOH, CH_2Cl_2 , $-25\text{ }^\circ\text{C}$, 0.5 h (44% over 2 steps).

Alcohol **3.40** was then Boc-protected on treatment with TFA to give the amine **3.41** in quantitative yields, which was coupled to the previously prepared dipeptide carboxylic acid **3.19** to give tripeptides **3.42** in a good yield as a 3:1 mixture of diastereomers based on ^1H NMR. (Scheme 3.6.2).



Scheme 3.6.2 *Reagents and Conditions:* i) TFA, CH₂Cl₂, rt, 2 h (100%), ii) **3.19**, HATU, DIPEA, DMF, rt, 18 h (71%).

Oxidation of alcohol **3.42** to α -keto heterocycle **3.43** was achieved with DMP and the crude product was Boc-protected on treatment with TFA to afford the target α -keto heterocycle **3.44** in a respectable yield following purification by rp-HPLC (Scheme 3.6.3).



Scheme 3.6.3 *Reagents and Conditions:* i) DMP, CH₂Cl₂, rt, 2 h, ii) TFA, CH₂Cl₂, rt, 1.5 h (46% over 2 steps).

3.6.2 Synthesis of aldehyde inhibitor

Given the potency of the aldehyde inhibitors of α -Chymotrypsin discussed in chapter two (particularly pyrrole **2.30**), it was proposed that incorporation of a C-terminal aldehyde into the optimised sequence would give rise to a potent inhibitor of Hip1. The target aldehyde **3.48** would be prepared by oxidation of tripeptide alcohol **3.46** followed by Boc-deprotection of aldehyde **3.47** (Figure 3.11).

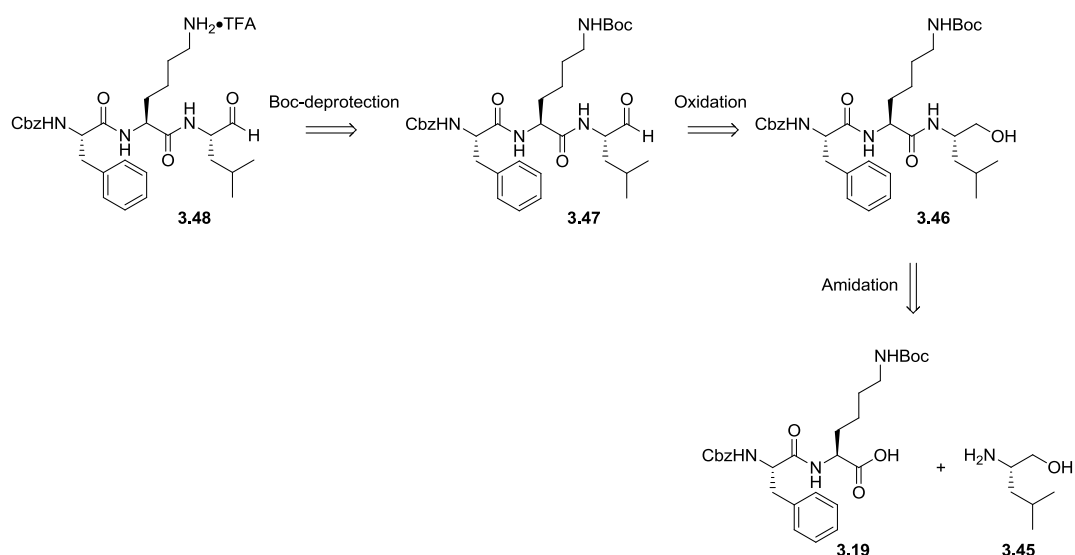


Figure 3.11 Retrosynthetic analysis of aldehyde **3.48**.

L-Leucinol **3.45** was coupled to dipeptide **3.19** to give alcohol **3.46** in a moderate yield and this was subsequently oxidised with DMP to afford aldehyde **3.47**. Boc-deprotection of **3.47** was initially trialled using anhydrous HCl. NMR analysis of the reaction mixture after 1.5 h reaction surprisingly revealed that aldehyde **3.47** had degraded. This suggested that the intermediate aldehyde is sensitive to acidic conditions and subsequent Boc-deprotection was attempted using tetra-*n*-butylammonium fluoride (TBAF). Refluxing of *N*-Boc protected amines in solutions of TBAF in THF has been demonstrated to selectively cleave Boc groups in the presence of acid and base sensitive functionalities.¹²³ Reaction of aldehyde **3.47** under these conditions, however, also resulted in degradation. Although **3.47** appears to be unstable towards various reaction conditions, Boc-deprotection was attempted with TFA as this condition was successful for cleaving the Boc group in α -keto heterocycle **3.43**. ¹H NMR (CD₃OD) of the product obtained after purification by rp-HPLC reveals that Boc-deprotection had proceeded cleanly, as demonstrated by the loss of the tertiary butyl signal at 1.43 ppm (Figure 3.12).

Surprisingly an expected signal for the formyl hydrogen of **3.47** (approximately 9.50 ppm) was absent and there was an added 1 H doublet at 4.18 ppm. Further investigation of the doublet by the 2-dimensional NMR experiment ^1H - ^1H COSY (spin-spin coupling correlations) revealed coupling between the signal and the α -hydrogen on the leucine residue, $J = 4.6$ Hz, suggesting vicinal coupling. The ^{13}C NMR spectrum of the **3.44** was also unexpected, with the appearance of a peak at 109 ppm, a diagnostic shift of a carbon directly attached to two heteroatoms (Figure 3.13). ^1H - ^{13}C HSQC (correlations of hydrogen nuclei directly attached to carbon nuclei) revealed a correlation between this signal and the doublet at 4.18 ppm in the ^1H spectra. In addition to this doublet, two diastereotopic singlets integrating for 3 H each at 3.39 ppm were present in the ^1H spectra, with ^1H - ^{13}C HSQC correlations to two peaks at 56 and 57 ppm in the ^{13}C spectra. From this analysis, methyl acetal **3.49** was proposed as the product (Scheme 3.6.4). The acetal likely formed during the workup when the crude product was washed with MeOH to remove residual TFA. ^1H NMR (CDCl_3) of the crude product from the reaction where the product was not washed with MeOH revealed retention of the aldehyde, supporting this proposed pathway for acetal formation. Although this demonstrates that acetal formation can be avoided by not washing the product with MeOH, it is was not possible to exclude the use of MeOH completely, as purification by rp-HPLC required dissolving the crude material in MeOH due to limited solubility in other solvents. The structure of acetal **3.49** is also supported by high resolution mass spectrometry (HRMS), with the base peak corresponding to $m/z = 571$, equivalent to $[\text{M}+\text{H}]^+$ for the proposed methyl acetal. Additionally,

peaks corresponding to $[M+H]^+$ for the corresponding hemiacetal ($m/z = 557$) and free aldehyde ($m/z = 525$) are also present.

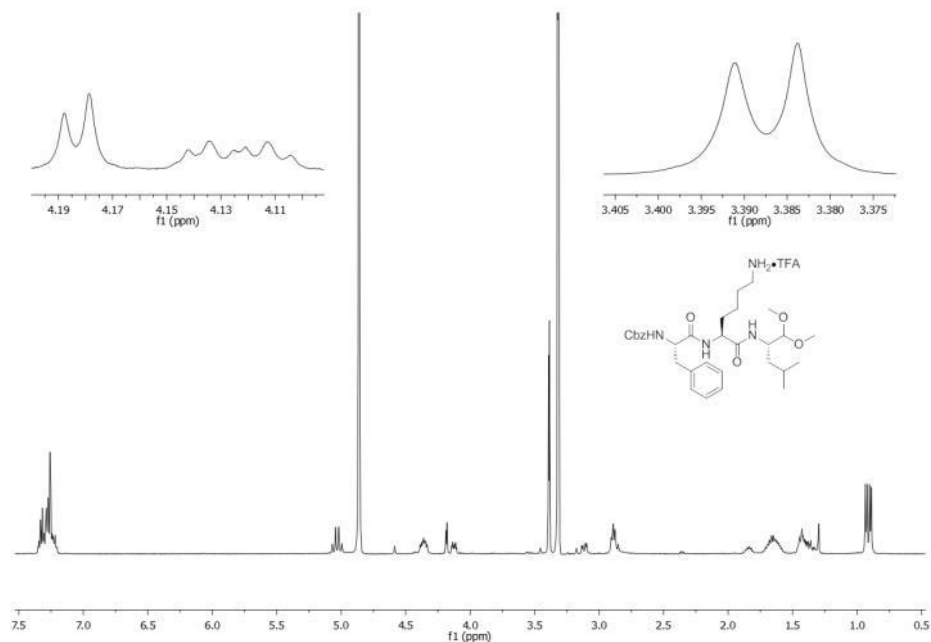


Figure 3.12 ^1H NMR (CD_3OD) of acetal **3.49**.

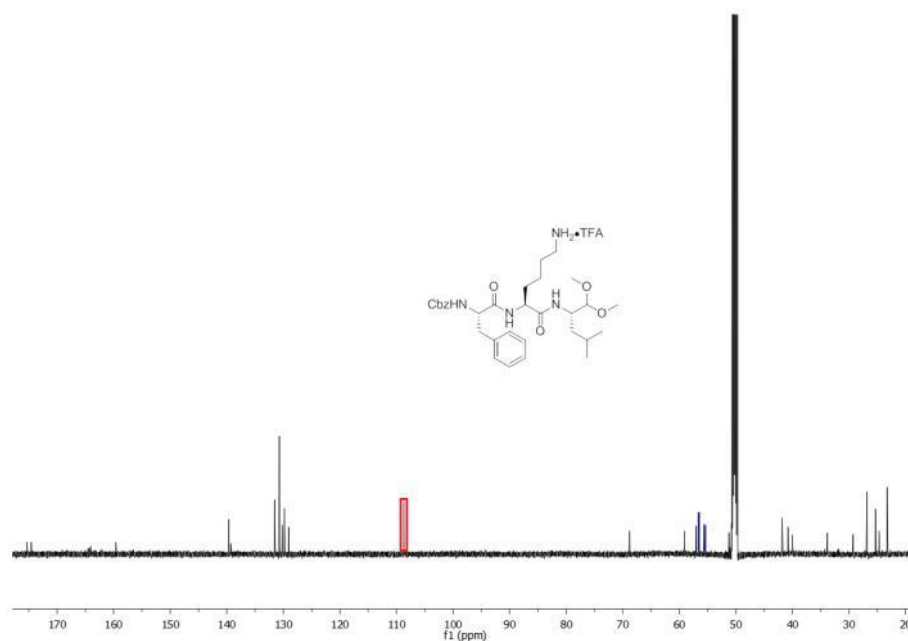
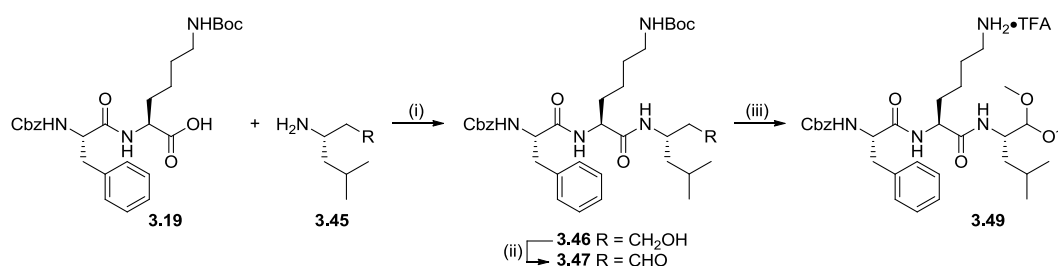


Figure 3.13 ^{13}C NMR (CD_3OD) of acetal **3.49**. The signal highlighted in red (109 ppm) corresponds to the acetal carbon, while those highlighted in blue (56 and 57 ppm) correspond to the two diastereotopic acetal methoxy groups.



Scheme 3.6.4 *Reagents and Conditions:* i) HATU, DIPEA, DMF, rt, 18 h (60%), ii) DMP, CH₂Cl₂, rt, 2 h, iii) TFA, CH₂Cl₂, rt, 1.5 h, then MeOH, TFA (29% over 2 steps).

3.6.3 Synthesis of the α -keto ester inhibitor

The final C-terminal electrophile investigated was an α -keto ester. Examples of peptidomimetic protease inhibitors featuring P₁ α -keto esters have been demonstrated to provide potent reversible inhibition of other serine proteases.¹²⁴

A study on Chymotrypsin selective inhibitors for which different C-terminal carbonyl electrophiles, including aldehydes, α -fluorinated ketones and α -diketones, demonstrated that inhibitors featuring C-terminal α -keto esters afforded the greatest amount of inhibition in proteolytic assays.⁴¹ In addition to increasing the electrophilicity of the reactive ketone, the adjacent ester is proposed to form a hydrogen bond with active site residues, stabilising the inhibitor-protease complex, resulting in the inhibitor having improved binding efficacy (Figure 3.14).¹²⁵ In the case of designing a reversible Hip1 inhibitor, the simple α -keto methyl ester **3.57** was prepared for assay against Hip1.

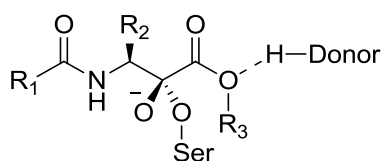


Figure 3.14 Proposed stabilised transition-state complex formed between serine proteases and α -keto ester inhibitors.

Retrosynthetic analysis of α -keto ester **3.57** identified the modified P₁ residue **3.54** which is prepared from commercially available L-leucinol **3.45**. Boc-protection of **3.45** will afford Boc-L-leucinol **3.50** which can be oxidised to the corresponding aldehyde **3.51**, and then converted to cyanohydrin **3.52**. Treatment with aqueous HCl will give α -hydroxy acid **3.53** which on esterification will afford the corresponding α -hydroxy methyl ester **3.54** (Figure 3.15).

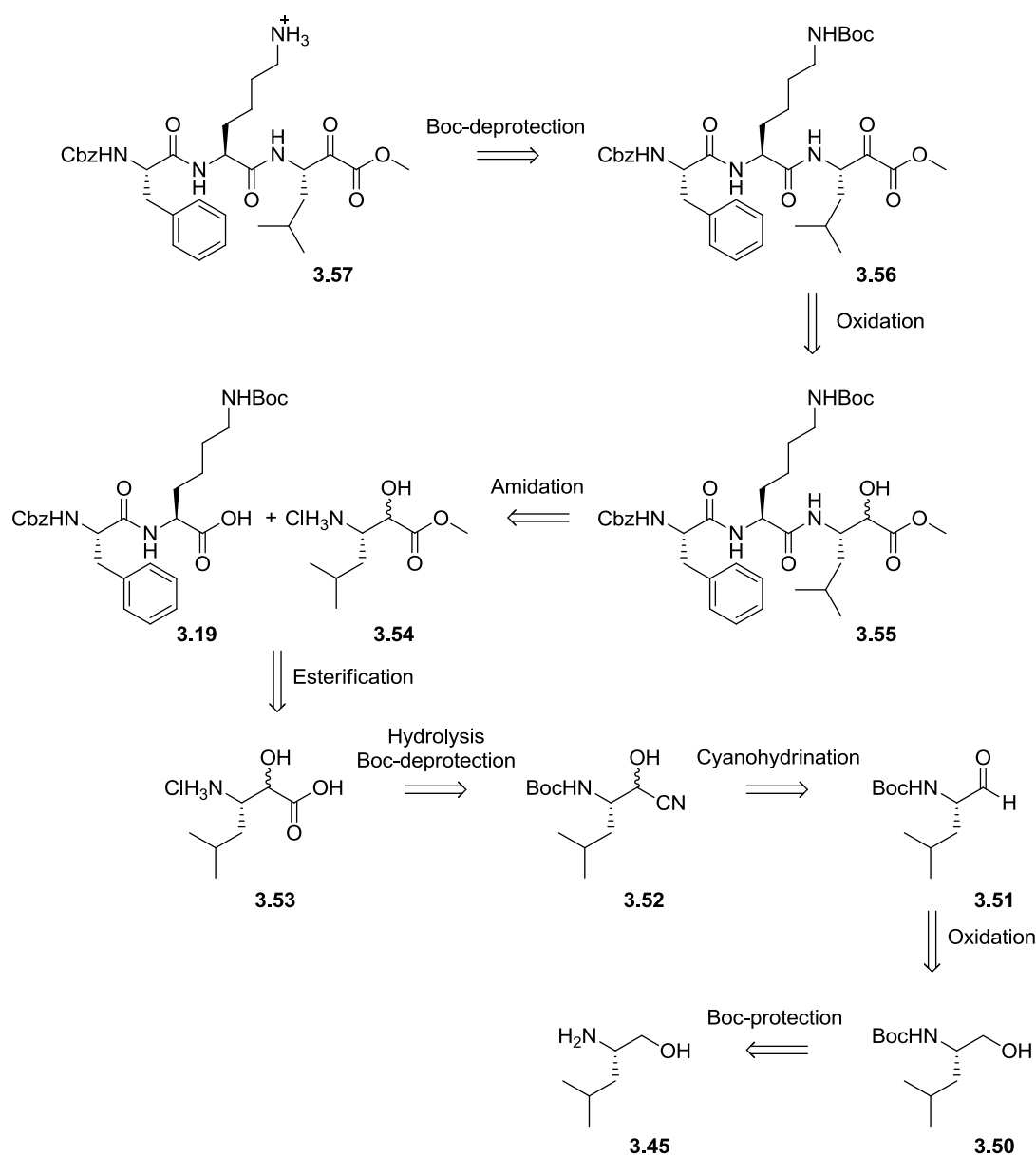
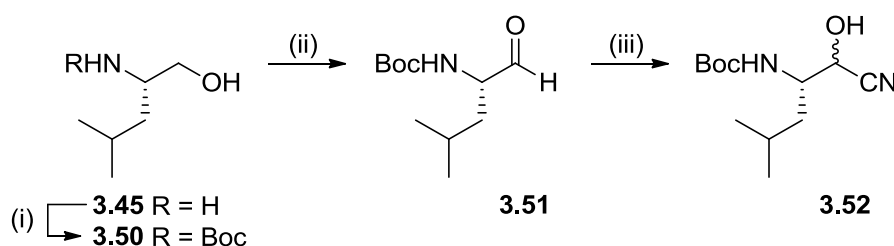


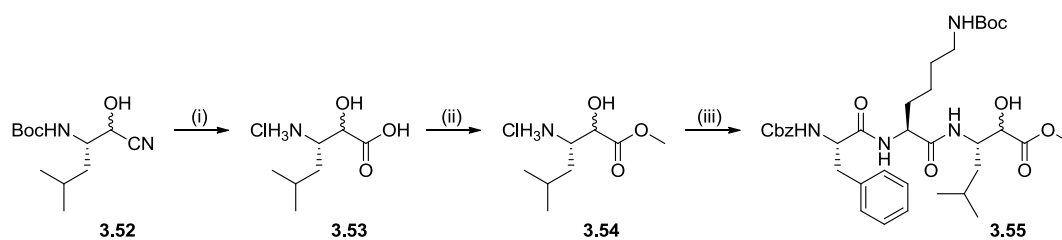
Figure 3.15 Retrosynthetic analysis of α -keto ester **3.57**.

Boc-protection of L-leucinol **3.45** was achieved using Boc anhydride¹²⁶ and the resulting Boc leucinol **3.50** was then oxidised to the corresponding aldehyde **3.51** under Parikh-Doering conditions.¹²⁷ Conversion of aldehyde **3.51** to cyanohydrins **3.52** as a 1:1 mixture of diastereomers, as determined by ¹H NMR, was achieved with acetone cyanohydrin under alkaline conditions in MeOH in an overall yield of 78% over the 3 steps (Scheme 3.6.5).



Scheme 3.6.5 Reagents and Conditions: i) Boc₂O, CH₂Cl₂, rt, 18 h, ii) sulfur trioxide pyridine complex, DMSO, TEA, 10 °C, 1 h, iii) acetone cyanohydrin, K₂CO₃, MeOH, rt, 1 h (78% over 3 steps).

Subsequent acidic hydrolysis of **3.52** with aqueous HCl gave the Boc-protected α-hydroxy acids **3.53**, again as a 1:1 mixture of diastereomers. Esterification to α-hydroxy methyl esters **3.54** was achieved with thionyl chloride in MeOH. Coupling of these esters to the core dipeptide unit **3.19** in the presence of HATU gave the tripeptides **3.55** in an overall yield of 63% over 3 steps and in an isomeric ratio of 1:1 (Scheme 3.6.6).



Scheme 3.6.6 *Reagents and Conditions:* i) HCl, H₂O, 1,4-dioxane, reflux, 18 h, ii) SOCl₂, MeOH, -10 °C → rt, 2.5 h, iii) **3.19**, HATU, DIPEA, DMF, rt, 18 h (63% over 3 steps).

Oxidation of alcohols **3.55** was achieved with DMP. The resulting α -keto ester **3.56** was Boc-protected using TFA. Similar to acetal **3.49**, addition of MeOH to the ketone of **3.56** appeared to have occurred based upon the ¹³C NMR spectrum (CD₃OD) which revealed loss of the ketone signal at 195 ppm and the appearance of a diagnostic peak corresponding to an addition product at 102 ppm (Figure 3.17). Interestingly however, the ¹H spectrum suggested hemiacetal formation (Scheme 3.6.7), as indicated by the presence of only one singlet at 3.87 ppm which would otherwise be expected to be present as two signals for an acetal which has diastereotopic methoxy groups. (Figure 3.16). Splitting of signals in the ¹³C spectrum and overlapping signals in the ¹H spectrum support assignment of the hemiacetal as two diastereomers on addition of MeOH at the ketone. Interestingly, the methyl peak of the hemiacetal integrates for 0.6 H rather than the expected 3.0 H. This is likely due to exchange between the methoxy group of the undeuterated hemiacetal isolated following purification with the NMR solvent, i.e., CD₃OD, giving rise to the reduced integration observed.

The ^1H spectrum in CDCl_3 lacked the methyl resonance observed at 3.87 ppm in the CD_3OD spectrum (Figure 3.16), while the ^{13}C spectra in CDCl_3 reveals the expected ketone signal at 195 ppm and lacks the signal at 102 ppm due to the hemiacetal resonance observed in the CD_3OD spectra (Figure 3.17). These cumulative findings suggest that the hemiacetal formed from MeOH is stable in methanolic solutions, but is readily converted back to the α -keto ester by solvent exchange with an aprotic solvent.

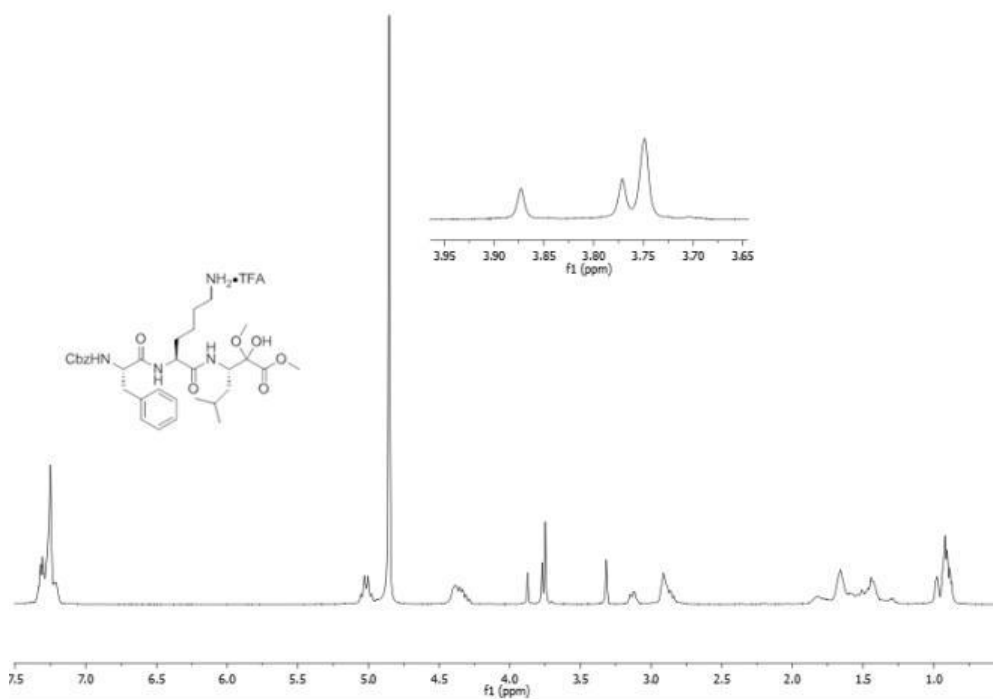


Figure 3.16 ^1H NMR (CD_3OD) of hemiacetal 3.58. The singlet at 3.87 ppm arises from the hemiacetal methoxy group, and the two singlets at 3.75 ppm correspond to the methyl esters of both diastereomers.

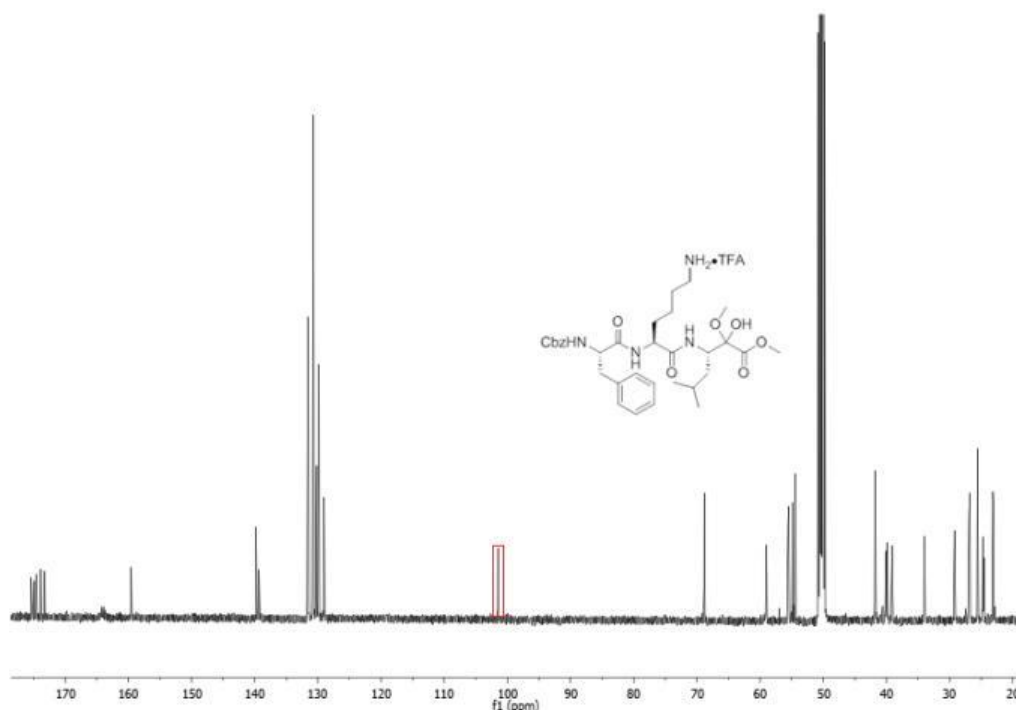
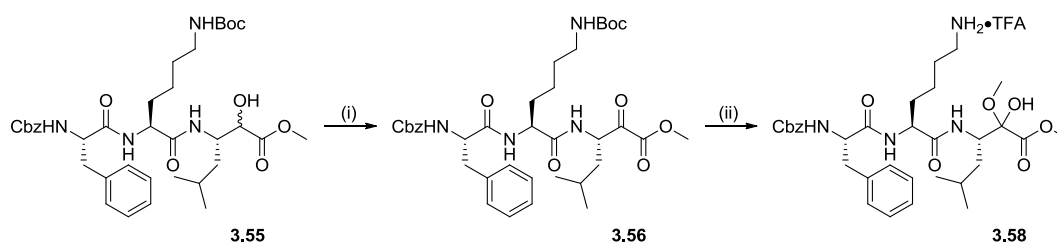


Figure 3.17 ^{13}C NMR (CD_3OD) of hemiacetal **3.58**. The signal highlighted in red (102 ppm) corresponds to the hemiacetal carbon. The signal corresponding to the methoxy group of the hemiacetal (55 ppm) has not been highlighted for clarity.

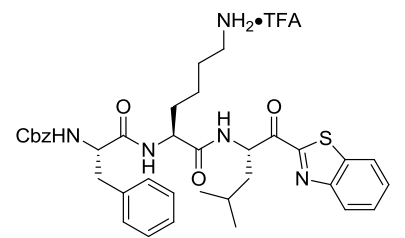
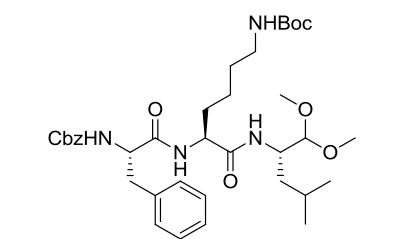
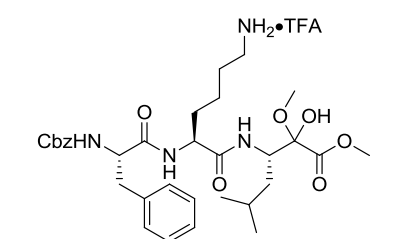


Scheme 3.6.7 *Reagents and Conditions:* i) DMP, CH_2Cl_2 , rt, 2 h, ii) TFA, CH_2Cl_2 , rt, 1.5 h, then MeOH, TFA (64% over 2 steps).

3.7 Extended Series Inhibition Assay

Inhibitors **3.44**, **3.49** and **3.58** were assayed against Hip1 using the same method described earlier and the inhibitory potencies are given in Table 3.7.1.

Table 3.7.1 % inhibition of Hip1 by tripeptide inhibitors and associated K_i values as determined by fluorometric assays.

Compound	Structure	% inhibition of Hip1 proteolytic activity					K_i (pM)
		1000 nM	500nM	100 nM	10 nM	1 nM	
3.44		100	100	100	100	95±5	178
3.49		-	-	70	71	45±2.7	-
3.58		100	100	100	100	97±3	309

Initial screening of the inhibitors demonstrated that all three are more potent against Hip1 compared to the lead inhibitor **3.23**. α -keto heterocycle **3.44** and hemiacetal **3.58** proved to be exceptionally potent, inhibiting Hip1 at 95% and 97% respectively at a concentration of 1 nM. K_i values of **3.44** and **3.58** were determined to be 178 pM and 309 pM, respectively (Appendix 1). This significantly improved activity over **3.23** is likely due to, in part, these inhibitors being able to react directly with the active site Ser₂₂₈ to achieve reversible binding, while boronate ester **3.23** is required to be hydrolytically cleaved to the boronic acid to react with Ser₂₂₈. Other factors such as the inhibitors' terminal electrophiles electrophilicity, shape and size are also expected to influence the binding efficacy. Additionally, the rate of interconversion between hydrates/hemiacetals/acetals and the active electrophile, in addition to the concentration of the active electrophile, is also presumed to affect the inhibitors potencies. For example, hemiacetal **3.58** will equilibrate to α -keto ester **3.57** which is expected to be the active form of the inhibitor. Similarly, acetal **3.49** which demonstrates relatively modest activity (45% inhibition at a concentration of 1 nM) is expected to be active on interconversion to aldehyde **3.48**, with the rate of interconversion and the concentration of the aldehyde in solution being expected to partially define the potency of the inhibitor.

3.8 Conclusions and Future Work

In summary, a novel series of tripeptide inhibitors containing P₁ boronate esters for the reversible inhibition of Hip1 has been synthesised and the associated inhibitory potencies characterised. Inhibitor **3.23** which features Phe at P₃ and Cbz at the N-terminus (P₄) was found to be a particularly potent inhibitor of Hip1 with a K_i = 16 nM.

An extended series of inhibitors containing either a C-terminal α -keto heterocycle, aldehyde or α -keto ester warhead were then designed based on the optimal sequence found in **3.23**. Initial screenings of these inhibitors against Hip1 shows α -keto heterocycle **3.44**, acetal **3.49** and hemiacetal **3.58** exhibit tight binding, with 95%, 45% and 97% inhibition of Hip1 activity at a concentration of 1 nM, respectively. K_i values for **3.44** and **3.58** were determined to be 178 and 309 pM, respectively, highlighting these compounds as highly potent inhibitors of Hip1.

Co-crystal structures of **3.23**, **3.36**, **3.44**, **3.49** and **3.58** bound to Hip1 are under investigation by our collaborator Nathan Goldfarb to provide insight into the binding mode of these inhibitors. *In vivo* efficacy against Mtb and cell cytotoxicity data will indicate the suitability of these inhibitors as adjunctive immunomodulatory therapeutic agents against Mtb. Investigations into other classical reversible serine electrophiles, including α -keto amides and carbamates, in addition to modifications to the nature of the electrophiles investigated thus far, including synthesis of the corresponding boronic acid of boronate ester **3.23**, will be valuable for further refining the inhibitors discussed.

CHAPTER FOUR:
Experimental Procedures

4 EXPERIMENTAL PROCEDURES

4.1 General Methods

4.1.1 General practices

Glassware

Oven-dried glassware was used for all reactions performed under an inert atmosphere of nitrogen or argon.

Reagents and Solvents

All commercially available starting materials and reagents were used without further purification unless otherwise stated. Dry dichloromethane (CH₂Cl₂) and tetrahydrofuran (THF) were obtained from an Innovative Technology Puresolv solvent purification system unless otherwise stated. Dry *N,N*-dimethylformamide (DMF) and methanol (MeOH) were purchased from Sigma Aldrich (St. Louis, MO, USA).

Cooled solutions

Cooling of solutions at <4 °C refers to cooling in an ice bath. Cooling of solutions below 0 °C was achieved by addition of dry ice to acetone until the desired temperature was reached.

Removal of volatiles *in vacuo*

Removal of volatiles *in vacuo* refers to removal of solvents and other volatiles under rotary evaporation. Residual volatiles were removed by use of high vacuum overnight.

Thin-layer chromatography

Thin-layer chromatography was performed on Merck aluminium TLC plates, silica gel (60 Å pore size) coated with fluorescent indicator F₂₅₄. Traces were visualised using 254 nm UV light on a Cole-Parmer 8-watt UV lamp with a 254 nm wavelength light tube and or a suitable dip including basic potassium permanganate dip and phosphomolybdic acid dip.

Flash Chromatography

Flash chromatography was performed on Grace Discovery Sciences Davisil chromatographic silica gel, 40-63 micron particle size, under a positive pressure of nitrogen. The eluting solvents hexane, ethyl acetate (EtOAc), dichloromethane (CH₂Cl₂) and methanol (MeOH) were used as received.

Reversed-Phase High Pressure Liquid Chromatography

Purification by Reversed-Phase High Pressure Liquid Chromatography (rp-HPLC) was performed using a Gilson semi-preparative reversed phase HPLC on a Phenomenex Luna C18(2) column with monitoring at 215 nm. The solvent gradient used is as specified in each protocol using solvent A = 0.1% TFA in Milli-Q water and solvent B = 0.1% TFA in acetonitrile (ACN) purchased from Sigma Aldrich (St. Louis, MO, USA). Appropriate fractions were combined and lyophilised on a Christ freeze dryer.

4.1.2 Analytical methods**NMR Spectroscopy**

Proton NMR spectra were obtained on an Agilent spectrometer (Agilent DD2 Console) operating at 500 MHz or an Oxford spectrometer (Agilent DD2 Console + Cryoprobe) operating at 600 MHz. Carbon NMR spectra were obtained on the

same spectrometers operating at 125 MHz or 150 MHz. Two-dimensional correlation experiments (COSY, HSQC, TOCSY, ROSEY and HMBC) were performed on the Agilent spectrometer operating at 500 MHz unless otherwise stated. All spectra were obtained at 23 °C. Chemical shifts are reported in parts per million (ppm) on a δ scale (internal standard is tetramethylsilane, TMS, shift = 0.00 ppm). Solvents used in NMR analysis include CDCl_3 (CHCl_3 at δ_{H} 7.26 ppm, CDCl_3 at δ_{C} 77.16 ppm); CD_3OD (CHD_2OD at δ_{H} 3.31 ppm, CD_3OD at δ_{C} 49.00 ppm); DMSO-d_6 ($(\text{CHD}_2)_2\text{SO}$ at δ_{H} 2.50 ppm, $(\text{CD}_3)_2\text{SO}$ at δ_{C} 39.52 ppm) and acetone- d_6 ($(\text{CHD}_2)_2\text{CO}$ at δ_{H} 2.05 ppm, $(\text{CD}_3)_2\text{CO}$ at δ_{C} 29.84 ppm). Spin multiplicities of signals are indicated as follows: singlet (s), broad singlet (br s), doublet (d), doublet of doublets (dd), doublet of doublet of triplets (ddt), triplet (t), doublet of triplets (dt), quartet (q) and multiplet (m). All coupling constants are reported in Hertz (Hz).

High Resolution Mass Spectrometry

High resolution mass spectrometry (HRMS) was performed on an Agilent 6230 ESI-TOF LCMS.

4.2 General Procedures

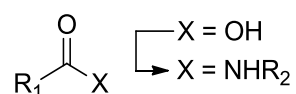
4.2.1 *In vitro* α -Chymotrypsin assay

The assay was adapted from the method of Zhang et al.¹²⁸ The activity of α -Chymotrypsin was assayed spectrophotometrically at 25 °C using a *Synergy H4 Hybrid Multi-Mode Microplate Reader* and each measurement was made in triplicate. A solution of α -Chymotrypsin (21.9 $\mu\text{g}/\text{mL}$) in 1 mM aqueous HCl was prepared fresh by a 1:40 dilution of a stock solution (874 $\mu\text{g}/\text{mL}$) in 1 mM aqueous HCl and kept on ice. A 1:100 dilution of the 21.9 $\mu\text{g}/\text{mL}$ solution in ice-cold 1 mM

aqueous HCl was prepared immediately before the start of each measurement. All compounds were analysed at seven different inhibitor concentrations. The assay was conducted in black 96-well plates as below: To each well was added *N*-[Tris(hydroxymethyl)methyl]-2-aminoethanesulfonic acid (TES) buffer (50 mM, pH = 8.0, adjusted with NaOH) (87.5 μ L), Ala-Ala-Phe-7-AMC substrate (20 mM) in DMSO (2.5 μ L), and an inhibitor (0.00064–10 mM) in DMSO (5 μ L). The reactions were initiated by addition of α -Chymotrypsin in 1 mM aqueous HCl (5 μ L, final concentration = 11 ng/mL). The excitation and emission wavelengths of the substrate were 380 nm and 460 nm respectively. Progress curves were monitored over 10 min for each concentration of every inhibitor. GraphPad Prism 5.0, GraphPad Software, Inc. was used for the determination of kinetic values and the half maximal inhibitory concentration (IC_{50}) of each inhibitor. The mean IC_{50} was determined by fitting the dose-response data to the built-in model-(inhibitor) vs. response- variable slope (without log transformation).

4.2.2 General reaction procedures

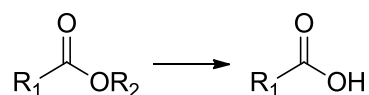
General Procedure A: HATU mediated amide coupling



To a stirred solution of the respective carboxylic acid (1.0 equiv) and appropriate amine (1.0 equiv) in dry DMF (20 mL / g carboxylic acid) was added sequentially HATU (1.2 equiv) and dry DIPEA dropwise (4.0 equiv), and the solution stirred at ambient temperature under a nitrogen atmosphere for 18 h. To the resulting solution was added 10% aq. NH_4Cl solution and the aqueous phase extracted with

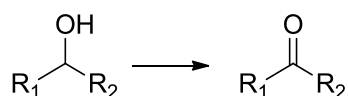
EtOAc (3x). The combined organic extracts were washed with brine (3x), dried over MgSO₄, filtered, and concentrated *in vacuo*. The crude product was purified by flash chromatography on silica to afford the desired pure amides.

General Procedure B: Ester hydrolysis with LiOH



To the respective ester (1.0 equiv) in THF (equal volume as aq. LiOH solution) was added aq. 1M LiOH (4.0 equiv) and the solution stirred at ambient temperature for 2 h. Volatiles were removed *in vacuo*, the solution washed with Et₂O and acidified to pH = 1 with 1M aq. HCl. The resulting mixture was extracted with EtOAc (3x), washed with brine, dried over MgSO₄, filtered, and concentrated *in vacuo* to afford the desired pure carboxylic acids.

General Procedure C: Oxidation of alcohols with DMP



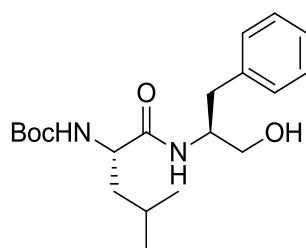
To the respective alcohol (1.0 equiv) in dry CH₂Cl₂ (25 mL / g alcohol) was added DMP (1.5 equiv) and the solution stirred at ambient temperature under a nitrogen atmosphere for 2 h. CH₂Cl₂ (25 mL / g alcohol) was added, the reaction quenched by addition of 10% Na₂S₂O₃ in sat. aq. NaHCO₃ solution (25 mL / g alcohol), and the resulting solution stirred at ambient temperature for 15 min. The mixture was extracted with CH₂Cl₂ (3x), washed with brine (1x), dried over MgSO₄, filtered, and concentrated *in vacuo* to afford the desired crude oxidised alcohols which were

either used without further purification in subsequent reactions or purified by rp-HPLC to afford the desired pure oxidised alcohols.

4.3 Experimental Work Described in Chapter Two

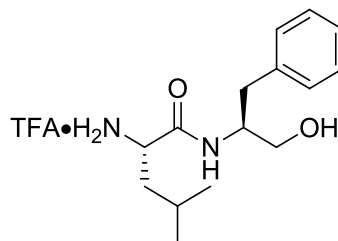
Diastereomers with selected data listed for minor isomers have NMR data reported which is distinguishable from the major isomer data.

tert-Butyl((*S*)-1-(((*S*)-1-hydroxy-3-phenylpropan-2-yl)amino)-4-methyl-1-oxopentan-2-yl)carbamate **2.23**



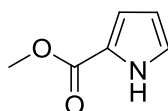
Boc-L-Leucine monohydrate (3.91 g, 15.7 mmol) was coupled to L-phenylalaninol (2.37 g, 15.7 mmol) according to general procedure A and the crude product was purified by flash chromatography on silica (80% EtOAc / Hexane) to afford **2.23** as a white solid (5.68 g, 99%). $R_f = 0.54$ (80% EtOAc / Hexane); $^1\text{H NMR}$ (500 MHz, CDCl_3) δ 0.91 (m, 6H, CHCH_3), 1.42 (m, 1H, CH_3CHCHH), 1.44 (s, 9H, $\text{C}(\text{CH}_3)_3$), 1.60 (m, 2H, CH_3CHCHH , CH_3CH), 2.88 (m, 2H, CH_2OH), 3.12 (br s, 1H, OH), 3.58 (m, 1H, $\text{CHHCHCH}_2\text{OH}$), 3.66 (m, 1H, $\text{CHHCHCH}_2\text{OH}$), 4.04 (m, 1H, CHCH_2OH), 4.14 (m, 1H, CO_2NHCH), 4.96 (m, 1H, NHCHCH_2OH), 6.56 (d, $J = 7.5$ Hz, 1H, CO_2NH), 7.25 (m, 5H, C_6H_5); $^{13}\text{C NMR}$ (125 MHz, CDCl_3) δ 24.6, 25.5, 27.4, 31.0, 39.5, 43.7, 55.6, 56.2, 66.2, 82.7, 129.2, 131.2, 131.9, 140.4, 158.6, 175.6. HRMS (ESI) 387.2324 ($\text{M}+\text{Na}$) $^+$; $\text{C}_{20}\text{H}_{32}\text{N}_2\text{NaO}_4$ requires 387.2254.

(S)-1-(((S)-1-Hydroxy-3-phenylpropan-2-yl)amino)-4-methyl-1-oxopentan-2-aminium 2,2,2-trifluoroacetate 2.24



To a solution of **2.23** (368 mg, 0.97 mmol) in dry CH₂Cl₂ (5 mL) was added TFA (0.5 mL, 6.5 mmol) and the solution left to stir at ambient temperature for 5 h under a nitrogen atmosphere. The resulting solution was concentrated *in vacuo*, washed with CH₂Cl₂ (3x) and MeOH (3x), concentrating *in vacuo* following each wash, to afford **2.24** as a crude orange oil (446 mg) which was used without further purification.

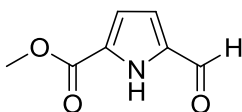
Methyl 1H-pyrrole-2-carboxylate 2.06



To a suspension of 60% sodium hydride dispersion in mineral oil (4.25 g, 127 mmol) in dry THF (40 mL) cooled at <4 °C under a nitrogen atmosphere was added dry MeOH (40 mL) over 1 h, and the resulting solution stirred at ambient temperature for 30 min. The resulting solution was added to a stirred solution of 2,2,2-trichloroacetyl pyrrole (22.4 g, 105 mmol) in dry THF (40 mL) at <4 °C under a nitrogen atmosphere over 1 h, the solution stirred for 45 min at <4 °C and then at ambient temperature for 18 h. Phosphate buffer, pH = 7 (50 mL) was added and

the pH of the solution lowered to pH = 7 by addition of 4M aq. HCl. Volatiles were removed *in vacuo*, added water (100 mL), and the aq. phase extracted with EtOAc (2x). The combined organic extracts were washed with brine (1x), dried over MgSO₄, filtered, and concentrated *in vacuo*. The resulting residue was triturated with hexane (3x 15 mL) and recrystallised from EtOAc / hexane to afford **2.06** as a pale brown crystalline solid (9.38 g, 71%). ¹H NMR (500 MHz, CDCl₃) δ 3.87 (s, 3H, CO₂CH₃), 6.28 (m, 1H, NHCH), 6.93 (m, 1H, NHCHCH), 6.97 (m, 1H, NHCCH), 9.07 (br s, 1H, NH); ¹³C NMR (125 MHz, CDCl₃) δ 51.4, 110.4, 115.3, 122.6, 123.0, 161.7. Experimental data as per literature.¹²⁹

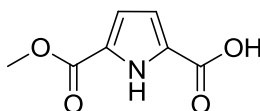
Methyl 5-formyl-1H-pyrrole-2-carboxylate **2.08**



Phosphoryl chloride (4.93 mL, 53.0 mmol) was added dropwise to a stirred solution of dry DMF (4.07 mL, 53.0 mmol) cooled to 15 °C under a nitrogen atmosphere over 15 min. DCE (12 mL) and a solution of **2.06** (6.00 g, 48.0 mmol) in DCE (12 mL) were added sequentially to the solution over 1 h. The resulting solution was heated at reflux for 15 min, cooled to ambient temperature, treated with a solution of sodium acetate tetrahydrate (35.9 g, 264 mmol) in water (70 mL) and heated at reflux for an additional 15 min. The aq. layer was extracted with CH₂Cl₂ (3x), the combined organics were washed with sat. aq. NaHCO₃ (3x), dried over MgSO₄, filtered, and concentrated *in vacuo*. The crude product was purified by flash chromatography on silica (98% CH₂Cl₂ / MeOH) to afford **2.08** as a yellow solid (5.00 g, 68%). R_f = 0.37 (2% MeOH / CH₂Cl₂); ¹H NMR (500 MHz, CDCl₃) δ 3.93

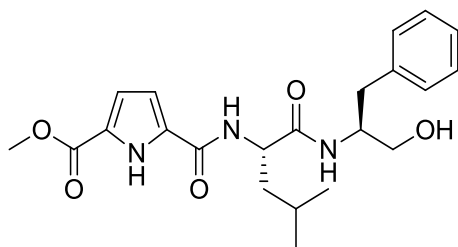
(s, 3H, CO₂CH₃), 6.95 (s, 1H, NHCCH), 6.95 (s, 1H, NHCCH), 9.68 (s, 1H, CHO), 9.80 (br s, 1H, NH); ¹³C NMR (125 MHz, CDCl₃) δ 52.2, 114.3, 124.9, 127.8, 128.5, 161.4, 185.8. Experimental data as per literature.¹³⁰

5-(Methoxycarbonyl)-1H-pyrrole-2-carboxylic acid **2.09**



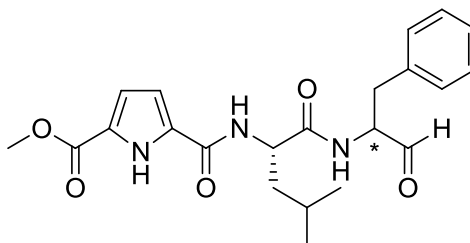
To a stirred solution of **2.08** (3.50 g, 23.0 mmol) in DMSO (25 mL) was added a solution of monosodium phosphate (21.4 g, 137 mmol) in water (30 mL). A solution of sodium chlorite (7.44 g, 67.0 mmol) in water (15 mL) was added dropwise over 20 min and the resulting solution stirred at ambient temperature for 3 h. The reaction was quenched by addition of sat. aq. NaHCO₃ (50 mL), water (100 mL) was added, and the mixture washed consecutively with Et₂O (50 mL) and EtOAc (50 mL). The mixture was acidified to pH = 1 with 1M aq. HCl and extracted with EtOAc (3x). The combined organics were washed with brine (1x), dried over MgSO₄, filtered, and concentrated *in vacuo* to afford **2.09** as white solid (2.51 g, 65%). ¹H NMR (500 MHz, DMSO-*d*₆) δ 3.77 (s, 3H, CO₂CH₃), 6.75 (d, *J* = 3.9 Hz, 1H, NHCCH), 6.80 (d, *J* = 3.9 Hz, 1H, NHCCH), 12.45 (s, 1H, NH), 12.80 (br s, 1H, CO₂H); ¹³C NMR (125 MHz, DMSO-*d*₆) δ 51.6, 115.3, 115.5, 126.2, 128.1, 160.5, 161.4. Experimental data as per literature.¹³⁰

Methyl 5-(((S)-1-(((S)-1-hydroxy-3-phenylpropan-2-yl)amino)-4-methyl-1-oxopentan-2-yl)carbamoyl)-1H-pyrrole-2-carboxylate **2.25**



Crude **2.24** (386 mg) was coupled to **2.09** (173 mg, 0.930 mmol) per general procedure A and the crude product was purified by flash chromatography on silica (80% EtOAc / Hexane) to afford **2.25** as a white solid (214 mg, 50%). $R_f = 0.32$ (80% EtOAc / Hexane); $^1\text{H NMR}$ (500 MHz, CDCl_3) δ 0.91 (m, 6H, 2x CHCH_3), 1.69 (m, 3H, CH_2CHCH_3 , CH_2CHCH_3), 2.91 (m, 2H, $\text{CH}_2\text{CHCH}_2\text{OH}$), 3.78 (m, 2H, CH_2OH), 3.90 (s, 3H, CO_2CH_3), 4.31 (m, 1H, CHCH_2OH), 5.15 (m, 1H, $\text{CHCH}_2\text{CHCH}_3$), 6.69 (m, 1H, NHCCH), 6.90 (m, 1H, NHCCH), 7.18 (m, 6H, C_6H_5 , $\text{NHCHCH}_2\text{CHCH}_3$), 8.52 (d, $J = 8.4$ Hz, 1H, NHCHCH_2OH), 11.45 (s, 1H, NH); $^{13}\text{C NMR}$ (125 MHz, CDCl_3) δ 25.2, 25.4, 27.6, 39.8, 44.3, 54.4, 54.7, 55.0, 65.8, 113.4, 118.9, 127.6, 129.0, 131.0, 131.9, 132.5, 140.6, 162.4, 164.9, 175.5. HRMS (ESI) 438.2000 ($\text{M}+\text{Na}$) $^+$; $\text{C}_{22}\text{H}_{29}\text{N}_3\text{NaO}_5$ requires 438.1999.

Methyl 5-(((S)-4-methyl-1-oxo-1-(((S/R)-1-oxo-3-phenylpropan-2-yl)amino)pentan-2-yl)carbamoyl)-1H-pyrrole-2-carboxylate 2.30

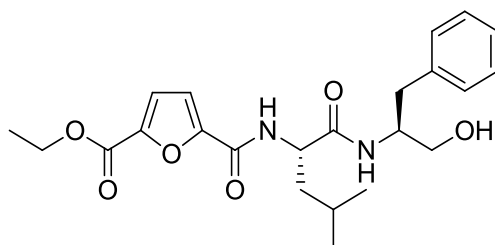


2.25 (69 mg, 0.170 mmol) was oxidised according to general procedure C and purified by rp-HPLC (10-70% aq. ACN over 25 min) to afford **2.30** as a fluffy white solid as a 94(S):6(R) mixture of diastereomers (15 mg, 22%). HRMS (ESI) 414.2011 (M+H)⁺; C₂₂H₂₈N₃O₅ requires 414.2024.

Data for major isomer from mixture: R_t: 10.7 min; ¹H NMR (500 MHz, CDCl₃) δ 0.92 (d, *J* = 6.2 Hz, 3H, CHCH₃), 0.96 (d, *J* = 6.2 Hz, 3H, CHCH₃), 1.68 (m, 3H, CH₂CHCH₃, CH₂CHCH₃), 3.06 (dd, *J* = 14.1 Hz, 7.0 Hz, 1H, CHHCHCHO), 3.17 (dd, *J* = 14.1 Hz, 7.0 Hz, 1H, CHHCHCHO), 3.83 (s, 3H, CO₂CH₃), 4.75 (m, 1H, CHCH₂CHO), 4.91 (m, 1H, CHCH₂CHCH₃), 6.62 (m, 1H, NHCCH), 6.66 (m, 1H, NHCHCH₂CHO), 6.88 (m, 1H, NHCCH), 7.11 (m, 5H, C₆H₅), 7.31 (m, 1H, NHCHCH₂CHCH₃), 9.66 (s, 1H, CHO), 10.90 (s, 1H, NH); ¹³C NMR (125 MHz, CDCl₃) δ 25.0, 25.3, 27.5, 37.7, 43.6, 53.9, 54.5, 62.5, 113.3, 118.3, 128.1, 129.7, 131.2, 131.9, 138.0, 162.5, 163.9, 175.2, 200.1.

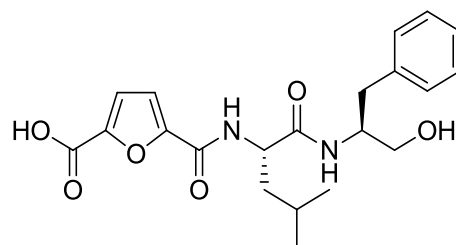
Selected data for minor isomer from mixture: R_t: 10.7 min; ¹H NMR (500 MHz, CDCl₃) δ 3.86 (s, 3H, CO₂CH₃), 9.62 (s, 1H, CHO), ¹³C NMR (125 MHz, CDCl₃) δ 24.9, 25.3, 27.5, 37.5, 43.9, 54.3, 62.5, 113.4, 118.3, 129.8, 131.4, 131.8, 138.3, 163.8, 201.2.

Ethyl 5-(((S)-1-(((S)-1-hydroxy-3-phenylpropan-2-yl)amino)-4-methyl-1-oxopentan-2-yl)carbamoyl)furan-2-carboxylate **2.26**



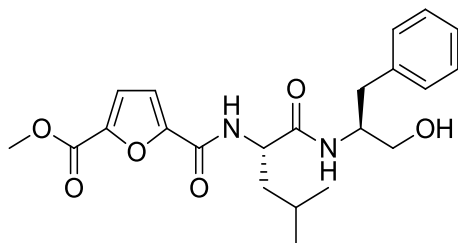
Crude **2.24** (679 mg) was coupled to **2.14** (364 mg, 2.00 mmol) per general procedure A and the crude product was purified by flash chromatography on silica (60 - 80% EtOAc / Hexane) to afford **2.26** as an off-white solid (344 mg, 45%). $R_f = 0.19$ (80% EtOAc / Hexane); $^1\text{H NMR}$ (500 MHz, CDCl_3) δ 0.91 (d, $J = 6.3$ Hz, 3H, CHCH_3), 0.93 (d, $J = 6.3$ Hz, 3H, CHCH_3), 1.42 (t, $J = 7.1$ Hz, 3H, $\text{CO}_2\text{CH}_2\text{CH}_3$), 1.68 (m, 3H, CH_2CHCH_3 , CH_2CHCH_3), 2.85 (dd, $J = 13.8, 7.6$ Hz, 1H, $\text{CHHCHCH}_2\text{OH}$), 2.90 (dd, $J = 13.8, 7.6$ Hz, 1H, $\text{CHHCHCH}_2\text{OH}$), 3.64 (dd, $J = 11.1, 5.2$ Hz, 1H, CHHOH), 3.71 (dd, $J = 11.1, 5.2$ Hz, 1H, CHHOH), 4.21 (m, 1H, $\text{CH}_2\text{CHCH}_2\text{OH}$), 4.41 (q, $J = 7.1$ Hz, 2H, $\text{CO}_2\text{CH}_2\text{CH}_3$), 4.60 (m, 1H, $\text{CHCH}_2\text{CHCH}_3$), 6.71 (d, $J = 8.0$ Hz, 1H, $\text{NHCHCH}_2\text{CHCH}_3$), 7.03 (d, $J = 8.4$ Hz, 1H, NHCHCH_2OH), 7.12 (m, 1H, OCCH), 7.19 (m, 6H, C_6H_5 , OCCH); $^{13}\text{C NMR}$ (125 MHz, CDCl_3) 24.7, 25.5, 27.4, 39.6, 43.4, 55.5, 55.6, 64.4, 66.5, 118.6, 121.5, 129.1, 131.1, 131.9, 140.2, 148.1, 151.9, 160.2, 160.9, 174.3. HRMS (ESI) 453.1997 ($\text{M}+\text{Na}$) $^+$; $\text{C}_{23}\text{H}_{30}\text{N}_2\text{NaO}_6$ requires 453.1996.

5-(((S)-1-(((S)-1-Hydroxy-3-phenylpropan-2-yl)amino)-4-methyl-1-oxopentan-2-yl)carbamoyl)furan-2-carboxylic acid 2.26*



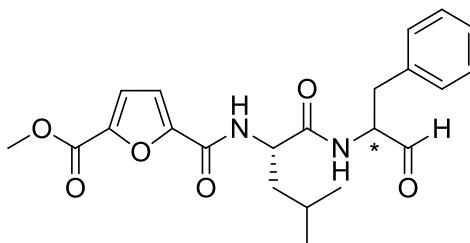
2.26 (182 mg, 0.453 mmol) was hydrolysed per general procedure B to afford **2.26*** as a white solid (135 mg, 79%). ^1H NMR (DMSO- d_6 , 500 MHz) δ 0.83 (d, J = 6.4 Hz, 3H, CHCH $_3$), 0.87 (d, J = 6.4 Hz, 3H, CHCH $_3$), 1.52 (m, 3H, CH $_2$ CHCH $_3$, CH $_2$ CHCH $_3$), 2.64 (dd, J = 13.7, 8.2 Hz, 1H, CHHCHCH $_2$ OH), 2.84 (dd, J = 13.7, 8.2 Hz, 1H, CHHCHCH $_2$ OH), 3.30 (m, 2H CH $_2$ OH), 3.88 (m, 1H, CH $_2$ CHCH $_2$ OH), 4.47 (m, 1H, CHCH $_2$ CHCH $_3$), 4.75 (br s, 1H, OH), 7.14 (m, 5H, C $_6$ H $_5$), 7.29 (d, J = 3.6 Hz, 1H, OCCH), 7.30 (d, J = 3.6 Hz, 1H, OCCH), 7.83 (d, J = 8.4 Hz, 1H, NHCHCH $_2$ OH), 8.37 (d, J = 8.4 Hz, 1H, NHCHCH $_2$ CHCH $_3$), 13.45 (br s, 1H, CO $_2$ H); ^{13}C NMR (DMSO- d_6 , 125 MHz) δ 24.7, 26.1, 27.4, 39.5, 43.7, 54.3, 55.5, 65.4, 117.9, 121.6, 128.9, 131.1, 132.2, 142.1, 148.8, 152.7, 159.9, 162.1, 174.3. HRMS (ESI) 403.2035 (M+H) $^+$; C $_{21}$ H $_{27}$ N $_2$ O $_6$ requires 403.1864.

Methyl 5-(((S)-1-(((S)-1-hydroxy-3-phenylpropan-2-yl)amino)-4-methyl-1-oxopentan-2-yl)carbamoyl)furan-2-carboxylate 2.29



To a solution of **2.26*** (93 mg, 0.223 mmol) in dry DMF (1.5 mL) was added sequentially K_2CO_3 (36 mg, 0.260 mmol) and methyl iodide (16 μ L, 0.260 mmol) and the solution stirred at ambient temperature under a nitrogen atmosphere for 24 h. Sat. aq. $NaHCO_3$ solution (2 mL) was added and the solution was extracted with EtOAc (3x). The combined organics were washed with brine (3x), dried over $MgSO_4$, filtered, and concentrated *in vacuo* to afford a crude residue which was purified by flash chromatography on silica (90 % EtOAc / Hexane) to afford **2.29** as a white solid (68 mg, 71 %). R_f = 0.34 (90 % EtOAc / Hexane); 1H NMR (500 MHz, $CDCl_3$) δ 0.93 (m, 6H, 2x $CHCH_3$), 1.69 (m, 3H, CH_2CHCH_3 , CH_2CHCH_3), 2.74 (br s, 1H, OH), 2.85 (dd, J = 13.9, 7.6 Hz, 1H, $CHHCHCH_2OH$), 2.91 (dd, J = 13.9, 7.6 Hz, 1H, $CHHCHCH_2OH$), 3.68 (m, 2H, CH_2OH), 3.95 (s, 3H, CO_2CH_3), 4.28 (m, 1H, $CHCH_2OH$), 4.58 (m, 1H, $CHCH_2CHCH_3$), 6.55 (d, J = 8.0 Hz, 1H, $NHCHCH_2OH$), 6.96 (d, J = 8.4 Hz, 1H, $NHCHCH_2CHCH_3$), 7.12 (m, 1H, OCCH), 7.20 (m, 6H, C_6H_5 , OCCH); ^{13}C NMR ($DMSO-d_6$, 125 MHz) δ 24.7, 25.5, 27.4, 39.6, 43.3, 54.4, 55.1, 55.6, 66.6, 118.6, 121.7, 129.1, 131.1, 131.9, 140.1, 147.8, 152.0, 160.2, 161.2, 174.2. HRMS (ESI) 439.1840 ($M+Na$) $^+$; $C_{22}H_{28}N_2NaO_6$ requires 439.1389.

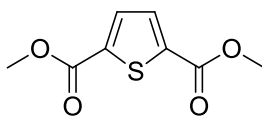
Methyl 5-(((S)-4-methyl-1-oxo-1-(((S/R)-1-oxo-3-phenylpropan-2-yl)amino)pentan-2-yl)carbamoyl)furan-2-carboxylate 2.31



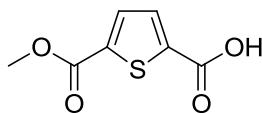
2.29 (56 mg, 0.135 mmol) was oxidised according to general procedure C and purified by rp-HPLC (10-70% aq. ACN over 15 min) to afford **2.31** as a fluffy white solid as a 79(S):21(R) mixture of diastereomers (16 mg, 28%). HRMS (ESI) 437.1647 (M+Na)⁺; C₂₂H₂₆N₂NaO₆ requires 437.1682.

Data for major isomer from mixture: R_t: 9.5 min; ¹H NMR (500 MHz, CDCl₃) δ 0.94 (d, *J* = 6.2 Hz, 3H, CHCH₃), 0.96 (d, *J* = 6.2 Hz, 3H, CHCH₃), 1.68 (m, 3H, CH₂CHCH₃, CH₂CHCH₃), 3.11 (dd, *J* = 14.1 Hz, 7.0 Hz, 1H, CHHCHCHO), 3.18 (dd, *J* = 14.1 Hz, 7.1 Hz, 1H, CHHCHCHO), 3.95 (s, 3H, CO₂CH₃), 4.64 (m, 1H, CHCH₂CHO), 4.73 (m, 1H, CHCH₂CHCH₃), 6.73 (m, 1H, NHCHCH₂CHO), 6.99 (d, *J* = 8.3 Hz, 1H, NHCHCH₂CHCH₃), 7.18 (m, 7H, C₆H₅, 2x OCCH), 9.64 (s, 1H, CHO); ¹³C NMR (125 MHz, CDCl₃) δ 24.6, 25.5, 27.4, 37.7, 43.2, 54.0, 55.1, 62.4, 118.6, 121.7, 129.8, 131.3, 131.9, 138.0, 147.8, 151.9, 160.2, 174.2, 200.1.

Selected data for minor isomer from mixture: R_t: 9.5 min; ¹H NMR (500 MHz, CDCl₃) δ 3.94 (s, 3H, CO₂CH₃), 9.62 (s, 1H, CHO), ¹³C NMR (125 MHz, CDCl₃) δ 25.4, 37.5, 43.6, 54.2, 55.0, 62.4, 121.7, 129.8, 131.4, 131.9, 138.1, 160.2, 174.4, 201.1.

Dimethyl thiophene-2,5-dicarboxylate 2.16

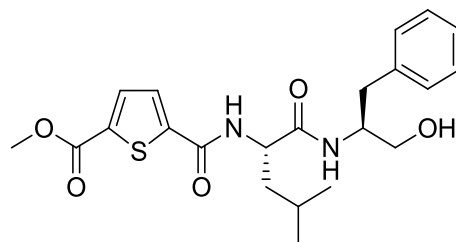
To a solution of 2,5-Thiophenedicarboxylic acid (2.50 g, 14.5 mmol) in dry MeOH (50 mL) was added SOCl₂ (4.43 mL, 61.0 mmol) over 10 min and the resulting solution heated at reflux for 18 h under a nitrogen atmosphere. The resulting precipitate was filtered, washed with MeOH (3x 10 mL) and air dried to afford **2.16** as an off-white solid (2.52 g, 88%). ¹H NMR (500 MHz, CDCl₃) δ 3.93 (s, 6H, 2x CO₂CH₃), 7.74 (s, 2H, 2x SCCH); ¹³C NMR (125 MHz, CDCl₃) δ 55.2, 135.7, 141.5, 164.7. Experimental data as per literature.¹³¹

5-(Methoxycarbonyl)thiophene-2-carboxylic acid 2.17

To a solution of **2.16** (923 mg, 4.61 mmol) suspended in acetone freshly distilled from dry calcium sulfate (13 mL) was added a solution of dry NaOH (221 mg, 5.53 mmol) in dry MeOH (2 mL) dropwise over 20 min, and the resulting solution stirred at ambient temperature under a nitrogen atmosphere for 18h. The solution was concentrated *in vacuo*, the residue dissolved in water (10 mL) and washed with EtOAc (3x 10 mL). The solution was acidified to pH = 1 with 1M HCl and the resulting precipitate filtered, washed with water (3x 10 mL) and air dried to afford **2.17** as a white solid (606 mg, 70%). ¹H NMR (500 MHz, DMSO-*d*₆) δ 3.85 (s, 3H, CO₂CH₃), 7.73 (d, *J* = 3.9 Hz, 1H, SCCH), 7.79 (d, *J* = 3.9 Hz, 1H, SCCH), 13.65 (br s,

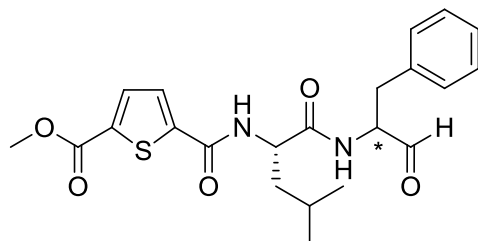
^1H , CO_2H); ^{13}C NMR (125 MHz, $\text{DMSO-}d_6$) δ 55.2, 136.3, 136.9, 140.7, 143.5, 164.5, 165.4. Experimental data as per literature.¹³²

Methyl 5-(((S)-1-(((S)-1-hydroxy-3-phenylpropan-2-yl)amino)-4-methyl-1-oxopentan-2-yl)carbamoyl)thiophene-2-carboxylate **2.27**



Crude **2.24** (864 mg) was coupled to **2.17** (491 mg, 2.64 mmol) per general procedure A and the crude product was purified by flash chromatography on silica (60% EtOAc / Hexane) to afford **2.27** as a yellow crystalline solid (445 mg, 43%). R_f = 0.29 (55% EtOAc / Hexane); ^1H NMR (500 MHz, Acetone- d_6) δ 0.91 (d, J = 6.5 Hz, 3H, CHCH_3), 0.93 (d, J = 6.5 Hz, 3H, CHCH_3), 1.68 (m, 3H, CH_2CHCH_3 , CH_2CHCH_3), 2.91 (dd, J = 13.7, 7.7 Hz, 1H, $\text{CHHCHCH}_2\text{OH}$), 2.93 (dd, J = 13.7, 7.7 Hz, 1H, $\text{CHHCHCH}_2\text{OH}$), 3.55 (2H, m, CH_2OH), 3.92 (s, 3H, CO_2CH_3), 4.11 (m, 1H, CHCH_2OH), 4.63 (m, 1H, $\text{CHCH}_2\text{CHCH}_3$), 7.17 (m, 5H, C_6H_5), 7.34 (d, J = 8.2 Hz, NHCHCH_2OH), 7.75 (d, J = 4.0 Hz, 1H, SCCH), 7.79 (d, J = 4.0 Hz, 1H, SCCH), 8.01 (d, J = 8.0 Hz, $\text{NHCHCH}_2\text{CHCH}_3$); ^{13}C NMR (125 MHz, Acetone- d_6) δ 23.9, 25.1, 27.3, 39.4, 43.4, 54.5, 54.9, 55.7, 65.5, 128.9, 130.7, 130.8, 131.9, 136.0, 139.4, 141.5, 148.2, 163.3, 164.4, 174.1. HRMS (ESI) 433.2052 ($\text{M}+\text{H}^+$); $\text{C}_{22}\text{H}_{29}\text{N}_2\text{O}_5\text{S}$ requires 433.1792.

Methyl 5-(((S)-4-methyl-1-oxo-1-(((S/R)-1-oxo-3-phenylpropan-2-yl)amino)pentan-2-yl)carbamoyl)thiophene-2-carboxylate **2.32**

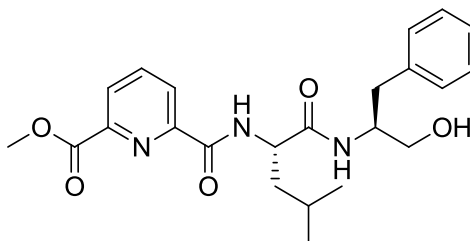


2.27 (61 mg, 0.141 mmol) was oxidised according to general procedure C, with the modification of using THF as the reaction solvent, and purified by rp-HPLC (10-70% aq. ACN over 15 min) to afford **2.32** as a fluffy white solid as a 74(S):26(R) mixture of diastereomers (12 mg, 20%). HRMS (ESI) 431.1642 (M+H)⁺; C₂₂H₂₇N₂O₅S requires 431.1633.

Data for major isomer from mixture: R_t : 7.3 min; ¹H NMR (600 MHz, CDCl₃) δ 0.94 (d, J = 6.3 Hz, 3H, CHCH₃), 0.95 (d, J = 6.3 Hz, 3H, CHCH₃), 1.68 (m, 3H, CH₂CHCH₃, CH₂CHCH₃), 3.10 (dd, J = 14.2 Hz, 6.9 Hz, 1H, CHHCHCHO), 3.17 (dd, J = 14.2 Hz, 6.9 Hz, 1H, CHHCHCHO), 3.92 (s, 3H, CO₂CH₃), 4.61 (m, 1H, CHCH₂CHO), 4.73 (m, 1H, CHCH₂CHCH₃), 6.44 (d, J = 8.0 Hz, 1H, NHCHCH₂CHO), 6.56 (d, J = 6.9 Hz, 1H, NHCHCH₂CHCH₃), 7.17 (m, 5H, C₆H₅), 7.44 (d, J = 4.0 Hz, 1H, SCCH), 7.74 (d, J = 4.0 Hz, 1H, SCCH), 9.64 (s, 1H, CHO); ¹³C NMR (150 MHz, CDCl₃) δ 24.9, 25.5, 27.5, 32.4, 37.7, 43.7, 54.5, 55.3, 62.4, 129.9, 130.9, 131.4, 131.9, 135.9, 137.8, 146.1, 163.4, 164.7, 174.3, 200.1.

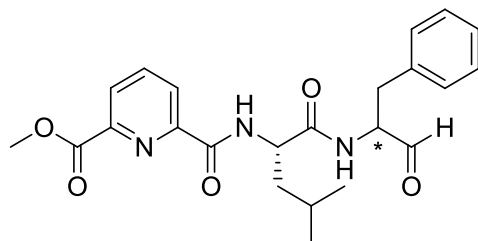
Selected data for minor isomer from mixture: R_t : 7.3 min; ¹H NMR (600 MHz, CDCl₃) δ 0.88 (m, 6H, 2x CHCH₃), 3.90 (s, 3H, CO₂CH₃), 7.71 (d, J = 4.0 Hz, 1H, SCCH), 9.63 (s, 1H, CHO), ¹³C NMR (150 MHz, CDCl₃) δ 25.4, 32.0.

Methyl 6-(((S)-1-(((S)-1-hydroxy-3-phenylpropan-2-yl)amino)-4-methyl-1-oxopentan-2-yl)carbamoyl)picolinate **2.28**



Crude **2.24** (744 mg) was coupled to 6-(methoxycarbonyl)-2-pyridinecarboxylic acid (392 mg, 2.20 mmol) per general procedure A and the crude product was purified by flash chromatography on silica (60 – 100% EtOAc / CH₂Cl₂) to afford **2.28** as a viscous yellow solid (322 mg, 62%). *R_f* = 0.25 (90% EtOAc / CH₂Cl₂); ¹H NMR (500 MHz, CDCl₃) δ 0.87 (m, 6H, 2x CHCH₃), 1.69 (m, 3H, CH₂CHCH₃, CH₂CHCH₃), 2.89 (m, 2H, CH₂CHCH₂OH), 3.66 (m, 2H, CH₂OH), 3.98 (s, 3H, CO₂CH₃), 4.13 (br s, 1H, OH), 4.24 (m, 1H, CHCH₂OH), 4.69 (m, 1H, CHCH₂CHCH₃), 7.09 (m, 6H, C₆H₅, NHCHCH₂OH), 7.97 (t, *J* = 7.8 Hz, 1H, NCCHCH), 8.18 (d, *J* = 7.8 Hz, NCCHCH), 8.30 (d, *J* = 7.8 Hz, NCCHCH), 8.60 (d, *J* = 8.7 Hz, 1H, NHCHCH₂CHCH₃); ¹³C NMR (125 MHz, CDCl₃) δ 24.7, 25.5, 27.5, 39.6, 41.3, 43.5, 54.9, 55.4, 55.7, 65.9, 128.3, 128.9, 130.1, 130.9, 131.9, 140.6, 141.2, 149.1, 152.3, 166.2, 167.7, 174.5. HRMS (ESI) 466.1750 (M+K)⁺; C₂₂H₂₉N₃O₅ requires 466.1739.

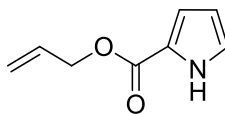
Methyl 6-(((*S/R*)-4-methyl-1-oxo-1-(((*S/R*)-1-oxo-3-phenylpropan-2-yl)amino)pentan-2-yl)carbamoyl)picolinate **2.33**



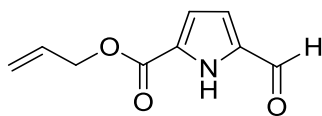
2.28 (71 mg, 0.169 mmol) was oxidised according to general procedure C and purified by rp-HPLC (10-70% aq. ACN over 15 min) to afford **2.33** as a fluffy white solid as an 87(*S*):13(*R*) mixture of diastereomers (30 mg, 52%). HRMS (ESI) 448.1847 ($M+Na$)⁺; C₂₃H₂₇N₃NaO₅ requires 448.1843.

Data for major isomer from mixture: R_t : 9.7 min; ¹H NMR (500 MHz, CDCl₃) δ 0.94 (d, J = 6.3 Hz, 3H, CHCH₃), 0.97 (d, J = 6.3 Hz, 3H, CHCH₃), 1.74 (m, 3H, CH₂CHCH₃, CH₂CHCH₃), 3.10 (dd, J = 14.2 Hz, 7.0 Hz, 1H, CHHCHCHO), 3.17 (dd, J = 14.2 Hz, 7.0 Hz, 1H, CHHCHCHO), 4.04 (s, 3H, CO₂CH₃), 4.61 (m, 1H, CHCH₂CHO), 4.73 (m, 1H, CHCH₂CHCH₃), 6.44 (d, J = 8.0 Hz, 1H, NHCHCH₂CHO), 7.14 (m, 5H, C₆H₅), 8.05 (t, J = 7.8 Hz, 1H, NCCHCH), 8.27 (d, J = 7.8 Hz, NCCHCH), 8.33 (d, J = 7.8 Hz, NCCHCH), 8.41 (d, J = 8.7 Hz, 1H, NHCHCH₂CHCH₃), 9.63 (s, 1H, CHO); ¹³C NMR (125 MHz, CDCl₃) δ 24.6, 25.5, 27.5, 37.6, 42.8, 54.6, 55.7, 62.4, 128.3, 129.6, 130.3, 131.3, 131.9, 138.1, 141.3, 149.4, 151.8, 166.6, 167.6, 174.7, 201.2.

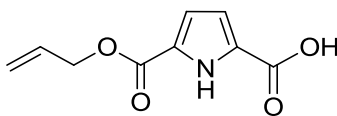
Selected data for minor isomer from mixture: R_t : 9.7 min; ¹H NMR (600 MHz, CDCl₃) δ 4.03 (s, 3H, CO₂CH₃), 9.62 (s, 1H, CHO), ¹³C NMR (125 MHz, CDCl₃) δ 25.4, 37.5, 43.2, 54.8, 62.4, 129.7, 131.3, 131.9, 141.3, 166.6, 174.9, 201.3.

Allyl 1H-pyrrole-2-carboxylate 2.39

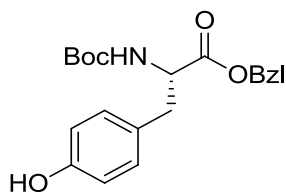
To a suspension of 60% sodium hydride dispersion in mineral oil (2.66 g, 79.0 mmol) in dry THF (20 mL) cooled at <4 °C under a nitrogen atmosphere was added allyl alcohol (20 mL) over 1 h, and the resulting solution stirred at ambient temperature for 30 min. The resulting solution was added to a stirred solution of 2,2,2-trichloroacetyl pyrrole (11.2 g, 53.1 mmol) in dry THF (20 mL) and allyl alcohol (20 mL) at <4 °C under a nitrogen atmosphere over 1 h, the solution stirred for an additional 45 min at <4 °C and then at ambient temperature for 18 h. Phosphate buffer, pH = 7 (25 mL) was added and the pH of the solution lowered to pH = 7 by addition of 4M aq. HCl. Volatiles were removed *in vacuo*, added water (50 mL) and the aq. phase extracted with EtOAc (2x). The combined organic extracts were washed with brine (1x), dried over MgSO₄, filtered, and concentrated *in vacuo*. The resulting residue was triturated with hexane (3x 15 mL) to afford **2.39** as a brown oil (8.53 g, 100%). ¹H NMR (500 MHz, CDCl₃) δ 4.79 (m, 2H, CH₂CHCH₂), 5.23 (m, 1H, CH₂CHCHH), 5.40 (m, 1H, CH₂CHCHH), 6.02 (m, 1H, CH₂CHCH₂), 6.28 (m, 1H, NHCH), 6.98 (m, 2H, NHCHCHCH), 9.60 (br s, 1H, NH); ¹³C NMR (125 MHz, CDCl₃) δ 67.6, 113.1, 118.2, 120.8, 125.2, 125.8, 135.0, 163.7. HRMS (ESI) 152.0687 (M+H)⁺; C₈H₁₀NO₂ requires 152.0706.

Allyl 5-formyl-1H-pyrrole-2-carboxylate 2.40

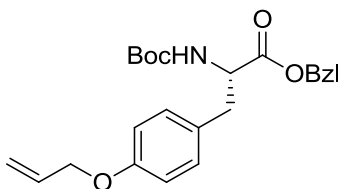
Phosphoryl chloride (2.42 mL, 37.5 mmol) was added dropwise to a stirred solution of DMF (2.82 mL, 37.5 mmol) cooled to 15 °C under a nitrogen atmosphere over 15 min. DCE (8 mL) and a solution of **2.39** (5.00 g, 31.0 mmol) in DCE (8 mL) were added sequentially to the solution over 1 h. The resulting solution was heated at reflux for 15 min, cooled to ambient temperature, treated with a solution of sodium acetate tetrahydrate (22.7 g, 167 mmol) in water (30 mL) and heated at reflux for an additional 15 min. The aq. layer was extracted with CH₂Cl₂ (3x), the combined organics were washed with sat. aq. NaHCO₃ (3x), dried over MgSO₄, filtered, and concentrated *in vacuo*. The crude product was purified by flash chromatography on silica (0-10% EtOAc / CH₂Cl₂) to afford **2.40** as an orange solid (1.31 g, 22%). *R_f* = 0.50 (10% EtOAc / CH₂Cl₂); ¹H NMR (500 MHz, CDCl₃) δ 4.83 (br d, *J* = 5.8 Hz, 2H, CH₂CHCH₂), 5.32 (m, 1H, CH₂CHCHH), 5.42 (m, 1H, CH₂CHCHH), 6.01 (m, 1H, CH₂CHCH₂), 6.96 (m, 2H, NHCHCH), 9.68 (s, 1H, CHO), 10.05 (br s, 1H, NH); ¹³C NMR (125 MHz, CDCl₃) δ 68.5, 118.5, 121.8, 122.4, 130.8, 134.2, 137.2, 162.7, 183.0. LRMS (ESI) 381.0 (2M+Na)⁺; (C₉H₉NO₃)₂Na requires 381.1.

5-((Allyloxy)carbonyl)-1H-pyrrole-2-carboxylic acid 2.41

To a stirred solution of **2.40** (1.10 g, 6.14 mmol) in DMSO (10 mL) was added a solution of monosodium phosphate (4.45 g, 37.1 mmol) in water (10 mL). A solution of sodium chlorite (2.01 g, 22.2 mmol) in water (5 mL) was added dropwise over 5 min and the resulting solution stirred at ambient temperature for 3 h. The reaction was quenched by addition of sat. aq. NaHCO₃ (25 mL), water (30 mL) was added and the aq. mixture was washed consecutively with Et₂O (25 mL) and EtOAc (25 mL). The mixture was acidified to pH = 1 with 1M aq. HCl and extracted with EtOAc (3x). The combined organics were washed with brine (1x), dried over MgSO₄, filtered, and concentrated *in vacuo* to afford **2.41** as a pale white solid (1.13 g, 94%). ¹H NMR (500 MHz, DMSO-*d*₆) δ 4.73 (br d, *J* = 5.0 Hz, 2H, CH₂CHCH₂), 5.24 (m, 1H, CH₂CHCHH), 5.39 (m, 1H, CH₂CHCHH), 6.00 (m, 1H, CH₂CHCH₂), 6.77 (m, 1H, NHCCHCH), 6.83 (m, 1H, NHCCHCH), 12.50 (s, 1H, NH), 12.85 (br s, 1H, CO₂H); ¹³C NMR (125 MHz, DMSO-*d*₆) δ 67.6, 118.2, 118.6, 120.9, 129.0, 131.1, 135.8, 162.6, 164.3. HRMS (ESI) 218.0421 (M+Na)⁺; C₉H₉NNaO₄ requires 218.0424.

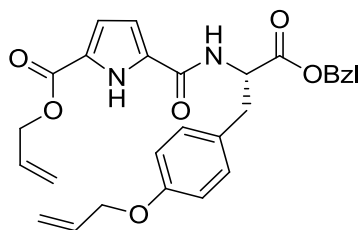
(S)-Benzyl 2-((tert-butoxycarbonyl)amino)-3-(4-hydroxyphenyl)propanoate 2.43

To a solution of Boc-L-tyrosine (5.86 g, 20.8 mmol) in dry THF (25 mL) was added sequentially DIPEA (3.79 mL, 20.8 mmol) and benzyl bromide (4.95 mL, 41.6 mmol), and the resulting solution left to stir at ambient temperature for 18 h under a nitrogen atmosphere. The mixture was concentrated *in vacuo*, added water (15 mL) and the mixture extracted with EtOAc (3x). The combined organics were washed with brine (1x), dried over MgSO₄, filtered, and concentrated *in vacuo*. The crude product was purified by flash chromatography on silica (0-50% EtOAc / Hexane) to afford **2.43** as a white solid (4.75 g, 55%). $R_f = 0.20$ (30% EtOAc / Hexane); ¹H NMR (500 MHz, CDCl₃) δ 1.43 (s, 9H, C(CH₃)₃), 3.02 (m, 2H, CHCH₂), 4.58 (m, 1H, CHCH₂), 5.01 (d, $J = 7.9$ Hz, 1H, NH), 5.10 (d, $J = 12.2$ Hz, 1H, CO₂CHHC₆H₅), 5.18 (d, $J = 12.2$ Hz, 1H, CO₂CHHC₆H₅), 6.06 (br s, 1H, OH), 6.69 (d, $J = 8.3$ Hz, 2H, 2x HOCCHCH), 6.88 (d, $J = 8.3$ Hz, 2H, 2x HOCCHCH), 7.33 (m, 5H, C₆H₅); ¹³C NMR (125 MHz, CDCl₃) δ 28.1, 37.1, 54.6, 67.1, 80.3, 115.4, 126.7, 128.4, 130.2, 134.9, 155.4, 172.0. Experimental data as per literature.¹³³

(S)-Benzyl 3-(4-(allyloxy)phenyl)-2-((tert-butoxycarbonyl)amino)propanoate**2.44**

To a solution of **2.43** (3.50 g, 9.43 mmol) in dry DMF (16 mL) was added sequentially dry K_2CO_3 (2.61 g, 18.9 mmol), TBAI (0.36 g, 1.12 mmol) and allyl bromide (2.85 mL, 33.0 mmol) and the solution stirred at 40 °C for 18 h under a nitrogen atmosphere. Water (10 mL) was added and the mixture extracted with EtOAc (3x). The combined organics were washed with 1M aq. HCl (15 mL), brine (3x), dried over $MgSO_4$, filtered, and concentrated *in vacuo*. The crude product was purified by flash chromatography on silica (0-30% EtOAc / Hexane) to afford **2.44** as a white solid (3.22 g, 92%). $R_f = 0.60$ (30% EtOAc / Hexane); 1H NMR (500 MHz, $CDCl_3$) δ 1.42 (s, 9H, $C(CH_3)_3$), 3.00 (m, 2H, $CHCH_2$), 4.50 (ddt~ddd, $J = 5.3, 3.0, 1.4$ Hz, 2H, OCH_2CHCH_2), 4.60 (m, 1H, $CHCH_2$), 4.98 (d, $J = 7.7$ Hz, 1H, **NH**), 5.11 (d, $J = 12.3$ Hz, 1H, $CO_2CH_2C_6H_5$), 5.18 (d, $J = 12.3$ Hz, 1H, $CO_2CH_2C_6H_5$), 5.29 (ddt~ddd, $J = 10.5, 2.8, 1.4$ Hz, 1H, OCH_2CHCHH), 5.42 (ddt~ddd, $J = 17.3, 10.5, 4.7$ Hz, 1H, OCH_2CHCHH), 6.06 (ddt, $J = 17.3, 10.5, 5.4$ Hz, 1H, OCH_2CHCH_2), 6.79 (d, $J = 8.3$ Hz, 2H, 2x $OCCHCH$), 6.95 (d, $J = 8.3$ Hz, 2H, 2x $OCCHCH$), 7.34 (m, 5H, C_6H_5); ^{13}C NMR (125 MHz, $CDCl_3$) δ 31.0, 40.1, 57.3, 69.7, 71.4, 82.5, 117.4, 120.3, 130.7, 131.1, 131.2, 131.2, 133.0, 136.0, 137.9, 157.8, 160.3, 174.5. HRMS (ESI) 450.1676 ($M+K$) $^+$; $C_{24}H_{29}NKO_5$ requires 450.1678.

(S)-Allyl 5-((3-(4-(allyloxy)phenyl)-1-(benzyloxy)-1-oxopropan-2-yl)carbamoyl)-1H-pyrrole-2-carboxylate 2.46

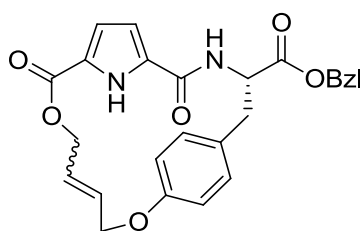


To a solution of **2.44** (400 mg, 0.973 mmol) in dry CH_2Cl_2 (0.5 mL) was added TFA (0.5 mL, 6.53 mmol) and the mixture stirred at ambient temperature for 1.5 h under a nitrogen atmosphere. The mixture was concentrated *in vacuo* and washed sequentially with CH_2Cl_2 (2x) and MeOH (2x), concentrating *in vacuo* following each wash to give **2.45** as a crude light brown oil (460 mg, 100%) which was used without further purification.

Crude **2.45** (460 mg) was coupled to **2.41** (240 mg, 1.23 mmol) according to general procedure A and the crude product was purified by flash chromatography on silica (0-40 % EtOAc / Hexane) to afford **2.46** as a yellow oil (390 mg, 76%). R_f = 0.49 (50% EtOAc / Hexane); ^1H NMR (500 MHz, CDCl_3) δ 3.16 (m, 2H, CHCH_2), 4.50 (ddt~ddd, J = 5.3, 3.0, 1.4 Hz, 2H, $\text{OCH}_2\text{CHCH}_2$), 4.81 (ddt~ddd, J = 5.8, 2.4, 1.1 Hz, 2H, $\text{CO}_2\text{CH}_2\text{CHCH}_2$), 5.03 (m, 1H, CHCH_2), 5.10 (d, J = 12.0 Hz, 1H, $\text{CO}_2\text{CHHC}_6\text{H}_5$), 5.25 (d, J = 12.0 Hz, 1H, $\text{CO}_2\text{CHHC}_6\text{H}_5$), 5.30 (m, 2H, OCH_2CHCHH , $\text{CO}_2\text{CH}_2\text{CHCHH}$), 5.39 (m, 1H, OCH_2CHCHH), 5.42 (m, 1H, $\text{CO}_2\text{CH}_2\text{CHCHH}$), 6.04 (m, 2H, $\text{OCH}_2\text{CHCH}_2$, $\text{CO}_2\text{CH}_2\text{CHCH}_2$), 6.41 (d, J = 7.8 Hz, 1H, NHCCH_2), 6.56 (m, 1H, NHCCH), 6.60 (d, J = 7.8 Hz, 1H, NHCCH), 6.77 (d, J = 8.6 Hz, 2H, 2x OCCHCH), 6.89 (d, J = 8.6 Hz, 2H, 2x OCCHCH), 6.92 (m, 1H, NHCCH), 7.38 (m, 5H, C_6H_5), 10.38 (s, 1H, NHCCH); ^{13}C

NMR (125 MHz, CDCl₃) δ 39.7, 56.2, 68.4, 70.4, 71.5, 112.7, 117.5, 118.4, 120.3, 121.4, 131.3, 131.3, 131.4, 130.0, 134.6, 135.9, 137.6, 160.5, 162.5, 173.9. HRMS (ESI) 511.1844 (M+Na)⁺; C₂₈H₂₈N₂NaO₆ requires 511.1839.

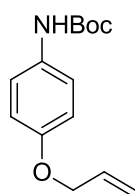
Benzyl (3*S*,13*E/Z*)-5,10-dioxo-11,16-dioxa-4,22-diazatricyclo[15.2.2.1^{6,9}]docosa-1(19),6,8,13,17,20-hexaene-3-carboxylate **2.47**



To a solution of **2.46** (100 mg, 0.205 mmol) in dry EtOAc (100 mL) was added Ti(O*i*Pr)₄ (0.24 mL, 0.811 mmol) and the solution was heated to 45 °C. Grubbs 2nd generation catalyst (17 mg, 0.02 mmol) in dry EtOAc (6 mL) was added portion wise (2 mL) at 1 h intervals over 3 h and the resulting solution stirred at 55 °C under an argon atmosphere following each addition. The solution was stirred for an additional 1 h, the reaction quenched by addition of 1M Tris(hydroxymethyl) phosphine in isopropyl alcohol (5 mL, 5 mmol) and stirred at 45 °C for 24 h under an argon atmosphere. Nitrogen-degassed water (15 mL) was added, the solution stirred vigorously for 10 minutes, and the aqueous phase removed (3x). The organic phase was washed with 1M aq. HCl, sat. NaHCO₃ (1x), brine (1x), dried over MgSO₄, filtered, and volatiles removed *in vacuo*. The crude product was purified by flash chromatography (0-40 % EtOAc / Hexane) to afford **2.47** as 2:1 mixture of E/Z isomers as a colourless oil (46 mg, 50%). ¹H NMR (500 MHz, CDCl₃) δ 3.16 (m, 2H, NHCHCH₂), 4.48 (dd, *J* = 11.0, 5.8 Hz, 1H, OCHHCHCH₂), 4.76 (m, 2H,

CO₂CH₂CHCH₂), 4.95 (dd, $J = 11.0, 5.8$ Hz, 1H, OCHHCHCH₂), 5.11 (m, 1H, NHCHCH₂), 5.23 (d, $J = 12.0$ Hz, 1H, CO₂CHHC₆H₅), 5.37 (d, $J = 12.0$ Hz, 1H, CO₂CHHC₆H₅), 5.89 (m, 2H, OCH₂CHCHCH₂), 6.67 (d, $J = 8.4$ Hz, 2H, OCCH₂CH₂), 6.77 (d, $J = 8.4$ Hz, 2H, OCCH₂CH₂), 6.83 (m, 1H, NHCCH), 6.97 (m, 1H, NHCCH), 7.41 (m, 5H, C₆H₅), 8.88 (s, 1H, NHCCHCH); ¹³C NMR (125 MHz, CDCl₃) δ 39.4, 54.1, 63.1, 66.0, 69.2, 70.4, 116.8, 119.2, 131.2, 131.4, 131.5, 131.7, 134.4, 158.6, 159.1, 174.1. HRMS (ESI) 483.1525 (M+Na)⁺; C₂₆H₂₄N₂NaO₆ requires 483.1526.

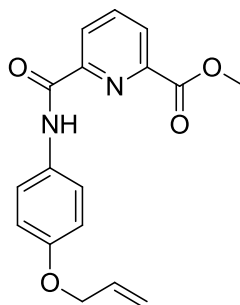
***tert*-Butyl (4-(allyloxy)phenyl)carbamate 2.52**



To a solution of *tert*-Butyl(4-hydroxyphenyl)carbamate (8.0 g, 38.2 mmol) in ACN (350 mL) was added sequentially K₂CO₃ (5.28 g, 38.2 mmol) and allyl bromide (3.23 mL, 38.2 mmol), the mixture stirred at reflux for 3h, and then stirred at ambient temperature under a nitrogen atmosphere for 18 h. The mixture was concentrated *in vacuo*, added water and the mixture extracted with EtOAc (3x). The combined organics were washed with brine (1x), dried over MgSO₄, filtered, and concentrated *in vacuo*. The crude product was purified by flash chromatography on silica (20% EtOAc / Hexane) to afford **2.52** as a white solid (7.26 g, 76%). $R_f = 0.47$ (20% EtOAc / Hexane); ¹H NMR (500 MHz, CDCl₃) δ 1.52 (s, 9H, C(CH₃)₃), 4.51 (ddt~ddd, $J = 5.3, 2.9, 1.3$ Hz, 2H, OCH₂CHCH₂), 5.28 (ddt~ddd, $J = 10.5, 2.9, 1.3$ Hz, 1H, OCH₂CHCHH), 5.41 (ddt~ddd, $J = 17.3, 10.5, 5.3$ Hz, 1H, OCH₂CHCHH), 6.05 (ddt, $J = 17.3, 10.5, 5.3$ Hz, 1H, OCH₂CHCH₂), 6.34 (br s, 1H, NH),

6.87 (m, 2H, 2x OCCHCH), 7.26 (m, 2H, 2x OCCHCH); ^{13}C NMR (125 MHz, CDCl_3) δ 31.0, 71.8, 80.2, 117.8, 120.2, 123.1 134.2, 136.0, 155.8, 157.3. Experimental data as per literature.¹³⁴

Methyl 6-((4-(allyloxy)phenyl)amino)picolinate **2.54**

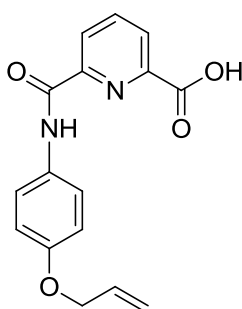


To a solution of **2.52** (2.93 g, 11.8 mmol) in dry CH_2Cl_2 (120 mL) was added TFA (20 mL, 261 mmol) under a nitrogen atmosphere. The reaction mixture was stirred at ambient temperature for 30 min and volatiles removed *in vacuo*. The resulting dark red oil was washed with CH_2Cl_2 and concentrated *in vacuo* (7x) to afford **2.53** as a dark red oil which crystallised on standing at 4°C (fridge) and was used without further purification (3.05 g, 100%).

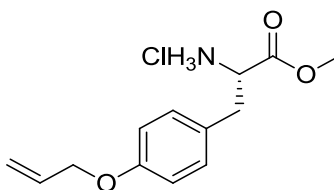
Crude **2.53** (3.05 g, 11.5 mmol) was coupled to 6-(methoxycarbonyl)picolinic acid (2.09 g, 11.5 mmol) per general procedure A and the crude product was purified by flash chromatography on silica (0-5% EtOAc / CH_2Cl_2) to afford **2.54** as a pale red solid (3.18 g, 89%). $R_f = 0.39$ (5% EtOAc / CH_2Cl_2); ^1H NMR (500 MHz, CDCl_3) δ 4.01 (s, 3H, OCH_3), 4.52 (ddt~ddd, $J = 5.3, 1.5$ Hz, 1.4 Hz, 2H, $\text{OCH}_2\text{CHCH}_2$), 5.27 (ddt~ddd, $J = 10.5, 3.0, 1.4$ Hz, 1H, OCH_2CHCHH), 5.40 (ddt~ddd, $J = 17.3, 3.0, 1.5$ Hz, 1H, OCH_2CHCHH), 6.04 (ddt, $J = 17.3, 10.5$ Hz, 5.3 Hz, 1H, $\text{OCH}_2\text{CHCH}_2$), 6.92 (m, 2H, 2x OCCHCH), 7.68 (m, 2H, 2x OCCHCH), 8.02 (t, $J = 7.8$ Hz, 1H, NCCHCH),

8.21 (d, $J = 7.8$ Hz, 1H, NCCHCH), 8.43 (d, $J = 7.8$ Hz, 1H, NCCHCH), 9.86 (s, 1H, NH); ^{13}C NMR (125 MHz, CDCl_3) δ 55.6, 71.7, 117.7, 120.3, 124.3, 128.0, 130.0, 133.4, 135.9, 141.4, 149.1, 152.9, 158.2, 163.5, 167.4. HRMS (ESI) 330.1458 ($\text{M}+\text{NH}_4$) $^+$; $\text{C}_{16}\text{H}_{20}\text{N}_3\text{O}_4$ requires 330.1448.

6-((4-(Allyloxy)phenyl)amino)picolinic acid **2.55**

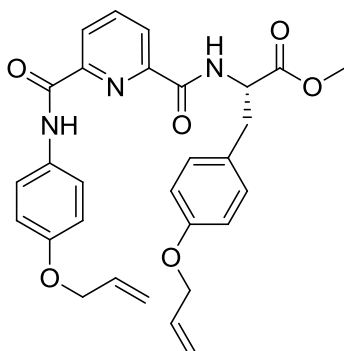


2.54 (2.50 g, 8.8 mmol) was hydrolysed according to general procedure B to afford **2.55** as a pale green solid (2.17 g, 91%). ^1H NMR (500 MHz, $\text{DMSO}-d_6$) δ 4.56 (m, 2H, $\text{OCH}_2\text{CHCH}_2$), 5.26 (ddt~ddd, $J = 10.5, 3.0, 1.4$ Hz, 1H, OCH_2CHCHH), 5.40 (ddt~ddd, $J = 17.3, 3.0, 1.6$ Hz, 1H, OCH_2CHCHH), 6.05 (ddt, $J = 17.3, 10.5, 5.4$ Hz, 1H, $\text{OCH}_2\text{CHCH}_2$), 7.00 (d, $J = 9.0$ Hz, 2H, 2x OCCHCH), 7.71 (d, $J = 9.0$ Hz, 2H, 2x OCCHCH), 8.28 (m, 2H, NCCHCH, NCCHCH), 8.37 (dd, $J = 7.5, 3.0$ Hz, 1H, NCCHCH), 10.77 (s, 1H, NH), 13.17 (br s, 1H, CO_2H); ^{13}C NMR (125 MHz, $\text{DMSO}-d_6$) δ 71.5, 117.9, 120.5, 125.4, 128.8, 129.9, 134.2, 136.9, 143.2, 149.1, 152.4, 158.1, 164.1, 167.8. HRMS (ESI) 321.0836 ($\text{M}+\text{Na}$) $^+$; $\text{C}_{16}\text{H}_{14}\text{N}_2\text{NaO}_4$ requires 321.0846.

(S)-3-(4-(Allyloxy)phenyl)-1-methoxy-1-oxopropan-2-aminium chloride 2.57

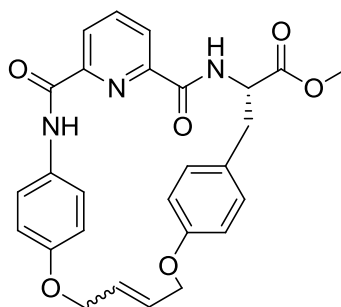
To a solution of Boc-L-Tyr(Allyl)-OH (7.00 g, 21.8 mmol) in dry MeOH (50 mL) was added thionyl chloride (6.33 mL, 87.2 mmol) dropwise at <4 °C under a nitrogen atmosphere, and the solution was left to stir at <4 °C for 1 h. The solution was warmed to ambient temperature and then stirred at ambient temperature for 18 h. The mixture was concentrated *in vacuo* and the resulting residue washed with MeOH and concentrated *in vacuo* (3x) to afford **2.57** as a yellow, crystalline solid (5.92 g, 100%). ^1H NMR (500 MHz, DMSO- d_6) δ 3.05 (dd, $J = 13.8, 7.2$ Hz, 2H, NCHCHH), 3.15 (dd, $J = 13.8, 7.2$ Hz, 2H, NCHCHH), 3.63 (s, 3H, OCH $_3$), 4.13 (m, 1H, NCHCH $_2$), 4.52 (br d, $J = 5.2$ Hz, 2H, OCH $_2$ CHCH $_2$), 5.37 (br d, $J = 17.2$ Hz, 1H, OCH $_2$ CHCHH), 6.02 (m, 1H, OCH $_2$ CHCH $_2$), 6.88 (d, $J = 8.6$ Hz, 2H, 2x OCCHCH), 7.14 (d, $J = 8.6$ Hz, 2H, 2x OCCHCH), 8.80 (br s, 3H, NH $_3$); ^{13}C NMR (125 MHz, DMSO- d_6) δ 38.1, 55.6, 55.6, 71.3, 117.8, 120.5, 129.7, 133.6, 136.9, 160.5, 172.5. Experimental data as per literature.¹³⁵

(S)-Methyl3-(4-(allyloxy)phenyl)-2-(6-((4-allyloxy)phenyl)carbamoyl)picolinamido)propanoate 2.58



2.55 (1.50 g, 5.03 mmol) was coupled to **2.57** (1.38 g, 5.09 mmol) according to general procedure A and the crude product was purified by flash chromatography on silica (60% EtOAc / Hexane) to afford **2.58** as a viscous yellow solid (2.59 g, 100%). $R_f = 0.54$ (60% EtOAc / Hexane); $^1\text{H NMR}$ (500 MHz, $\text{DMSO-}d_6$) δ 3.21 (m, 2H, NHCHCH_2), 3.68 (s, 3H, OCH_3), 4.42 (br d, $J = 5.1$ Hz, 2H, $\text{OCH}_2\text{CHCH}_2$), 4.49 (br d, $J = 5.1$ Hz, 2H, $\text{OCH}_2\text{CHCH}_2$), 4.69 (m, 1H, NHCHCH_2), 5.17 (m, 1H, OCH_2CHCHH), 5.28 (m, 2H, OCH_2CHCHH , OCH_2CHCHH), 5.41 (m, 1H, OCH_2CHCHH), 5.94 (m, 1H, $\text{OCH}_2\text{CHCH}_2$), 6.06 (m, 1H, $\text{OCH}_2\text{CHCH}_2$), 6.78 (d, $J = 8.4$ Hz, 2H, 2x OCCHCH), 7.06 (d, $J = 8.4$ Hz, 2H, 2x OCCHCH), 7.30 (d, $J = 8.5$ Hz, 2H, 2x OCCHCH), 7.77 (d, $J = 8.5$ Hz, 2H, 2x OCCHCH), 8.20 (m, 2H, NCCHCH), 8.32 (m, 1H, NCCHCH), 9.63 (d, $J = 7.8$ Hz, 1H, NHCHCH_2), 10.79 (s, 1H, NHCCHCH); $^{13}\text{C NMR}$ (125 MHz, $\text{DMSO-}d_6$) δ 38.5, 57.7, 57.7, 71.1, 71.5, 117.5, 117.9, 120.4, 120.5, 125.8, 127.9, 128.1, 132.6, 133.1, 134.2, 136.8, 136.9, 142.9, 151.2, 152.0, 158.2, 160.0, 164.3, 166.4, 176.2. HRMS (ESI) 538.1942 ($\text{M}+\text{Na}$) $^+$; $\text{C}_{29}\text{H}_{29}\text{N}_3\text{NaO}_6$ requires 538.1948.

Methyl(11S,19E/Z)-3,9-dioxo-17,22-dioxa-2,10,30-triazatetracyclo[21.2.2.2^{13,16}.1^{4,8}]triaconta-1(25),4,6,8(30),13,15,19,23,26,28-decaene-11-carboxylate **2.59**



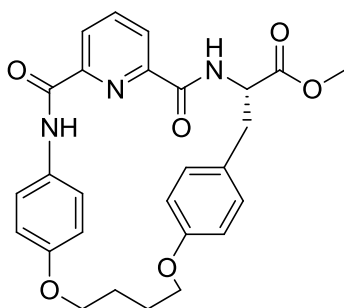
To a solution of **2.58** (60 mg, 0.12 mmol) in dry CH₂Cl₂ (150 mL) heated at reflux was added Grubbs 2nd generation catalyst (10 mg, 0.01 mmol) in dry CH₂Cl₂ (2 mL) and the resulting solution stirred at reflux for 0.5 h under an argon atmosphere. An additional portion of Grubbs 2nd generation catalyst (10 mg, 0.01 mmol) in dry CH₂Cl₂ (2 mL) was added and the solution was stirred at reflux for 18 h. The reaction quenched by addition of 1M Tris(hydroxymethyl) phosphine in isopropyl alcohol (3 mL, 3mmol) and stirred at reflux for 24 h under an argon atmosphere. Nitrogen-degassed water (20 mL) was added, the solution stirred vigorously for 10 minutes, and the aqueous phase removed (3x). The organic phase was washed with 1M aq. HCl, sat. NaHCO₃ (1x), brine (1x), dried over MgSO₄, filtered, and volatiles removed *in vacuo*. The crude product was purified by flash chromatography (0-100 % EtOAc / Hexane) to afford **2.59** as 1.7:1 mixture of E/Z isomers as a white solid (18 mg, 50%). ¹H NMR (500 MHz, CDCl₃) δ 3.13 (m, 1H, NHCHCHH), 3.35 and 3.43 (dd, *J* = 3.7, 14.0 Hz, 1H, NHCHCHH), 3.84 and 3.87 (s, 3H, CO₂CH₃), 3.95 (m, 1H, OCHHCHCHCHH), 4.13 (m, 1H, OCHHCHCHCHH), 4.55 (m, 1H, OCHHCHCHCHH), 4.67 (m, 1H, OCHHCHCHCHH), 5.20 and 5.30 (m, 1H,

NHCHCH₂), 5.76 and 6.08 (m, 2H, OCHHCHCHHH), 6.80 (d, $J = 8.4$ Hz, 2H, 2x OCCHCH), 6.97 (m, 2H, 2x OCCHCH), 7.09 (d, $J = 8.4$ Hz, 2H, 2x OCCHCH), 7.46 (d, $J = 8.4$ Hz, 1H, 2x OCCHCH), 8.09 (m, 2H, NCCHCH, NHCHCH₂), 8.39 (m, 1H, NCCHCH), 8.47 (m, 1H, NCCHCH), 9.20 (s, 1H, NHCCHCH); ¹³C NMR (125 MHz, CDCl₃) δ 32.4, 39.5, 39.7, 54.6, 54.9, 55.2, 69.7, 69.9, 70.2, 70.5, 117.2, 117.4, 117.6, 118.0, 124.1, 124.2, 127.8, 127.9, 129.8, 130.3, 130.5, 130.7, 133.2, 133.2, 133.3, 133.4, 142.2, 150.8, 150.9, 151.5, 151.5, 158.0, 160.5, 163.3, 163.3, 165.2, 165.2, 174.0, 174.1. HRMS (ESI) 510.1638 (M+Na)⁺; C₂₇H₂₅N₃NaO₆ requires 510.1635.

Methyl(11S)-3,9-dioxo-17,22-dioxa-2,10,30-

triazatetracyclo[21.2.2.2^{13,16}.1^{4,8}]triaconta-1(25),4,6,8(30),13,15,23,26,28-

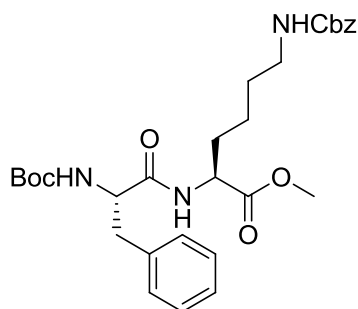
nonaene-11-carboxylate 2.60



To a solution of **2.59** (15 mg, 0.03 mmol) in CH₂Cl₂ (4 mL), EtOAc (3 mL) and MeOH (3 mL) was added 10 % palladium on activated carbon and the resulting mixture stirred under a hydrogen atmosphere for at ambient temperature for 18 h. The mixture was filtered through a short pad of silica and concentrated *in vacuo* to afford crude **2.60** as a white solid (14 mg, 90%) which was used without further purification.

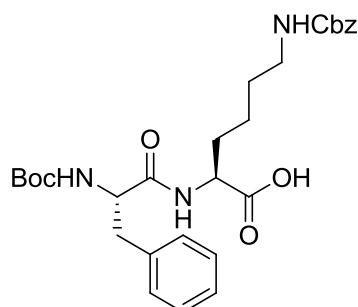
4.4 Experimental Work Described in Chapter Three

(S)-Methyl 6-((benzyloxy)carbonylamino)-2-((S)-2-((tert-butoxycarbonyl)amino)-3-phenylpropanamido)hexanoate **3.05**



N^α -Boc-L-Phenylalanine (300 mg, 1.13 mmol) was coupled to N^ϵ -Z-L-Lysine methyl ester hydrochloride (374 mg, 1.13 mmol) according to general procedure A and the crude product purified by flash chromatography on silica (50% EtOAc / Hexane) to afford **3.05** as a colourless gum (570 mg, 93%). R_f = 0.44 (50% EtOAc / Hexane); ^1H NMR (500 MHz, CDCl_3) δ 1.23 (m, 2H, $\text{NHCH}_2\text{CH}_2\text{CH}_2\text{CH}_2\text{CH}$), 1.34 (s, 9H, $\text{C}(\text{CH}_3)_3$), 1.46 (m, 2H, $\text{NHCH}_2\text{CH}_2\text{CH}_2\text{CH}_2\text{CH}$), 1.63 (m, 1H, $\text{NHCH}_2\text{CH}_2\text{CH}_2\text{CHHCH}$) 1.73 (m, 1H, $\text{NHCH}_2\text{CH}_2\text{CH}_2\text{CHHCH}$), 2.83 (m, 1H, $\text{CO}_2\text{NHCHCHH}$), 3.11 (m, 2H, $\text{CO}_2\text{NHCHCHH}$, $\text{NHCHHCH}_2\text{CH}_2\text{CH}_2\text{CH}$), 3.17 (m, 1H, $\text{NHCHHCH}_2\text{CH}_2\text{CH}_2\text{CH}$), 3.64 (s, 3H, CO_2CH_3), 4.53 (m, 2H, $\text{CO}_2\text{NHCHCHH}$, $\text{NHCH}_2\text{CH}_2\text{CH}_2\text{CH}_2\text{CH}$), 5.04 (d, J = 12.1 Hz, 1H, $\text{CO}_2\text{CHHCH}_6\text{H}_5$), 5.11 (d, J = 12.1 Hz, 1H, $\text{CO}_2\text{CHHCH}_6\text{H}_5$), 5.42 (d, J = 8.2 Hz, 1H, $\text{CO}_2\text{NHCH}_2\text{C}_6\text{H}_5$), 5.82 (br s, 1H, $\text{NHCH}_2\text{CH}_2\text{CH}_2\text{CH}_2\text{CH}$), 7.20 (m, 10H, 2x C_6H_5); ^{13}C NMR (125 MHz, CDCl_3) δ 30.9, 31.9, 34.4, 41.2, 43.2, 54.7, 54.9, 58.2, 69.2, 80.2, 82.7, 129.3, 130.7, 130.7, 131.1, 131.1, 131.9, 139.4, 139.4, 158.5, 159.3, 174.8, 175.0. HRMS (ESI) 564.2676 ($\text{M}+\text{Na}$) $^+$; $\text{C}_{29}\text{H}_{39}\text{N}_3\text{NaO}_7$ requires 564.2680.

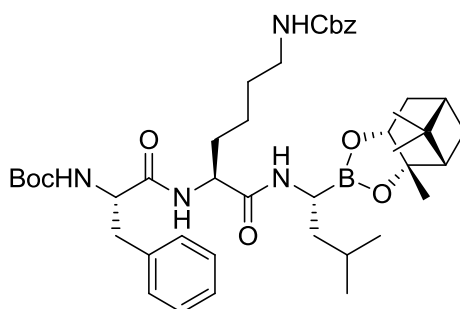
(S)-Methyl 6-((benzyloxy)carbonylamino)-2-((S)-2-((tert-butoxycarbonyl)amino)-3-phenylpropanamido)hexanoic acid **3.07**



3.05 (487 mg, 0.90 mmol) was hydrolysed according to general procedure B to afford **3.07** as a viscous colourless solid (472 mg, 100%). ^1H NMR (500 MHz, DMSO- d_6) δ 1.22 (m, 2H, $\text{NHCH}_2\text{CH}_2\text{CH}_2\text{CH}_2\text{CH}$), 1.30 (s, 9H, $\text{C}(\text{CH}_3)_3$), 1.41 (m, 2H, $\text{NHCH}_2\text{CH}_2\text{CH}_2\text{CH}_2\text{CH}$), 1.61 (m, 1H, $\text{NHCH}_2\text{CH}_2\text{CH}_2\text{CHHCH}$) 1.73 (m, 1H, $\text{NHCH}_2\text{CH}_2\text{CH}_2\text{CHHCH}$), 2.72 (m, 1H, $\text{NHCHHCH}_2\text{CH}_2\text{CH}_2\text{CH}$), 2.98 (m, 3H, $\text{CO}_2\text{NHCHCH}_2$, $\text{NHCHHCH}_2\text{CH}_2\text{CH}_2\text{CH}$), 4.20 (m, 2H, $\text{CO}_2\text{NHCHCH}_2$, $\text{NHCH}_2\text{CH}_2\text{CH}_2\text{CH}_2\text{CH}$), 5.00 (br, s, 2H, $\text{CO}_2\text{CH}_2\text{C}_6\text{H}_5$), 6.87 (d, $J = 8.7$ Hz, 1H, NHCHCO_2H), 7.27 (m, 10H, 2x C_6H_5), 8.06 (d, $J = 7.7$ Hz, 1H, $\text{NHCHCH}_2\text{C}_6\text{H}_5$), 12.60 (br s, 1H, CO_2H); ^{13}C NMR (125 MHz, DMSO- d_6) δ 31.2, 32.2, 34.0, 40.4, 43.2, 54.9, 58.7, 68.2, 81.1, 81.3, 129.3, 130.8, 131.1, 131.4, 132.3, 140.4, 141.3, 158.3, 159.2, 174.9, 176.6. HRMS (ESI) 550.2521 ($\text{M}+\text{Na}$) $^+$; $\text{C}_{29}\text{H}_{39}\text{N}_3\text{NaO}_7$ requires 550.2524.

Benzyl **N**[(5*S*)-5-[(2*S*)-2-[[*(tert*-butoxy)carbonyl]amino]3-3-phenylpropanamido]-5-[[*(1R*)-3-methyl-1-[[*(1S,2S,6R,8S)*]-2,9,9-trimethyl-3,5-dioxo-4-boratricyclo[6.1.1.0^{2,6}]decan-4-yl]butyl]carbamoyle]pentyl]carbamate

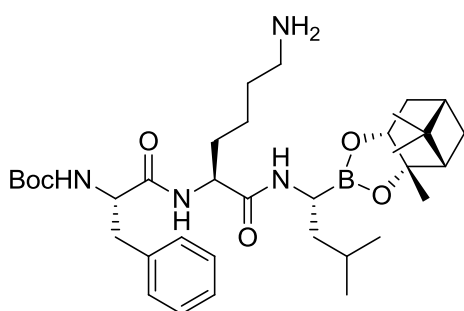
3.09



3.07 (70 mg, 0.132 mmol) was coupled to (*R*)-3-Methyl-1-((3*aS*,4*S*,6*S*,7*aR*)-3*a*,5,5-trimethylhexahydro-4,6-methanobenzo[d][1,3,2]dioxaborol-2-yl)butan-1-aminium 2,2,2-trifluoroacetate (50 mg, 0.132 mmol) according to general procedure A and the crude product purified by flash chromatography on silica (60% EtOAc / Hexane) to afford **3.09** as a white solid (93 mg, 92%). $R_f = 0.36$ (60% EtOAc / Hexane); $^1\text{H NMR}$ (500 MHz, CD_3OD) δ 0.85 (s, 3H, bridge CH_3), 0.95 (d, $J = 6.5$ Hz, 6H, 2x CHCH_2CH_3), 1.27 (s, 3H, bridge CH_3), 1.35 (s, 3H, CH_3CO), 1.38 (s, 9H, $\text{C}(\text{CH}_3)_3$), 1.39 (m, 2H, BOCCH , BOCHCHH), 1.44 (m, 4H, CH_3CHCH_2 , $\text{NHCH}_2\text{CH}_2\text{CH}_2\text{CH}_2\text{CH}$), 1.80 (m, 5H, $\text{NHCH}_2\text{CH}_2\text{CH}_2\text{CH}_2\text{CH}$, CH_3CHCH_2), 1.95 (t, $J = 5.6$ Hz, 1H, $\text{BOCHCH}_2\text{CHCHH}$), 2.13 (m, 1H, $\text{BOCHCH}_2\text{CHCHH}$), 2.32 (m, 1H, BOCHCHH), 2.72 (t, $J = 7.4$ Hz, BCH), 2.85 (m, 1H, $\text{NHCHCHHC}_6\text{H}_5$), 3.12 (m, 3H, $\text{NHCHCHHC}_6\text{H}_5$, $\text{NHCH}_2\text{CH}_2\text{CH}_2\text{CH}_2\text{CH}$), 4.17 (br d, $J = 8.5$ Hz, BOCH), 4.31 (m, 1H, $\text{NHCHCH}_2\text{C}_6\text{H}_5$), 4.51 (m, 1H, $\text{NHCH}_2\text{CH}_2\text{CH}_2\text{CH}_2\text{CH}$), 5.07 (m, 2H, $\text{NHCO}_2\text{CH}_2\text{C}_6\text{H}_5$), 7.28 (m, 10 H, 2x C_6H_5); $^{13}\text{C NMR}$ (125 MHz, CD_3OD) δ 24.0, 24.9, 25.1, 25.9, 28.0, 28.7, 29.1, 29.8, 30.0, 31.1, 33.2, 38.9, 40.2, 40.5, 42.6, 42.7, 43.0, 43.5, 52.6, 54.8,

58.8, 68.6, 78.7, 82.2, 85.6, 129.1, 130.1, 130.2, 130.7, 130.8, 131.6, 139.6, 159.3, 160.1, 175.8, 178.9. HRMS (ESI) 797.4639 ($M+Na$)⁺; $C_{43}H_{63}BN_4NaO_8$ requires 797.4631.

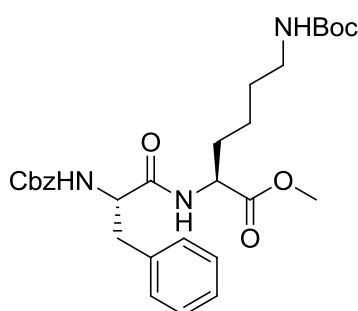
N-tert-Butyl(((S)-1-(((S)-6-amino-1-(((R)-3-methyl-1-((3aS,4S,6S,7aR)-3a,5,5-trimethylhexahydro-4,6-methanobenzo[d][1,3,2]dioxaborol-2-yl)butyl)amino)-1-oxohexan-2-yl)amino)-1-oxo-3-phenylpropan-2-yl)carbamate 3.11



To a solution of **3.09** (14 mg, 0.02 mmol) in MeOH (5 mL) and EtOAc (1.5 mL) was added 10% palladium on activated carbon (4 mg, 0.004 mmol) and the resulting mixture stirred under a hydrogen atmosphere at ambient temperature for 4 h. The mixture was filtered through a short pad of silica and concentrated *in vacuo* to afford **3.11** as a white solid (11 mg, 98%). ¹H NMR (500 MHz, CD₃OD) δ 0.86 (s, 3H, bridge CH₃), 0.94 (m, 6H, 2x CH₂CHCH₃), 1.25 (s, 3H, CH₃CO), 1.30 (m, 4H, CHCH₂CH₃, NHCH₂CH₂CH₂CH₂CH), 1.38 (s, 9H, C(CH₃)₃), 1.46 (m, 2H, BOCCH, BOCHCHH), 1.85 (m, 5H, NHCH₂CH₂CH₂CH₂CH, CHCH₂CH₃), 2.05 (m, 2H, BOCHCH₂CHCHH, BOCHCHH), 2.15 (t, *J* = 5.6 Hz, 1H, BOCHCH₂CHCHH), 2.63 (t, *J* = 7.0 Hz, 1H, BCH), 2.85 (m, 3H, NHCHCHHC₆H₅, NHCH₂CH₂CH₂CH₂CH), 3.10 (dd, *J* = 13.4, 5.1 Hz, 1H, CHHC₆H₅), 3.96 (d, *J* = 8.6 Hz, 1H, BOCH), 4.00 (m, 1H, NHCHCH₂C₆H₅), 4.31 (m, 1H, NHCH₂CH₂CH₂CH₂CH), 7.26 (m, 10 H, 2x C₆H₅); ¹³C

NMR (125 MHz, DMSO- d_6) δ 23.9, 25.5, 25.9, 26.8, 28.7, 29.0, 30.0, 31.0, 31.2, 31.6, 33.4, 38.7, 40.3, 41.1, 42.7, 42.9, 43.1, 47.1, 54.3, 62.9, 78.7, 81.2, 86.0, 129.3, 131.1, 132.3, 141.3, 158.3, 166.5, 176.5. HRMS (ESI) 663.4362 ($M+Na$)⁺; $C_{35}H_{57}BN_4NaO_6$ requires 663.4263.

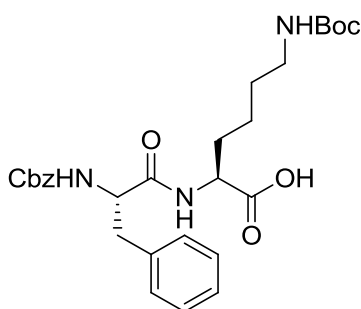
(S)-Methyl2-((S)-2-(((benzyloxy)carbonyl)amino)-3-phenylpropanamido)-6-((tert-butoxycarbonyl)amino)hexanoate 3.17



To a solution of N^{ϵ} -Boc-L-Lysine methyl ester hydrochloride (935 mg, 3.20 mmol) and N-Z-L-Phenylalanine (1.13 g, 3.80 mmol) in dry DMF (11 mL) was added sequentially DIPEA (2.2 mL, 12.6 mmol), hydroxybenzotriazole (851 mg, 6.30 mmol) and EDCI (906 mg, 4.70 mmol), and the resulting solution stirred at ambient temperature under a nitrogen atmosphere for 16 h. The mixture was partitioned between 1M aq. HCl and CH_2Cl_2 and the aq. phase extracted with CH_2Cl_2 (3x). The organic extracts were combined, washed with sat. aq. $NaHCO_3$ (1x), brine (2x), dried over $MgSO_4$, filtered, and concentrated *in vacuo*. The crude product purified by flash chromatography on silica (25 – 50% EtOAc / Hexane) to afford **3.17** as a white solid (1.56 g, 92%). R_f = 0.36 (50% EtOAc : Hexane); 1H NMR (500 MHz, CD_3OD) δ 1.34 (m, 2H, $NHCH_2CH_2CH_2CH_2CH$), 1.42 (s, 9H, $C(CH_3)_3$), 1.47 (m, 2H, $NHCH_2CH_2CH_2CH_2CH$), 1.68 (m, 1H, $NHCH_2CH_2CH_2CH_2CH$), 1.83 (m, 1H,

NHCH₂CH₂CH₂CHHCH), 2.85 (dd, *J* = 13.9, 5.4 Hz, 1H, CHCHHC₆H₅), 3.01 (m, 2H, NHCH₂CH₂CH₂CH₂CH), 3.13 (dd, *J* = 13.9, 5.4 Hz, 1H, CHCHHC₆H₅), 3.69 (s, 3H, CO₂CH₃), 4.42 (m, 2H, CHCH₂C₆H₅, NHCH₂CH₂CH₂CH₂CH), 5.03 (m, 2H, CO₂CH₂C₆H₅), 7.27 (m, 10H, 2x C₆H₅); ¹³C NMR (125 MHz, CD₃OD) δ 25.3, 30.1, 31.6, 33.5, 40.4, 42.3, 54.0, 54.9, 58.9, 68.8, 81.1, 129.0, 129.9, 130.2, 130.7, 130.7, 131.6, 139.4, 139.7, 159.4, 159.8, 175.1, 175.5. HRMS (ESI) HRMS (ESI) 564.2672 (M+Na)⁺; C₂₉H₃₉N₃NaO₇ requires 564.2680.

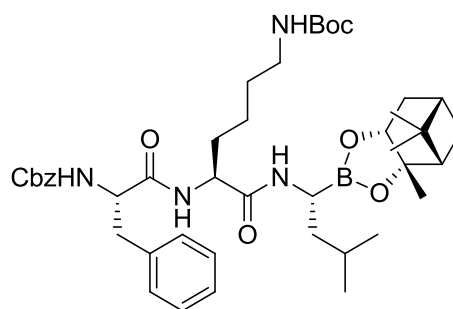
(S)-2-((S)-2-(((Benzyloxy)carbonyl)amino)-3-phenylpropanamido)-6-((tert-butoxycarbonyl)amino)hexanoic acid **3.19**



To a solution of **3.17** (1.56 g, 2.88 mmol) in dioxane (18 mL) and water (9 mL) was added 1M aq. NaOH (2.9 mL, 2.90 mmol) and the mixture was stirred at ambient temperature for 2 h. The resulting solution was washed with Et₂O and acidified to pH = 1 with 1M aq. HCl. The aq. phase was extracted with EtOAc (3x), the organic extracts combined and washed with brine (1x) dried over MgSO₄, filtered, and concentrated *in vacuo* to afford **3.19** as a white solid (1.42 g, 93%). ¹H NMR (500 MHz, DMSO-*d*₆) δ 1.30 (m, 2H, NHCH₂CH₂CH₂CH₂CH), 1.36 (s, 9H, C(CH₃)₃), 1.59 (m, 3H, NHCH₂CH₂CH₂CHHCH), 1.72 (m, 1H, NHCH₂CH₂CH₂CHHCH), 2.71 (dd, *J* = 13.9, 3.9 Hz, 1H, CHCHHC₆H₅), 2.89 (m, 2H, NHCH₂CH₂CH₂CH₂CH), 3.00 (dd, *J* = 13.9, 3.9

Hz, 1H, CHCHHC₆H₅), 4.16 (m, 1H, NHCH₂CH₂CH₂CH₂CH), 4.29 (m, 1H, CHCH₂C₆H₅), 6.76 (t, *J* = 5.6 Hz, 1H, NHCH₂CH₂CH₂CH₂CH), 7.25 (m, 10H, 2x C₆H₅), 7.45 (d, *J* = 8.8 Hz, 1H, CO₂NHCHCH₂C₆H₅), 8.22 (d, *J* = 7.6 Hz, 1H, NHCHCO₂H), 12.56 (br s, 1H, CO₂H); ¹³C NMR (125 MHz, DMSO-*d*₆) δ 25.9, 31.4, 32.2, 33.9, 40.5, 55.1, 59.0, 68.3, 80.5, 82.3, 129.3, 130.6, 130.8, 131.1, 131.4, 132.3, 140.1, 141.2, 158.7, 158.9, 174.8, 176.6. HRMS (ESI) HRMS (ESI) 550.2516 (M+Na)⁺; C₂₈H₃₇N₃NaO₇ requires 550.2524.

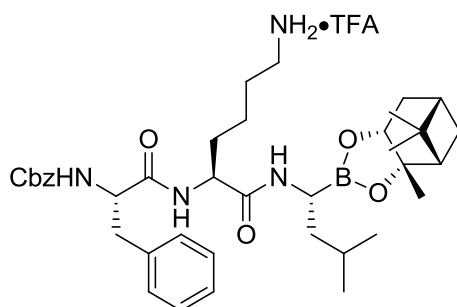
Benzyl N-[(1*S*)-1-[(1*S*)-5-amino-1-[(1*R*)-3-methyl-1-[(1*S*,2*S*,6*R*,8*S*)-2,9,9-trimethyl-3,5-dioxa-4-boratricyclo[6.1.1.0^{2,6}]decan-4-yl]butyl]carbamoyl]pentyl]carbamoyl}-2-phenylethyl]carbamate **3.21**



3.19 (263 mg, 0.499 mmol) was coupled to (*R*)-3-Methyl-1-((3*aS*,4*S*,6*S*,7*aR*)-3*a*,5,5-trimethylhexahydro-4,6-methanobenzo[*d*][1,3,2]dioxaborol-2-yl)butan-1-aminium 2,2,2-trifluoroacetate (189 mg, 0.499 mmol) according to general procedure A and the crude product purified by flash chromatography on silica (60 % EtOAc / Hexane) to afford **3.21** as a white crystalline solid (316 mg, 82%). *R*_f = 0.49 (65% EtOAc / Hexane); ¹H NMR (500 MHz, CD₃OD) δ 0.86 (s, 3H, bridge CH₃), 0.94 (m, 6H, 2x CHCH₂CHCH₃), 1.30 (m, 10 H, bridge CH₃, CH₃CO, CHCH₂CHCH₃, NHCH₂CH₂CH₂CH₂CH), 1.43 (s, 9H, C(CH₃)₃), 1.48 (m, 2H, NHCH₂CH₂CH₂CH₂CH),

1.78 (m, 7H, BOCCH, BOCHCHH, CHCH₂CHCH₃, BOCHCH₂CH, BOCHCHH, NHCH₂CH₂CH₂CH₂CH), 1.95 (t, *J* = 5.4 Hz, 1H, BOCHCH₂CHCHH), 2.13 (m, 1H, BOCHCH₂CHCHH), 2.33 (m, 1H, BOCHCHH), 2.74 (t, *J* = 7.5 Hz, 1H, BCH), 2.86 (dd, *J* = 13.4, 4.5 Hz, 1H, CHCHHC₆H₅), 3.03 (m, 2H, NHCH₂CH₂CH₂CH₂CH), 3.15 (dd, *J* = 13.4, 4.5 Hz, 1H, CHCHHC₆H₅), 4.18 (br d, *J* = 7.1 Hz, 1H, BOCH), 4.39 (m, 1H, m, 1H, CHCH₂C₆H₅), 4.51 (m, 1H, NHCH₂CH₂CH₂CH₂CH), 5.00 (d, *J* = 12.5 Hz, 1H, NHCO₂CHHC₆H₅), 5.05 (d, *J* = 12.5 Hz, 1H, NHCO₂CHHC₆H₅), 6.55 (m, 1H, NHCH₂CH₂CH₂CH₂CH), 7.27 (m, 10H, 2x C₅H₅); ¹³C NMR (125 MHz, CD₃OD) δ 23.8, 24.8, 24.2, 25.8, 28.0, 28.7, 29.0, 30.1, 31.0, 31.5, 33.5, 38.8, 40.2, 40.5, 42.4, 42.6, 43.0, 52.6, 54.8, 59.1, 68.9, 78.7, 85.6, 129.1, 130.0, 130.2, 130.7, 130.7, 131.6, 139.3, 139.7, 159.8, 159.8, 175.5, 178.9. HRMS (ESI) 775.5507 (M+H)⁺; C₄₃H₆₄BN₄O₈ requires 775.4812.

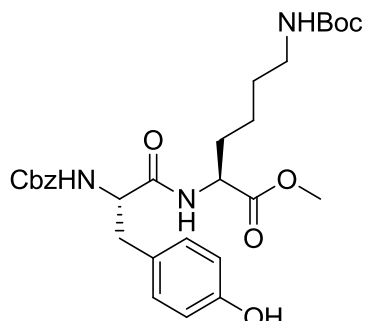
(S)-5-((S)-2-(((Benzyloxy)carbonyl)amino)-3-phenylpropanamido)-6-(((R)-3-methyl-1-((3*aS*,4*S*,6*S*,7*aR*)-3*a*,5,5-trimethylhexahydro-4,6-methanobenzo[d][1,3,2]dioxaborol-2-yl)butyl)amino)-6-oxohexan-1-aminium 2,2,2-trifluoroacetate **3.23**



To a solution of **3.21** (126 mg, 0.163 mmol) in dioxane (5 mL) was added 4M HCl in dioxane (0.24 mL, 0.960 mmol) and the reaction mixture was stirred at RT for

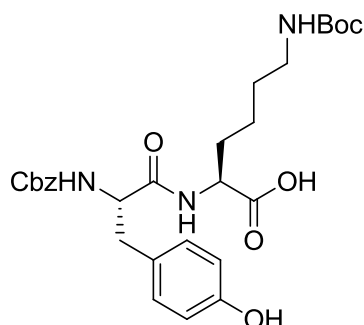
18 h. The mixture was concentrated *in vacuo*, washed with MeOH and concentrated *in vacuo* (3x) to afford a crude white solid which was purified by rp-HPLC (10-70% aq. ACN over 15 min) to afford **3.23** as a fluffy white solid (35 mg, 33%). $R_t = 18.3$ min; $^1\text{H NMR}$ (500 MHz, CD_3OD) δ 0.87 (s, 3H, bridge CH_3), 0.94 (d, $J = 6.5$ Hz, 6H, 2x $\text{CHCH}_2\text{CHCH}_3$), 1.28 (s, 3H, bridge CH_3), 1.36 (s, 3H, CH_3CO), 1.42 (m, 4H, $\text{CHCH}_2\text{CHCH}_3$, $\text{NHCH}_2\text{CH}_2\text{CH}_2\text{CH}_2\text{CH}$), 1.64 (m, 2H, $\text{NHCH}_2\text{CH}_2\text{CH}_2\text{CH}_2\text{CH}$), 1.77 (m, 3H, BOCCH , BOCHCHH , $\text{CHCH}_2\text{CHCH}_3$), 1.87 (m, 2H, BOCHCH_2CH , BOCHCHH), 1.95 (t, $J = 5.3$ Hz, 1H, $\text{BOCHCH}_2\text{CHCHH}$), 2.14 (m, 1H, $\text{BOCHCH}_2\text{CHCHH}$), 2.34 (m, 1H, BOCHCHH), 2.75 (t, $J = 7.8$ Hz, 1H, BCH), 2.89 (m, 3H, $\text{CHCHHC}_6\text{H}_5$, $\text{NHCH}_2\text{CH}_2\text{CH}_2\text{CH}_2\text{CH}$), 3.13 (dd, $J = 13.9, 4.6$ Hz, 1H, $\text{CHCHHC}_6\text{H}_5$), 4.19 (br d, $J = 6.9$ Hz, 1H, BOCH), 4.36 (m, 1H, $\text{CHCH}_2\text{C}_6\text{H}_5$), 4.55 (m, 1H, $\text{NHCH}_2\text{CH}_2\text{CH}_2\text{CH}_2\text{CH}$), 5.01 (d, $J = 12.5$ Hz, 1H, $\text{NHCO}_2\text{CHHC}_6\text{H}_5$), 5.06 (d, $J = 12.5$ Hz, 1H, $\text{NHCO}_2\text{CHHC}_6\text{H}_5$), 7.28 (m, 10H, 2x C_6H_5), 8.41 (d, $J = 8.1$ Hz, 1H, $\text{NHCHCH}_2\text{CH}_2\text{CH}_2\text{CH}_2\text{NH}_2$); $^{13}\text{C NMR}$ (125 MHz, CD_3OD) δ 23.8, 24.7, 25.8, 28.0, 28.7, 29.0, 29.2, 31.0, 33.1, 38.8, 39.9, 40.5, 41.7, 42.6, 42.9, 52.4, 54.7, 59.1, 68.9, 78.8, 85.8, 129.1, 129.9, 130.3, 130.7, 130.8, 131.5, 139.3, 139.6, 159.9, 175.7, 178.5. HRMS (ESI) 675.4311 ($\text{M}+\text{H}$) $^+$; $\text{C}_{38}\text{H}_{56}\text{BN}_4\text{O}_7$ requires 675.4198.

(S)-Methyl 2-((S)-2-(((benzyloxy)carbonyl)amino)-3-(4-hydroxyphenyl)propanamido)-6-((tert-butoxycarbonyl)amino)hexanoate 3.18



N-Z-L-Tyrosine (286 mg, 0.908 mmol) was coupled to *N*^ε-Boc-L-Lysine methyl ester hydrochloride (270 mg, 0.908 mmol) according to general procedure A and the residue purified by flash chromatography on silica (55% EtOAc / Hexane) to afford **3.18** as a white solid (304 mg, 60%). *R*_f = 0.36 (60% EtOAc / Hexane); ¹H NMR (500 MHz, CDCl₃) δ 1.40 (m, 4H, NHCH₂CH₂CH₂CH₂CH, NHCH₂CH₂CH₂CH₂CH), 1.46 (s, 9H, C(CH₃)₃), 1.62 (m, 1H, NHH₂CH₂CH₂CHHCH), 1.79 (m, 1H, NHCH₂CH₂CH₂CHHCH), 2.81 (m, 2H, CO₂NHCHCHH, NHCHHCH₂CH₂CH₂CH), 3.08 (m, 1H, NHCHHCH₂CH₂CH₂CH), 3.34 (m, 1H, CO₂NHCHCHH), 3.69 (s, 3H, CO₂CH₃), 4.50 (m, 1H, CO₂NHCHCH₂C₆H₄), 4.54 (m, 1H, NHCH₂CH₂CH₂CH₂CH), 4.84 (br s, 1H, OH), 5.13 (m, 2H, CO₂CH₂C₆H₅), 5.27 (m, 1H, NHCHCH₂C₆H₄), 6.52 (m, 1H, NHCH₂CH₂CH₂CH₂CH₂), 7.80 (d, *J* = 7.8 Hz, 2H, 2x CHCHOH), 7.01 (d, *J* = 7.8 Hz, 2H, 2x CHCHOH), 7.35 (m, 5H, C₆H₅); ¹³C NMR (125 MHz, CDCl₃) δ 24.4, 31.1, 32.9, 34.2, 39.7, 41.3, 43.3, 54.8, 55.1, 58.5, 70.5, 118.5, 129.1, 130.8, 130.9, 131.2, 133.2, 138.7, 158.6, 158.9, 159.2, 173.2, 174.6. HRMS (ESI) 580.2628 (M+Na)⁺; C₂₉H₃₉N₃NaO₈ requires 580.2629.

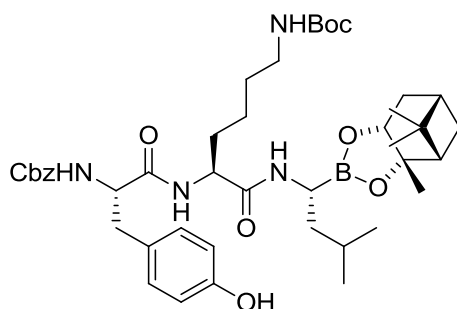
(S)-2-((S)-2-(((Benzyloxy)carbonyl)amino)-3-(4-hydroxyphenyl)propanamido)-6-((tert-butoxycarbonyl)amino)hexanoic acid **3.20**



3.18 (250 mg, 0.490 mmol) was hydrolysed according to general procedure B to afford **3.20** as a white solid (239 mg, 98%). ^1H NMR (500 MHz, DMSO- d_6) δ 1.29 (m, 2H, $\text{NHCH}_2\text{CH}_2\text{CH}_2\text{CH}_2\text{CH}$), 1.36 (s, 9H, $\text{C}(\text{CH}_3)_3$), 1.38 (m, 2H, $\text{NHCH}_2\text{CH}_2\text{CH}_2\text{CH}_2\text{CH}$), 1.60 (m, 1H, $\text{NHCH}_2\text{CH}_2\text{CH}_2\text{CHHCH}$), 1.71 (m, 1H, $\text{NHCH}_2\text{CH}_2\text{CH}_2\text{CHHCH}$), 2.60 (m, 1H, $\text{NHCHHCH}_2\text{CH}_2\text{CH}_2\text{CH}$), 2.89 (m, 3H, $\text{NHCHCH}_2\text{C}_5\text{H}_4$, $\text{NHCHHCH}_2\text{CH}_2\text{CH}_2\text{CH}$), 4.19 (m, 2H, $\text{NHCHCH}_2\text{C}_5\text{H}_4$, $\text{NHCH}_2\text{CH}_2\text{CH}_2\text{CH}_2\text{CH}$), 4.94 (m, 2H, $\text{NHCO}_2\text{CH}_2\text{C}_5\text{H}_5$), 6.64 (d, $J = 8.0$ Hz, 2H, 2x CHCHOH), 6.75 (t, $J = 5.3$ Hz, 1H, $\text{NHCH}_2\text{CH}_2\text{CH}_2\text{CH}_2\text{CH}$), 7.08 (d, $J = 8.0$ Hz, 2H, 2x CHCHOH), 7.28 (m, 5H, C_6H_5), 8.16 (d, $J = 7.6$ Hz, 1H, NHCHCO_2H), 9.16 (br s, 1H, OH), 12.60 (br s, 1H, CO_2H); ^{13}C NMR (125 MHz, DMSO- d_6) δ 25.9, 31.4, 32.3, 33.9, 39.8, 55.0, 59.4, 68.3, 80.5, 82.3, 117.9, 129.9, 130.7, 131.2, 131.4, 133.2, 140.2, 158.7, 158.9, 158.9, 174.9, 176.6. HRMS (ESI) 566.2470 ($\text{M}+\text{Na}$) $^+$; $\text{C}_{28}\text{H}_{37}\text{N}_3\text{NaO}_8$ requires 566.2473.

Benzyl N-[(1S)-1-[[[(1S)-5-[[[(tert-butoxy)carbonyl]amino]-1-[[[(1R)-3-methyl-1-[[[(1S,2S,8S)-2,9,9-trimethyl-3,5-dioxo-4-boratricyclo[6.1.1.0^{2,6}]decan-4-yl]butyl]carbamoyl]pentyl]carbamoyl]-2-(4-hydroxyphenyl)ethyl]carbamate

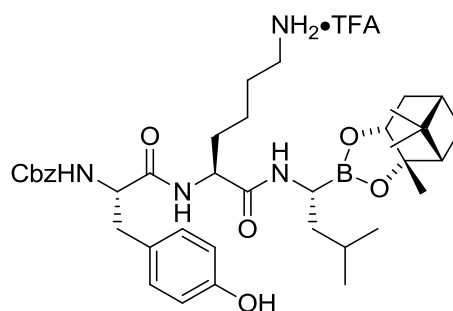
3.22



3.20 (72 mg, 0.132 mmol) was coupled to (*R*)-3-Methyl-1-((3*aS*,4*S*,6*S*,7*aR*)-3*a*,5,5-trimethylhexahydro-4,6-methanobenzo[*d*][1,3,2]dioxaborol-2-yl)butan-1-aminium 2,2,2-trifluoroacetate (50 mg, 0.132 mmol) according to general procedure A and the crude product purified by flash chromatography on silica (60 % EtOAc / Hexane) to afford **3.22** as a white solid (70 mg, 67%). $R_f = 0.38$ (60 % EtOAc / Hexane); $^1\text{H NMR}$ (500 MHz, CD_3OD) δ 0.86 (s, 3H, bridge CH_3), 0.94 (d, $J = 6.5$ Hz, 6H, 2x $\text{CHCH}_2\text{CHCH}_3$), 1.32 (m, 10H, bridge CH_3 , CH_3CO , BOCCH , BOCHCHH , $\text{CHCH}_2\text{CHCH}_3$), 1.46 (m, 11H, $\text{C}(\text{CH}_3)_3$, $\text{NHCH}_2\text{CH}_2\text{CH}_2\text{CH}_2\text{CH}$), 1.78 (m, 5H, $\text{NHCH}_2\text{CH}_2\text{CH}_2\text{CH}_2\text{CH}$, $\text{CHCH}_2\text{CHCH}_3$), 1.95 (t, $J = 5.3$ Hz, 1H, $\text{BOCHCH}_2\text{CHCHH}$), 2.13 (m, 1H, $\text{BOCHCH}_2\text{CHCHH}$), 2.33 (m, 1H, BOCHCHH), 2.73 (t, $J = 7.4$ Hz, BCH), 2.80 (m, 1H, $\text{CHCHHC}_6\text{H}_4$), 3.03 (m, 3H, $\text{CHCHHC}_6\text{H}_4$, $\text{NHCH}_2\text{CH}_2\text{CH}_2\text{CH}_2\text{CH}$), 4.18 (br d, $J = 8.5$ Hz, 1H, BOCH), 4.32 (m, 1H, $\text{NHCHCH}_2\text{C}_6\text{H}_4$), 4.51 (m, 1H, $\text{NHCH}_2\text{CH}_2\text{CH}_2\text{CH}_2\text{CH}$), 5.00 (d, $J = 12.5$ Hz, 1H, $\text{NHCO}_2\text{CHHC}_6\text{H}_5$), 5.08 (d, $J = 12.5$ Hz, 1H, $\text{NHCO}_2\text{CHHC}_6\text{H}_5$), 6.55 (br s, 1H, OH), 6.71 (d, $J = 8.4$ Hz, 2H, 2x CHCHOH), 7.07 (d, $J = 8.4$ Hz, 2H, 2x CHCHOH), 7.30 (m, 4H, C_6H_4); $^{13}\text{C NMR}$ (125 MHz, CD_3OD)

δ 23.8, 24.8, 25.2, 25.8, 28.0, 28.7, 29.0, 30.1, 31.0, 31.6, 33.4, 38.8, 40.2, 40.5, 42.4, 42.6, 43.0, 43.6, 52.6, 54.8, 59.4, 68.9, 78.6, 81.2, 85.6, 117.6, 129.9, 130.2, 130.2, 130.7, 130.7, 132.6, 139.3, 158.6, 159.9, 175.7, 178.9. HRMS (ESI) 813.4583 ($M+Na$)⁺; $C_{43}H_{63}BN_4NaO_9$ requires 813.4580.

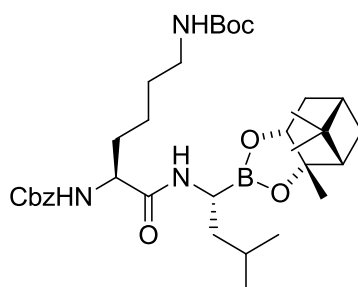
(S)-5-((S)-2-(((Benzyloxy)carbonyl)amino)-3-(4-hydroxyphenyl)propanamido)-6-(((R)-3-methyl-1-((3aS,4S,6S,7aR)-3a,5,5-trimethylhexahydro-4,6-methanobenzo[d][1,3,2]dioxaborol-2-yl)butyl)amino)-6-oxohexan-1-aminium 2,2,2-trifluoroacetate 3.24



To a solution of **3.22** (16 mg, 0.02 mmol) in CH_2Cl_2 (2 mL) was added TFA (0.01 mL, 0.10 mmol) and the reaction mixture was stirred at ambient temperature for 2 h. The mixture was concentrated *in vacuo* and washed with MeOH (3x), concentrating *in vacuo* following each wash to afford **3.24** (15.3 mg, 95%) as a white solid. 1H NMR (500 MHz, CD_3OD): δ 0.86 (s, 3H, bridge CH_3), 0.96 (m, 6H, 2x $CHCH_2CHCH_3$), 1.27 (s, 3H, bridge CH_3), 1.44 (m, 9H, bridge CH_3 , CH_3CO , $BOCCH$, $BOCHCHH$, $CHCHHCHCH_3$), 1.64 (m, 4H, $CHCHHCHCH_3$, $NHCH_2CH_2CH_2CH_2CH$, $NHCH_2CHHCH_2CH_2CH$), 1.87 (2H, $NHCH_2CHHCH_2CH_2CH$, $CHCHHCHCH_3$), 1.95 (t, $J = 5.3$ Hz, 1H, $BOCHCH_2CHCHH$), 2.17 (m, 1H, $BOCHCH_2CHCHH$), 2.41 (m, 1H, $BOCHCHH$), 2.86 (m, 4H, BCH , $NHCHHC_6H_4$, $NHCH_2CH_2CH_2CH_2CH$), 3.01 (dd, $J = 13.9$,

6.4 Hz, 1H, CHHC₆H₄), 3.97 (m, 1H, BOCH), 4.31 (m, 2H, NHCHCH₂C₆H₄, NHCH₂CH₂CH₂CH₂CH), 5.02 (d, *J* = 12.5 Hz, 1H, NHCO₂CHHC₆H₅), 5.09 (d, *J* = 12.5 Hz, 1H, NHCO₂CHHC₆H₅), 6.72 (d, *J* = 8.2 Hz, 2H, 2x CHCHOH), 7.08 (d, *J* = 8.2 Hz, 2H, 2x CHCHOH), 7.32 (m, 4H, C₆H₄); ¹³C NMR (125 MHz, CD₃OD) δ 23.8, 24.8, 25.6, 25.8, 28.4, 28.8, 28.9, 30.4, 31.3, 33.5, 38.0, 39.2, 40.0, 42.1, 42.5, 43.1, 44.6, 53.3, 55.1, 59.6, 68.7, 79.5, 79.7, 117.6, 129.9, 130.1, 130.2, 130.7, 132.6, 132.6, 139.4, 158.6, 159.7, 175.7. HRMS (ESI) 843.3743 (M+K)⁺; C₄₀H₅₆BF₃N₄KO₉ requires 843.3724.

Benzyl tert-butyl ((S)-6-(((R)-3-methyl-1-((3a*S*,4*S*,6*S*,7a*R*)-3a,5,5-trimethylhexahydro-4,6-methanobenzo[*d*][1,3,2]dioxaborol-2-yl)butyl)amino)-6-oxohexane-1,5-diyl)dicarbamate **3.30**

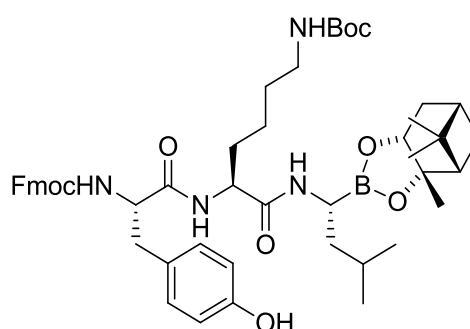


N^α-*Z*-*N*^ε-Boc-L-Lysine (262 mg, 0.689 mmol) was coupled to (*R*)-3-Methyl-1-((3a*S*,4*S*,6*S*,7a*R*)-3a,5,5-trimethylhexahydro-4,6-methanobenzo[*d*][1,3,2]dioxaborol-2-yl)butan-1-aminium 2,2,2-trifluoroacetate (262 mg, 0.689 mmol) according to general procedure A and the crude product purified by flash chromatography on silica (50% EtOAc / Hexane) to afford dipeptide **3.30** as a crystalline white solid (397 mg, 92%). *R*_f = 0.30 (50% EtOAc / Hexane); ¹H NMR (500 MHz, CD₃OD) δ 0.88 (s, 3H, bridge CH₃), 0.93 (d, *J* = 6.3 Hz, 6H, 2x CHCH₂CHCH₃), 1.29 (s, 3H, bridge CH₃), 1.37 (m, 3H, CH₃CO), 1.43 (s, 9H,

C(CH₃)₃), 1.49 (m, 5H, BOCCH, BOCHCHH, CHCH₂CHCH₃, NHCH₂CH₂CHHCH₂CH), 1.75 (m, 5H, NHCH₂CHHCHHCH₂CH, CHCH₂CHCH₃), 1.86 (m, 1H, NHCH₂CHHCH₂CH₂CH), 1.96 (t, *J* = 5.5 Hz, 1H, BOCHCH₂CHCHH), 2.13 (m, 1H, BOCHCH₂CHCHH), 2.34 (m, 1H, BOCHCHH), 2.71 (t, *J* = 7.8 Hz, 1H, BCH), 3.02 (t, *J* = 6.6 Hz, 2H, NHCH₂CH₂CH₂CH₂CH), 4.18 (br d, *J* = 8.6 Hz, 1H, BOCH), 4.30 (m, 1H, NHCH₂CH₂CH₂CH₂CH), 5.09 (m, 2H, NHCO₂CH₂C₆H₅), 7.33 (m, 5H, C₆H₅); ¹³C NMR (125 MHz, CD₃OD) δ 23.9, 24.7, 25.1, 25.9, 28.0, 28.7, 29.0, 30.1, 31.0, 31.6, 33.7, 39.9, 40.5, 42.2, 42.7, 43.0, 54.4, 54.8, 69.1, 78.5, 81.2, 85.4, 130.2, 130.3, 130.7, 139.3, 159.5, 159.9, 179.8. HRMS (ESI) 650.4587 (M+Na)⁺; C₃₄H₅₄BN₃NaO₇ requires 650.3897.

(9*H*-Fluoren-9-yl)methyl N-[(1*S*)-1-[[[(1*S*)-5-[[[(*tert*-butoxy)carbonyl]amino]-1-[[[(1*R*)-3-methyl-1-[(1*S*,2*S*,8*S*)-2,9,9-trimethyl-3,5-dioxo-4-boratricyclo[6.1.1.0^{2,6}]decan-4-yl]butyl]carbamoyl]pentyl]carbamoyl]-2-(4-hydroxyphenyl)ethyl]carbamate

3.34



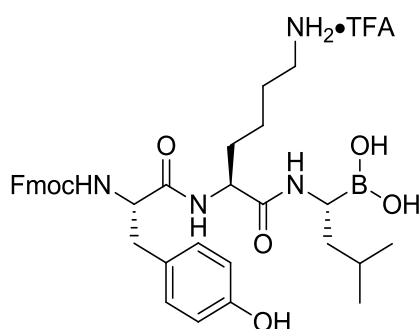
To a solution of **3.30** (353 mg, 0.563 mmol) in MeOH (120 mL) and EtOAc (40 mL) was added 10% palladium on activated carbon (120 mg, 1.12 mmol) and the resulting mixture stirred under a hydrogen atmosphere at ambient temperature

for 3 h. The mixture was filtered through a short pad of silica and concentrated *in vacuo* to afford **3.32** as a white solid which was used without further purification (277 mg, 100%).

Crude **3.32** (197 mg) was coupled to Fmoc-L-Tyrosine (161 mg, 0.399 mmol) according to general procedure A with the modification of stirring for 4h and the crude product purified by flash chromatography on silica (50 – 60 % EtOAc / Hexane) to afford **3.34** as a white solid (200 mg, 58%). $R_f = 0.22$ (60% EtOAc / Hexane); $^1\text{H NMR}$ (500 MHz, Acetone- d_6) δ 0.83 (s, 3H, bridge CH_3), 0.89 (m, 6H, 2x CH_3CH), 1.25 (s, 3H, bridge CH_3), 1.32 (m, 5H, CH_3CO , $\text{NHCH}_2\text{CH}_2\text{CH}_2\text{CH}_2\text{CH}$), 1.39 (s, 9H, $\text{C}(\text{CH}_3)_3$), 1.45 (m, 4H, BOCCH , BOCHCHH , $\text{CHCH}_2\text{CHCH}_3$), 1.75 (m, 5H, $\text{NHCH}_2\text{CH}_2\text{CH}_2\text{CH}_2\text{CH}$, $\text{CHCH}_2\text{CHCH}_3$), 1.94 (t, $J = 5.3$ Hz, 1H, $\text{BOCHCH}_2\text{CHCHH}$), 2.13 (m, 2.10, $\text{BOCHCH}_2\text{CHCHH}$), 2.29 (m, 1H, BOCHCHH), 2.92 (m, 2H, $\text{CHCHHC}_6\text{H}_4$, $\text{NHCHHCH}_2\text{CH}_2\text{CH}_2\text{CH}$), 3.02 (t, $J = 6.6$ Hz, 1H, BCH), 3.07 (m, 2H, $\text{CHCHHC}_6\text{H}_4$, $\text{NHCHHCH}_2\text{CH}_2\text{CH}_2\text{CH}$), 4.22 (m, 3H, $\text{NHCHCH}_2\text{C}_6\text{H}_4$, BOCH , $\text{NHCO}_2\text{CHHCH}$), 4.36 (m, 1H, $\text{NHCO}_2\text{CHHCH}$), 4.46 (m, 2H, $\text{NHCO}_2\text{CHHCH}$, $\text{NHCH}_2\text{CH}_2\text{CH}_2\text{CH}_2\text{CH}$), 6.00 (m, 1H, $\text{NHCHCH}_2\text{C}_6\text{H}_4$), 6.67 (d, $J = 7.6$ Hz, 1H, $\text{NHCH}_2\text{CH}_2\text{CH}_2\text{CH}_2\text{CHNH}$), 6.77 (d, $J = 8.3$ Hz, 2H, 2x CHCHOH), 7.13 (d, $J = 8.3$ Hz, 2H, 2x CHCHOH), 7.34 (t, $J = 7.4$ Hz, 2H, 2x CHCCHCH), 7.42 (t, $J = 7.4$ Hz, 2H, 2x CHCCHCHCH), 7.54 (d, $J = 8.4$ Hz, 1H, $\text{NHCH}_2\text{CH}_2\text{CH}_2\text{CH}_2\text{CH}$), 7.66 (d, $J = 7.4$ Hz, 2H, 2x CHCCHCHCH), 7.82 (br s, 1H, OH), 7.86 (d, $J = 7.4$ Hz, 2H, 2x CHCCHCHCHCH); $^{13}\text{C NMR}$ (125 MHz, Acetone- d_6) δ 24.3, 25.1, 25.3, 26.1, 27.8, 28.7, 29.4, 30.5, 31.1, 33.1, 34.4, 38.5, 39.5, 40.6, 42.4, 42.7, 42.9, 49.7, 54.1, 54.5, 59.4, 69.1, 69.8, 72.9, 79.5, 80.3, 86.9, 117.9, 122.6, 122.6,

127.9, 128.0, 129.8, 130.3, 130.7, 133.0, 143.8, 146.7, 146.7, 158.9, 158.9, 174.0, 175.7. HRMS (ESI) 462.2343 ($M+2Na$)²⁺; $C_{34}H_{54}BN_3Na_2O_7/2$ requires 462.2393.

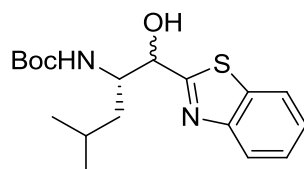
(S)-5-((S)-2-(((9H-Fluoren-9-yl)methoxy)carbonyl)amino)-3-(4-hydroxyphenyl)propanamido)-6-(((R)-1-borono-3-methylbutyl)amino)-6-oxohexan-1-aminium 2,2,2-trifluoroacetate **3.36**



To a solution of **3.34** (92 mg, 0.105 mmol) in THF (2 mL) and dioxane (1.5 mL) was added 4M HCl in dioxane (0.16 mL, 0.630 mmol) and the reaction mixture was stirred at ambient temperature for 18 h. The mixture was concentrated *in vacuo* and washed with MeOH (3x), concentrating *in vacuo* following each wash to afford a crude pale yellow solid which was purified by rp-HPLC (10-90% aq. ACN over 15 min) to afford **3.36** as a fluffy pale yellow solid (37 mg, 47 %). $R_t = 16.5$ min; ¹H NMR (500 MHz, CD₃OD) δ 0.90 (d, $J = 6.5$ Hz, 6H, 2x CHCH₂CHCH₃), 1.35 (m, 4H, CHCH₂CHCH₃, NHCH₂CH₂CH₂CH₂CH), 1.63 (m, 3H, NHCH₂CH₂CH₂CH₂CH, CH₃CHCH₂), 1.78 (m, 1H, NHCH₂CH₂CH₂CHHCH), 1.86 (m, 1H, NHCH₂CH₂CH₂CHHCH), 2.71 (t, $J = 7.6$ Hz, 1H, BCH), 2.85 (m, 3H, CHCHHC₆H₄, NHCH₂CH₂CH₂CH₂CH), 3.00 (dd, $J = 14.1, 5.9$ Hz, 1H, CHCHHC₆H₄), 4.20 (m, 2H, CHCH₂C₆H₄, NHCO₂CHHCH), 4.27 (m, 1H, NHCO₂CHHCH), 4.40 (m, 1H, NHCO₂CHHCH), 4.50 (m, 1H, NHCH₂CH₂CH₂CH₂CH), 6.73 (d, $J = 8.3$ Hz, 2H, 2x

CHCHOH), 7.09 (d, $J = 8.3$ Hz, 2H, 2x CHCHOH), 7.30 (m, 2H, 2x CHCCHCH), 7.40 (dt, $J = 7.4, 3.1$ Hz, 2H, 2x CHCCHCHCH), 7.60 (dd, $J = 14.6, 7.4$ Hz, 2H, 2x CHCCHCHCH), 7.80 (d, $J = 7.4$ Hz, 2H, 2x CHCCHCHCHCH); ^{13}C NMR (125 MHz, CD_3OD) δ 23.7, 23.9, 24.8, 25.0, 25.2, 28.2, 31.5, 33.2, 39.2, 42.2, 49.5, 52.2, 59.5, 69.4, 117.6, 117.6, 122.2, 127.4, 127.5, 129.4, 130.0, 130.1, 132.6, 143.8, 143.8, 146.4, 158.6, 159.8, 173.5, 175.8. HRMS (ESI) 667.3454 ($\text{M}+\text{Na}$) $^+$; $\text{C}_{35}\text{H}_{45}\text{BN}_4\text{NaO}_7$ requires 667.3272.

***tert*-Butyl ((1 *S/R*, 2*S*)-1-(benzo[*d*]thiazol-2-yl)-1-hydroxy-4-methylpentan-2-yl)carbamate 3.40**



A solution of *n*-butyllithium in hexanes (2.5 M, 2.34 mL, 5.85 mmol) was added dropwise to a stirred solution of benzothiazole (0.65 mL, 5.85 mmol) in THF freshly distilled from sodium (10 mL) over 0.25 h at -78°C under an argon atmosphere, and the solution was left to stir for an additional 0.5 h at -78°C . A solution of Boc-L-leucine *N,O*-dimethylhydroxamide (162 mg, 0.585 mmol) in THF freshly distilled from sodium (5 mL) was added dropwise over 0.5 h at -78°C , and the solution was left to stir for an additional 1.75 h at -78°C . The reaction was quenched by addition of sat. aq. NH_4Cl (10 mL) and the mixture allowed to warm to ambient temperature. The resulting mixture was concentrated *in vacuo* and partitioned between EtOAc and water. The aq. phase was extracted with EtOAc (3x), the organic extracts were combined, washed with brine (1x), dried over MgSO_4 ,

filtered, and concentrated *in vacuo* to afford an oily yellow solid which was used without further purification.

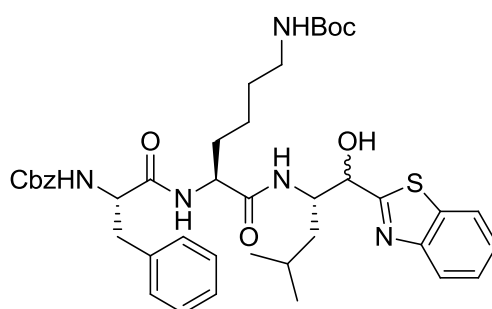
To a stirred solution of crude oily solid (147 mg) in dry CH₂Cl₂ (20 mL) and dry MeOH (5 mL) at -25°C was added sodium borohydride (70 mg, 1.85 mmol) and the solution stirred for 0.5 h at -25°C under a nitrogen atmosphere. The reaction was quenched by addition of acetone (5 mL) and the mixture allowed to warm to ambient temperature. The resulting mixture was concentrated *in vacuo* and partitioned between EtOAc and water. The aq. phase was extracted with EtOAc (3x), the organic extracts combined, washed with brine (1x), dried over MgSO₄, filtered, and concentrated *in vacuo* to afford an oily yellow solid which was purified by flash chromatography on silica (15% EtOAc / CH₂Cl₂) to afford **3.40** as a pale-yellow oil as a 3:1 mixture of diastereomers (90 mg, 44% over 2 steps). HRMS (ESI) 373.1563 (M+Na)⁺; C₁₈H₂₆N₂NaO₃S requires 373.1556.

Data for major isomer from mixture: R_f = 0.41 (15% EtOAc / CH₂Cl₂); ¹H NMR (500 MHz, CDCl₃) δ 0.90 (m, 6H, 2x CHCH₂CHCH₃), and 1.43 (s, 9H, C(CH₃)₃), 1.60 (m, 1H, CHCHHCHCH₃), 1.69 (m, 2H, CHCHHCHCH₃, CHCH₂CHCH₃), 4.21 (m, 1H, CHCH₂CHCH₃), 4.86 (d, J = 8.0 Hz, 1H, NH), 5.18 (br s, 1H, OH), 5.39 (m, 1H, CHOH), 7.38 (m, 1H, NCCHCH), 7.46 (m, 1H, SCCHCH), 7.89 (m, 1H, NCCHCH), 7.99 (m, 1H, SCCHCH); ¹³C NMR (CDCl₃, 125 MHz) δ 24.3, 26.0, 27.4, 31.0, 41.2, 57.5, 78.6, 83.0, 124.4, 125.6, 127.5, 128.6, 137.6, 155.7, 160.0, 176.7.

Selected data for minor isomer from mixture: R_f = 0.41 (15% EtOAc / CH₂Cl₂); ¹H NMR (500 MHz, CDCl₃) δ 0.94 (d, J = 6.6 Hz, 2H, 2x CHCH₂CHCH₃), 1.35 (s, 9H, C(CH₃)₃), 4.09 (m, 1H, CHCH₂CHCH₃), 5.12 (m, 1H, NH); ¹³C NMR (CDCl₃, 125 MHz)

δ 24.6, 25.9, 27.6, 30.9, 42.2, 57.0, 77.2, 82.5, 124.4, 125.5, 137.6, 155.6, 159.3, 177.9.

tert*-Butyl N-[(5*S*)-5-[[[(1*S*/*R*,2*S*)-1-(1,3-benzothiazol-2-yl)-1-hydroxy-4-methylpentan-2-yl]carbamoyl]-5-[(2*S*)-2-[[[(benzyloxy)carbonyl]amino]-3-phenylpropanamido]pentyl]carbamate **3.42*



To a stirred solution of **3.40** (83 mg, 0.237 mmol) in dry CH_2Cl_2 (6 mL) was added TFA (1.5 mL, 19.6 mmol) and the solution stirred for 2 h at ambient temperature under a nitrogen atmosphere. The mixture was concentrated *in vacuo* and the resulting residue washed with methanol and concentrated *in vacuo* (5x) to afford **3.41** as a yellow oil (85 mg, 100%) which was used without further purification.

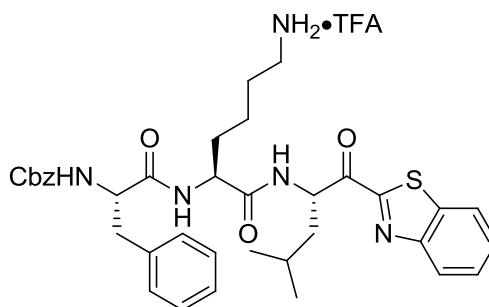
Crude **3.41** (85 mg) was coupled to **3.19** (136 mg, 0.258 mmol) per general procedure A and the crude product was purified by flash chromatography on silica (70% EtOAc / Hexane) to afford **3.42** as an off-white solid (127 mg, 71%). HRMS (ESI) 782.3588 ($\text{M}+\text{Na}$)⁺; $\text{C}_{41}\text{H}_{53}\text{N}_5\text{NaO}_7\text{S}$ requires 782.3556.

Data for major isomer from mixture: $R_f = 0.49$ (80% EtOAc / Hexane); ^1H NMR (500 MHz, CD_3OD) δ 0.84 (d, $J = 6.3$ Hz, 3H, $\text{CHCH}_2\text{CHCH}_3$), 0.88 (d, $J = 6.3$ Hz, 3H, $\text{CHCH}_2\text{CHCH}_3$), 1.28 (m, 5H, $\text{CHCH}_2\text{CHCH}_3$, $\text{NHCH}_2\text{CH}_2\text{CH}_2\text{CH}_2\text{CH}$, $\text{NHCH}_2\text{CHHCH}_2\text{CH}_2\text{CH}$), 1.42 (s, 9H, $\text{C}(\text{CH}_3)_3$), 1.60 (m, 4H, $\text{CHCH}_2\text{CHCH}_3$,

NHCH₂CHHCH₂CH₂CH, NHCH₂CH₂CH₂CH₂CH), 2.83 (m, 1H, CHCHHC₆H₅), 2.94 (m, 2H, NHCH₂CH₂CH₂CH₂CH), 3.12 (m, 1H CHCHHC₆H₅), 4.32 (m, 1H, CHCH₂CHCH₃), 4.43 (m, 1H, CHCH₂C₆H₅), 4.57 (m, 1H, CHCHOH), 4.99 (m, 3H, NHCO₂CH₂C₅H₆, CHCHOH), 7.23 (m, 10H, 2x C₆H₅), 7.38 (m, 1H, NCCHCH), 7.47 (m, 1H, SCCHCH), 7.95 (m, 2H, NCCH, SCCH); ¹³C NMR (CD₃OD, 125 MHz) δ 23.2, 25.1, 27.0, 30.1, 31.8, 34.3, 40.3, 42.4, 55.0, 55.1, 55.9, 59.0, 68.9, 76.7, 124.3, 124.9, 127.5, 128.5, 129.0, 130.0, 130.2, 130.7, 131.7, 137.3, 139.3, 139.7, 155.7, 159.5, 159.7, 175.0, 175.2, 178.7, 179.8.

Selected data for minor isomer from mixture: R_f = 0.49 (80% EtOAc / Hexane); ¹H NMR (500 MHz, CD₃OD) δ 0.96 (d, J = 6.3 Hz, 3H, CHCH₂CHCH₃); ¹³C NMR (CD₃OD, 125 MHz) δ 23.9, 24.9, 27.2, 31.6, 40.7, 42.9, 55.0, 55.7, 58.9, 75.4, 124.3, 124.8, 127.3, 129.9, 130.7, 137.2, 139.8, 155.7, 159.6, 174.6, 175.1, 179.8.

(S)-6-(((S)-1-(Benzo[d]thiazol-2-yl)-4-methyl-1-oxopentan-2-yl)amino)-5-(((S)-2(((benzyloxy)carbonyl)amino)-3-phenylpropanamido)-6-oxohexan-1-aminium 2,2,2-trifluoroacetate 3.44

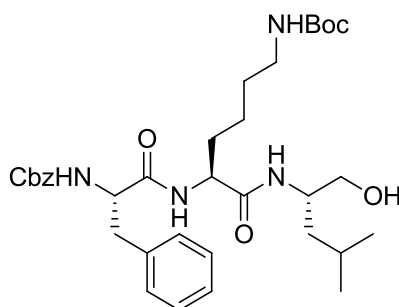


3.42 (37 mg, 0.05 mmol) was oxidised according to general procedure C with the modification of using distilled water instead of sodium bicarbonate in the aqueous

workup to afford **3.43** as a crude white solid (34 mg) which was used without further purification.

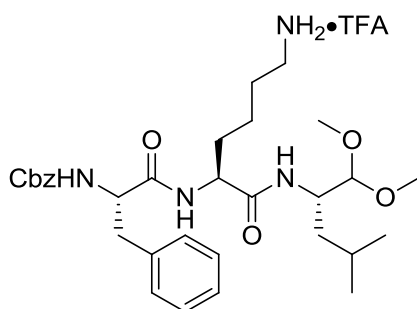
Crude **3.43** (26 mg, 0.03 mmol) was dissolved in dry CH₂Cl₂ (1 mL), added TFA (0.02 mL, 0.240 mmol), and the solution left to stir at ambient temperature for 1.5 h under a nitrogen atmosphere. The mixture was concentrated *in vacuo*, the resulting residue was dissolved in MeOH, concentrated *in vacuo* (3x) and triturated with Et₂O (2x) to afford a crude pale brown solid which was purified by rp-HPLC (10-80% aq. ACN over 15 min) to afford **3.44** as a fluffy white solid (12.1 mg, 46%). R_t: 10.1 min; ¹H NMR (500 MHz, CD₃OD) δ 1.01 (d, *J* = 5.6 Hz, 3H, CHCH₂CHCH₃), 1.09 (d, *J* = 5.6 Hz, 3H, CHCH₂CHCH₃), 1.38 (m, 2H, NHCH₂CH₂CH₂CH₂CH), 1.67 (m, 3H, NHCH₂CHHCH₂CH₂CH, NHCH₂CH₂CH₂CHHCH, CHCHHCHCH₃), 1.86 (m, 4H, NHCH₂CHHCH₂CH₂CH, NHCH₂CH₂CH₂CHHCH, CHCHHCHCH₃, CHCH₂CHCH₃), 2.88 (m, 3H, NHCH₂CH₂CH₂CH₂CH, CHCHHC₆H₅), 3.12 (dd, *J* = 13.8 Hz, 5.1 Hz, 1H, CHCHHC₆H₅), 4.38 (m, 1H, CHCH₂C₆H₅), 4.48 (m, 1H, NHCH₂CH₂CH₂CH₂CH), 5.03 (m, 2H, NHCO₂CH₂C₆H₅), 5.76 (m, 1H, CHCH₂CHCH₃), 7.27 (m, 10H, 2x C₆H₅), 7.64 (m, 2H, SCCHCHCH), 8.13 (d, *J* = 7.9 Hz, 1H, NCCH), 8.23 (d, *J* = 7.9 Hz, 1H, SCCH); ¹³C NMR (125 MHz, CD₃OD) δ 23.1, 24.6, 24.9, 27.8, 29.1, 34.0, 40.1, 41.8, 42.4, 55.1, 56.8, 59.1, 68.8, 125.0, 127.8, 129.0, 129.8, 129.8, 130.2, 130.6, 130.7, 131.6, 139.6, 139.6, 156.1, 166.8, 175.0, 175.3, 196.2. HRMS (ESI) 680.2905 (M+Na)⁺; C₃₆H₄₃N₅NaO₅S requires 680.2877.

tert-Butyl N-[(5*S*)-5-[(2*S*)-2-[[[(benzyloxy)carbonyl]amino]-3-phenylpropanamido]-5-[[[(2*S*)-1-hydroxy-4-methylpentan-2-yl]carbamoyl]pentyl]carbamate **3.46**



3.19 (350 mg, 0.664 mmol) was coupled to L-Leucinol (0.09 mL, 0.730 mmol) according to general procedure A and the crude product purified by flash chromatography on silica on silica (90% EtOAc / Hexane) to afford **3.46** as a white solid (249 mg, 60%). $R_f = 0.50$ (EtOAc); $^1\text{H NMR}$ (500 MHz, CDCl_3) δ 0.92 (m, 6H, 2x CH_3CH), 1.31 (m, 4H, $\text{NHCH}_2\text{CH}_2\text{CH}_2\text{CH}_2\text{CH}$, $\text{CHCH}_2\text{CHCH}_3$), 1.42 (m, 1H, $\text{NHCH}_2\text{CHHCH}_2\text{CH}_2\text{CH}$), 1.44 (s, 9H, $\text{C}(\text{CH}_3)_3$), 1.60 (m, 2H, $\text{NHCH}_2\text{CHHCH}_2\text{CH}_2\text{CH}$, $\text{CHCH}_2\text{CHCH}_3$), 1.84 (m, 2H, $\text{NHCH}_2\text{CH}_2\text{CH}_2\text{CH}_2\text{CH}$), 3.06 (m, 4H, $\text{NHCH}_2\text{CH}_2\text{CH}_2\text{CH}_2\text{CH}$, $\text{CHCH}_2\text{C}_6\text{H}_5$), 3.22 (br s, 1H, OH), 3.51 (dd, $J = 11.2, 5.4$ Hz, 1H, CHHOH), 3.69 (dd, $J = 11.2, 5.4$ Hz, 1H, CHHOH), 4.03 (m, 1H, CHCH_2OH), 4.35 (m, 1H, $\text{CHCH}_2\text{C}_6\text{H}_5$), 4.47 (m, 1H, $\text{NHCH}_2\text{CH}_2\text{CH}_2\text{CH}_2\text{CH}$), 4.79 (m, 1H, $\text{NHCHCH}_2\text{CH}_2\text{CH}_2\text{CH}_2$), 5.07 (m, 2H, $\text{NHCO}_2\text{CH}_2\text{C}_6\text{H}_5$), 5.54 (m, 1H, $\text{NHCHCH}_2\text{CH}_2\text{CH}_2\text{CH}_2\text{NH}$), 6.50 (m, 1H, NHCHCH_2OH), 6.80 ($\text{NHCHCH}_2\text{C}_6\text{H}_5$), 7.27 (m, 10H, 2x C_6H_5); $^{13}\text{C NMR}$ (125 MHz, CDCl_3) δ 24.9, 25.2, 27.5, 31.1, 32.1, 32.4, 34.5, 40.8, 42.5, 42.7, 52.7, 56.3, 59.0, 68.0, 69.9, 82.0, 129.8, 130.7, 130.9, 131.2, 131.4, 131.9, 138.6, 138.7, 158.9, 159.0, 173.9, 173.9. HRMS (ESI) 627.3758 ($\text{M}+\text{H}$) $^+$; $\text{C}_{34}\text{H}_{51}\text{N}_4\text{O}_7$ requires 627.3752.

Benzyl **N-[(1S)-1-[[[(1S)-1-[[[(2S)-1,1-dimethoxy-4-methylpentan-2-yl]carbamoyl]-5-(2,2,2-trifluoroacetamido)pentyl]carbamoyl]-2-phenylethyl]carbamate 3.49**

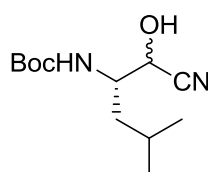


3.46 (200 mg, 0.319 mmol) was oxidised according to general procedure C to afford a crude white solid which was used without further purification.

Crude **3.46** (53 mg) was dissolved in dry CH_2Cl_2 (2 mL), added TFA (0.04 mL, 0.523 mmol), and the solution left to stir at ambient temperature for 1.5 h under a nitrogen atmosphere. The mixture was concentrated *in vacuo*, washed with MeOH, concentrated *in vacuo* (3x), and triturated with Et_2O (2x) to afford a crude residue which was purified by rp-HPLC (10-70% aq. ACN over 25 min) to afford **3.49** as a fluffy white solid (13 mg, 29%). $R_t = 11.4$ min; $^1\text{H NMR}$ (600 MHz, CD_3OD) δ 0.87 (d, $J = 6.5$ Hz, 3H, CHCH_2CH_3), 0.91 (d, $J = 6.5$ Hz, 3H, $\text{CHCH}_2\text{CHCH}_3$), 1.34 (m, 1H, CHCHHCHCH_3), 1.40 (m, 3H, CHCHHCHCH_3 , $\text{NHCH}_2\text{CH}_2\text{CH}_2\text{CH}_2\text{CH}$), 1.63 (m, 4H, $\text{CHCH}_2\text{CHCH}_3$, $\text{NHCH}_2\text{CH}_2\text{CH}_2\text{CH}_2\text{CH}$, $\text{NHCH}_2\text{CH}_2\text{CH}_2\text{CHHCH}$), 1.82 (m, 1H, $\text{NHCH}_2\text{CH}_2\text{CH}_2\text{CHHCH}$), 2.86 (m, 3H, $\text{NHCH}_2\text{CH}_2\text{CH}_2\text{CH}_2\text{CH}$, $\text{CHCHHC}_6\text{H}_5$), 3.09 (dd, $J = 14.0, 5.0$ Hz, 1H, $\text{CHCHHC}_6\text{H}_5$), 3.38 (s, 3H, OCH_3), 3.39 (s, 3H, OCH_3), 4.10 (m, 1H, CHCHOCH_3), 4.16 (d, $J = 4.6$ Hz, 1H, CHCHOCH_3), 4.34 (m, 2H, $\text{CHCH}_2\text{C}_6\text{H}_5$, $\text{NHCH}_2\text{CH}_2\text{CH}_2\text{CH}_2\text{CH}$), 4.98 (d, $J = 12.6$ Hz, 1H, $\text{NHCO}_2\text{CHHC}_6\text{H}_5$), 5.03 (d, $J = 12.6$

Hz, 1H, NHCO₂CHHC₆H₅), 7.25 (m, 10H, 2x C₆H₅); ¹³C NMR (150 MHz, CD₃OD) δ 23.3, 24.7, 25.3, 26.9, 29.3, 33.9, 40.0, 40.8, 41.8, 50.8, 55.6, 56.6, 57.1, 59.1, 68.8, 108.7, 129.0, 129.8, 130.2, 130.7, 131.5, 139.3, 139.6, 159.6, 174.6, 175.3. HRMS (ESI) 571.3485 (M+H)⁺; C₃₁H₄₇N₄O₆ requires 571.3489.

tert*-Butyl ((1 *S*/*R*, 2*S*)-1-cyano-1-hydroxy-4-methylpentan-2-yl)carbamate **3.52*



To a solution of L-leucinol (1.51 g, 12.9 mmol) in dry CH₂Cl₂ (16 mL) was added Boc anhydride (2.81 g, 12.9 mmol) over 5 min and the solution was left to stir at ambient temperature for 18 h. The resulting solution was concentrated *in vacuo* to afford **3.50** (3.00 g) as a crude yellow oil which was used without further purification.

To a solution of crude **3.50** (2.91 g) in DMSO (27 mL) was added sequentially sulfur trioxide pyridine complex (6.39 g, 40.2 mmol) in DMSO (22 mL) and triethylamine (5.6 mL, 40.2 mmol), and the solution stirred at 10 °C for 1 h under a nitrogen atmosphere. The solution was poured onto water and extracted with EtOAc (5x), washed with 10% aq. citric acid solution (1x), brine (4x), dried over MgSO₄, filtered, and concentrated *in vacuo* to afford **3.51** (2.51 g) as a crude viscous yellow oil which was used without further purification.

To a solution of crude **3.51** (1.83 g) in dry MeOH (9 mL) was added sequentially acetone cyanohydrin (0.94 mL, 10.3 mmol) and potassium carbonate (0.23 g, 1.66 mmol) and the solution stirred at ambient temperature for 1 h under a nitrogen

atmosphere. The resulting solution was concentrated *in vacuo*, poured onto water and extracted with EtOAc (3x). The combined organics were washed with brine (1x), dried over MgSO₄, filtered, and concentrated *in vacuo* to afford a crude residue which was purified by flash chromatography on silica (25 % EtOAc / Hexane) to afford **3.52** as a viscous yellow oil as a 1:1 mixture of diastereomers (969 mg, 78% over 3 steps). Experimental data as per literature.¹³⁶

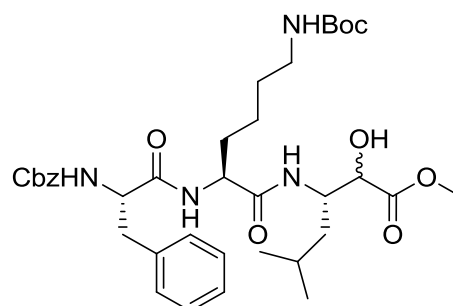
Data for isomer 1 from mixture: $R_f = 0.29$ (25% EtOAc / Hexane); ¹H NMR (500 MHz, CDCl₃) δ 0.96 (m, 6H, 2x CHCH₂CHCH₃), 1.37 (m, 1H, CHCHHCHCH₃), 1.48 (s, 9H, C(CH₃)₃), 1.55 (s, 1H, CHCHHCHCH₃), 1.72 (m, 1H, CHCH₂CHCH₃), 3.77 (m, 1H, CHCH₂CHCH₃), 4.34 (m, 1H, OH), 4.54 (m, 1H, CHCHOH), 4.79 (m, 1H, NH); ¹³C NMR (125 MHz, CDCl₃) δ 24.2, 27.3, 30.9, 40.5, 55.2, 68.2, 84.2, 120.5, 156.8.

Data for isomer 2 from mixture: $R_f = 0.29$ (25% EtOAc / Hexane); ¹H NMR (500 MHz, CDCl₃) δ 0.96 (m, 6H, 2x CHCH₂CHCH₃), 1.37 (m, 1H, CHCHHCHCH₃), 1.47 (s, 9H, C(CH₃)₃), 1.55 (s, 1H, CHCHHCHCH₃), 1.72 (m, 1H, CHCH₂CHCH₃), 3.98 (m, 1H, CHCH₂CHCH₃), 4.34 (m, 1H, OH), 4.49 (m, 1H, CHCHOH), 4.79 (m, 1H, NH); ¹³C NMR (125 MHz, CDCl₃) δ 24.4, 27.4, 30.9, 42.2, 56.1, 70.9, 84.2, 121.2, 160.8.

Methyl (2*S*/*R*,3*S*)-3-[(2*S*)-2-[(2*S*)-2-[[[(benzyloxy)carbonyl]amino]-3-phenylpropanamido]-6-

[[[(*tert*-butoxy)carbonyl]amino]hexanamido]-2-hydroxy-5-methylhexanoate

3.55



To a solution of **3.52** (879 mg, 3.6 mmol) in dioxane (3 mL) was added 32% aq. hydrochloric acid (8 mL, 81.6 mmol) and the solution stirred under reflux for 18 h. The resulting solution was concentrated *in vacuo* to afford crude **3.53** as a brown solid (925 mg) which was used without further purification.

Thionyl chloride (3.5 mL, 48.2 mmol) was added to a solution of dry MeOH (19 mL) cooled to -40°C and the solution stirred for 10 min under a nitrogen atmosphere. Crude **3.53** (460 mg) was dissolved in dry MeOH (4.5 mL), the solution cooled to -10°C and added to the thionyl chloride/MeOH solution. The resulting solution was left to stir at ambient temperature for 2.5 h under a nitrogen atmosphere. The solution was concentrated *in vacuo* to afford crude **3.54** as a viscous orange oil (381 mg) which was used without further purification.

Crude **3.54** (160 mg) was coupled to **3.19** (400 mg, 0.759 mmol) per general procedure A and the crude product was purified by flash chromatography on silica (50-60% EtOAc / CH₂Cl₂) to afford **3.55** as a flaky white solid as 1:1 mixture of

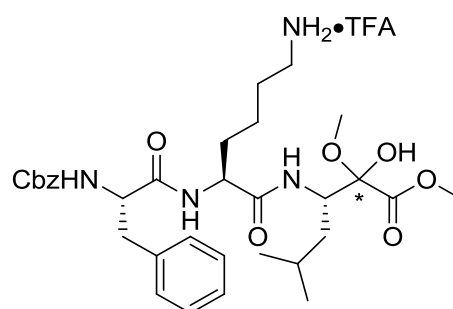
diastereomers (328 mg, 63%). HRMS (ESI) 707.3621 ($M+Na$)⁺; $C_{36}H_{52}N_4NaO_9$ requires 707.3621.

Data for isomer 1 from mixture: $R_f = 0.41$ (60% EtOAc / CH_2Cl_2); 1H NMR (500 MHz, $CDCl_3$) δ 0.91 (m, 6H, 2x $CHCH_2CHCH_3$), 1.18 (m, 4H, $CHCH_2CHCH_3$, $NHCH_2CH_2CH_2CH_2CH$), 1.43 (s, 10H, $C(CH_3)_3$, $NHCH_2CHHCH_2CH_2CH$), 1.57 (m, 3H, $NHCH_2CHHCH_2CHHCH$, $CHCH_2CHCH_3$), 1.79 (m, 1H, $NHCH_2CH_2CH_2CHHCH$), 3.79 (s, 3H, OCH_3), 4.38 (m, 4H, $NHCH_2CH_2CH_2CH_2CH$, $CHCH_2C_6H_5$, $CHCH_2CHCH_3$, $CHOH$), 4.89 (m, 1H, $NHCH_2CH_2CH_2CH_2CH$), 5.06 (m, 1H, $NHCO_2CH_2C_6H_5$), 5.52 (m, 1H, $NHCHCH_2C_6H_5$), 6.54 (d, $J = 8.5$ Hz, 1H, $NHCH_2CH_2CH_2CH_2CHNH$), 6.67 (m, 1H, $NHCHCH_2CHCH_3$), 7.25 (m, 10H, 2x C_6H_5); ^{13}C NMR (125 MHz, $CDCl_3$) δ 24.8, 25.5, 27.4, 31.1, 31.9, 34.4, 40.5, 42.6, 43.3, 52.7, 55.3, 56.0, 59.0, 69.8, 74.7, 75.8, 81.9, 129.8, 130.7, 130.9, 131.2, 131.4, 131.9, 138.7, 138.7, 158.9, 173.4, 174.1, 175.6, 176.8.

Data for isomer 2 from mixture: $R_f = 0.41$ (60% EtOAc / CH_2Cl_2); 1H NMR (500 MHz, $CDCl_3$) δ 0.91 (m, 6H, 2x $CHCH_2CHCH_3$), 1.18 (m, 4H, $CHCH_2CHCH_3$, $NHCH_2CH_2CH_2CH_2CH$), 1.43 (s, 10H, $C(CH_3)_3$, $NHCH_2CHHCH_2CH_2CH$), 1.57 (m, 3H, $NHCH_2CHHCH_2CHHCH$, $CHCH_2CHCH_3$), 1.79 (m, 1H, $NHCH_2CH_2CH_2CHHCH$), 3.76 (s, 3H, OCH_3), 4.38 (m, 4H, $NHCH_2CH_2CH_2CH_2CH$, $CHCH_2C_6H_5$, $CHCH_2CHCH_3$, $CHOH$), 4.82 (m, 1H, $NHCH_2CH_2CH_2CH_2CH$), 5.06 (m, 2H, $NHCO_2CH_2C_6H_5$), 5.52 (m, 1H, $NHCHCH_2C_6H_5$), 6.48 (m, 1H, $NHCH_2CH_2CH_2CH_2CHNH$), 6.76 (m, 1H, $NHCHCH_2CHCH_3$), 7.25 (m, 10H, 2x C_6H_5); ^{13}C NMR (125 MHz, $CDCl_3$) δ 24.2, 26.1, 27.3, 31.1, 31.9, 34.6, 40.6, 42.6, 43.3, 53.1, 55.5, 56.1, 59.0, 69.8, 74.7, 75.8, 81.9,

129.8, 130.7, 130.9, 131.2, 131.4, 131.9, 138.7, 138.7, 158.9, 173.8, 174.1, 175.6, 176.8.

Benzyl N-[(1S)-1-[[[(1S)-1-[[[(3S/R,4S)-3-hydroxy-2,3-dimethoxy-6-methylhept-1-en-4-yl]carbamoyl]-5-(2,2,2-trifluoroacetamido)pentyl]carbamoyl]-2-phenylethyl]carbamate 3.58



3.56 (60 mg, 0.09 mmol) was oxidised according to general procedure C to afford **3.57** as a crude residue (92 mg) which was used without further purification.

Crude **3.57** (68 mg) was dissolved in dry CH_2Cl_2 (1 mL), added TFA (0.05 mL, 0.530 mmol), and the solution was left to stir at ambient temperature for 1.5 h under a nitrogen atmosphere. The mixture was concentrated *in vacuo* and the resulting residue dissolved in MeOH, concentrated *in vacuo* (3x), and triturated with Et_2O (2x) to afford a crude yellow/brown solid which was purified by rp-HPLC (10-90% aq. ACN over 20 min) to afford **3.58** as a fluffy white solid as a 2:1 mixture of diastereomers (44 mg, 64%). HRMS (ESI) 637.3205 ($\text{M}+\text{Na}$)⁺; $\text{C}_{32}\text{H}_{46}\text{N}_4\text{NaO}_8$ requires 637.3208.

Data for major isomer from mixture: R_t : 17.1 min; ^1H NMR (600 MHz, CD_3OD) δ 0.94 (m, 6H, 2x $\text{CHCH}_2\text{CHCH}_3$), 1.58 (m, 9H, $\text{CHCH}_2\text{CHCH}_3$, $\text{NHCH}_2\text{CH}_2\text{CH}_2\text{CH}_2\text{CH}$), 2.88 (m, 3H, $\text{NHCH}_2\text{CH}_2\text{CH}_2\text{CH}_2\text{CH}$, $\text{CHCHHC}_6\text{H}_5$), 3.13 (dd, $J = 13.8, 4.6$ Hz, 1H,

CHCHHC₆H₅), 3.75 (s, 3H, CO₂CH₃), 3.88 (s, 3H, OHCOCH₃) 4.36 (m, 3H, CHCH₂C₆H₅, CHCH₂CHCH₃, NHCH₂CH₂CH₂CH₂CH), 5.02 (m, 2H, CO₂CH₂C₅H₅), 7.26 (m, 10H, 2x C₆H₅); ¹³C NMR (150 MHz, CD₃OD) δ 23.2, 24.7, 25.6, 26.8, 29.2, 33.9, 39.1, 39.9, 40.1, 41.8, 54.4, 54.8, 55.5, 59.0, 68.8, 101.5, 129.0, 129.9, 130.2, 130.7, 131.4, 139.3, 139.7, 159.6, 173.9, 174.6, 175.4.

Selected data for minor isomer from mixture: R_t: 17.1 min; ¹H NMR (600 MHz, CD₃OD) δ 3.78 (s, 3H, CO₂CH₃), ¹³C NMR (150 MHz, CD₃OD) δ 23.0, 24.6, 25.5, 27.0, 33.9, 39.1, 40.1, 54.4, 55.6, 59.0, 139.7, 173.2, 174.9, 175.3.

4.5 References

1. Wade, L.; Simek, J., *Organic Chemistry*. 8 ed.; Pearson: 2012.
2. Petsko, G.; Ringe, D., *Protein Structure and Function* Oxford University Press: 2009.
3. Berg, J. M.; Tymoczko, J. L.; Stryer., L., *Biochemistry*. W H Freeman: 2002.
4. Bulaj, G., Formation of disulfide bonds in proteins and peptides. *Biotechnol. Adv.* **2005**, *23* (1), 87-92.
5. Hatanaka, H.; Oka, M.; Kohda, D.; Shin-ichiTate; Suda, A.; Tamiya, N.; Inagaki, F., Tertiary Structure of Erabutoxin b in Aqueous Solution as Elucidated by Two-dimensional Nuclear Magnetic Resonance. *J. Mol. Bio.* **1994**, *240* (2), 155-166.
6. Fermi, G.; Perutz, M. F.; Shaanan, B.; Fourme, R., The crystal structure of human deoxyhaemoglobin at 1.74 Å resolution. *J. Mol. Bio.* **1984**, *175* (2), 159-174.
7. Brix, K.; Stocker, W., *Proteases: Structure and Function*. Springer: 2014.
8. Goll, D. E.; Thompson, V. F.; Li, H.; Wei, W.; Cong, J., The Calpain System. *Physiol. Rev.* **2003**, *83*, 731-801.
9. Lopez-Otin, C.; Bond, J. S., Proteases: multifunctional enzymes in life and disease. *J. Bio. Chem.* **2008**, *283* (45), 30433-30437.
10. Antalis, T. M.; Shea-Donohue, T.; Vogel, S. N.; Sears, C.; Fasano, A., Mechanisms of disease: protease functions in intestinal mucosal pathobiology. *Nat. Rev. Gastroenterol. Hepatol.* **2007**, *4* (7), 393-402.
11. Turk, V.; Stoka, V.; Vasiljeva, O.; Renko, M.; Sun, T.; Turk, B.; Turk, D., Cysteine cathepsins: from structure, function and regulation to new frontiers. *Biochem. Biophys. Res. Commun.* **2012**, *1824* (1), 68-88.
12. Maes, D.; Bouckaert, J.; Poortmans, F.; Wyns, L.; Looze, Y., Structure of Chymopapain at 1.7 Å Resolution. *Biochem.* **1996**, *35*, 16292-16298.
13. Demuth, H.-U., Recent Developments in Inhibiting Cysteine and Serine Proteases. *J. Enzyme Inhib. Med. Chem.* **2008**, *3* (4), 249-278.

14. Leung, D.; Abbenante, G.; Fairlie, D. P., Protease inhibitors: current status and future prospects. *J. Med. Chem.* **2000**, *43* (3), 305-341.
15. Schechter, I.; Berger, A., On the size of the active site in proteases. I. Papain. *Biochem. Biophys. Res. Commun.* **1967**, *27* (2), 157-162.
16. Otto, H.-H.; Schirmeister, T., Cysteine Proteases and Their Inhibitors. *Chem. Rev.* **1997**, *97* (1), 133-172.
17. Shokhen, M.; Traube, T.; Vijayakumar, S.; Hirsch, M.; Uritsky, N.; Albeck, A., Differentiating serine and cysteine protease mechanisms by new covalent QSAR descriptors. *Chembiochem* **2011**, *12* (7), 1023-1026.
18. Jenal, U.; Fuchs, T., An essential protease involved in bacterial cell-cycle control. *EMBO J.* **1998**, *17* (19), 5658-5669.
19. Glading, A.; Lauffenburger, D. A.; Wells, A., Cutting to the chase: calpain proteases in cell motility. *Trends Cell Biol.* **2002**, *12* (1), 46-54.
20. Good, J. R., TagA, a putative serine protease/ABC transporter of Dictyostelium that is required for cell fate determination at the onset of development. *Development* **2003**, *130* (13), 2953-2965.
21. Chakraborti, S.; Dhalla, N. S.; Chakraborti, S.; Dhalla, N. S., *Proteases in Health and Disease*. Springer: 2013.
22. De Strooper, B., Proteases and proteolysis in Alzheimer disease: a multifactorial view on the disease process. *Physiol. Rev.* **2010**, *90* (2), 465-494.
23. Edwards, D.; Høyer-Hansen, G.; Blasi, F.; Sloane, B., *The Cancer Degradome: Proteases and Cancer Biology*. Springer: 2008.
24. Pietsch, M.; Gutschow, M., Alternate substrate inhibition of cholesterol esterase by thieno[2,3-d][1,3]oxazin-4-ones. *J. Biol. Chem.* **2002**, *277* (27), 24006-13.
25. Powers, J. C.; Asgian, J. L.; Ekici, O. D.; James, K. E., Irreversible Inhibitors of Serine, Cysteine, and Threonine Proteases. *Chem. Rev.* **2002**, *102*, 4639-4750.
26. Fear, G.; Komarnytsky, S.; Raskin, I., Protease inhibitors and their peptidomimetic derivatives as potential drugs. *Pharmacol. Ther.* **2007**, *113* (2), 354-368.
27. Drag, M.; Salvesen, G. S., Emerging principles in protease-based drug discovery. *Nat. Rev. Drug Discov.* **2010**, *9* (9), 690-701.
28. Abell, A. D.; Jones, M. A.; Coxon, J. M.; Morton, J. D.; Aitken, S. G.; McNabb, S. B.; Lee, H. Y.; Mehrtens, J. M.; Alexander, N. A.; Stuart, B. G.; Neffe, A. T.; Bickerstaffe, R., Molecular modeling, synthesis, and biological evaluation of macrocyclic calpain inhibitors. *Angew. Chem. Int. Ed.* **2009**, *48* (8), 1455-1458.
29. Chua, K. C.; Pietsch, M.; Zhang, X.; Hautmann, S.; Chan, H. Y.; Bruning, J. B.; Gutschow, M.; Abell, A. D., Macrocyclic protease inhibitors with reduced peptide character. *Angew. Chem. Int. Ed.* **2014**, *53* (30), 7828-7831.
30. Sanderson, P. E. J., Small, noncovalent serine protease inhibitors. *Med. Res. Rev.* **1999**, *19* (2), 179-197.
31. Aoyagi, T.; Takeuchi, T.; Matsuzaki, A.; Kawamura, K.; Kondo, S., Leupeptins, new protease inhibitors from Actinomycetes. *J. Antibiot.* **1969**, *22* (6), 283-286.
32. Thompson, R. C.; Bauer, C. A., Reaction of peptide aldehydes with serine proteases. Implications for the entropy changes associated with enzymic catalysis. *Biochem.* **1979**, *18* (8), 1552-1558.

33. Das, J.; Kimball, D. S., Thrombin active site inhibitors. *Bioorg. Med. Chem.* **1995**, *3* (8), 999-1007.
34. Shao, Y. M.; Yang, W. B.; Kuo, T. H.; Tsai, K. C.; Lin, C. H.; Yang, A. S.; Liang, P. H.; Wong, C. H., Design, synthesis, and evaluation of trifluoromethyl ketones as inhibitors of SARS-CoV 3CL protease. *Bioorg. Med. Chem. Lett.* **2008**, *16* (8), 4652-4660.
35. Imperiali, B.; Abeles, R. H., Inhibition of serine proteases by peptidyl fluoromethyl ketones. *Biochem.* **1986**, *25* (13), 3760-3767.
36. Maryanoff, B. E.; Costanzo, M. J., Inhibitors of proteases and amide hydrolases that employ an alpha-ketoheterocycle as a key enabling functionality. *Bioorg. Med. Chem.* **2008**, *16* (4), 1562-1595.
37. Han, W.; Hu, Z.; Jiang, X.; Decicco, C., Alpha-ketoamides, alpha-ketoesters and alpha-diketones as HCV NS3 protease inhibitors. *Bioorg. Med. Chem. Lett.* **2000**, *10* (8), 711-713.
38. Smoum, R.; Rubinstein, A.; Dembitsky, V. M.; Srebnik, M., Boron containing compounds as protease inhibitors. *Chem. Rev.* **2012**, *112* (7), 4156-4220.
39. Jr, C. A. L.; Richard, W., Thiohemiacetal formation by inhibitory aldehydes at the active site of papain. *Biochem.* **1977**, *16* (22), 4890-4895.
40. Smith, R. A.; Copp, L. J.; Donnelly, S. A.; Spencer, R. W.; Krantz, A., Inhibition of cathepsin B by peptidyl aldehydes and ketones: slow-binding behavior of a trifluoromethyl ketone. *Biochem.* **1988**, *27* (17), 6568-6573.
41. Angelastro, M. R.; Mehdi, S.; Burkhart, J. P.; Peet, N. P.; Bey, P., Alpha Diketone and Alpha Keto Ester Derivatives of N-Protected Amino Acids and Peptides as Novel Inhibitors of Cysteine and Serine Proteinases. *J. Med. Chem.* **1990**, *33* (1), 11-13.
42. Sajid, M.; McKerrow, J. H., Cysteine proteases of parasitic organisms. *Mol. Biochem. Parasitol.* **2002**, *120* (1), 1-21.
43. Palmer, J. T.; Rasnick, D.; Klaus, J. L.; Bromme, D., Vinyl Sulfones as Mechanism-Based Cysteine Protease Inhibitors. *J. Med. Chem.* **1995**, *38* (17), 3193-3196.
44. Altmann, E.; Cowan-Jacob, S. W.; Missbach, M., Novel Purine Nitrile Derived Inhibitors of the Cysteine Protease Cathepsin K. *J. Med. Chem.* **2004**, *47* (24), 5833-5836.
45. Di Cera, E., Serine proteases. *IUBMB Life* **2009**, *61* (5), 510-515.
46. Craik, D. J.; Fairlie, D. P.; Liras, S.; Price, D., The Future of Peptide - based Drugs. *Chem. Biol. Drug. Des.* **2013**, *81*, 136-147.
47. Adessi, C.; Soto, C., Converting a Peptide into a Drug: Strategies to Improve Stability and Bioavailability. *Curr. Med. Chem.* **2002**, *9*, 963-978.
48. Loughlin, W. A.; Tyndall, J. D. A.; Glenn, M. P.; Fairlie, D. P., Beta-Strand Mimetics. *Chemical Reviews* **2004**, *104*, 6085-6117.
49. Fairlie, D. P.; Tyndall, J. D. A.; Robert C. Reid; Allan K. Wong; Abbenante, G.; Scanlon, M. J.; March, D. R.; Bergman, D. A.; Chai, C. L. L.; Burkett, B. A., Conformational Selection of Inhibitors and Substrates by Proteolytic Enzymes: Implications for Drug Design and Polypeptide Processing. *J. Med. Chem.* **2000**, *43*, 1271-1281.

50. Ridky, T. W.; Cameron, C. E.; Cameron, J.; Leis, J.; Copeland, T.; Wlodawer, A.; Weber, I. T.; Harrison, R. W., Human Immunodeficiency Virus, Type 1 Protease Substrate Specificity Is Limited by Interactions between Substrate Amino Acids Bound in Adjacent Enzyme Subsites *J. Biol. Chem.* **1996**, *271* (9), 4709-4717.
51. Illingworth, C. J. R.; Parkes, K. E. B.; Snell, C. R.; Reynolds, C. A., Quantitative measurement of protease ligand conformation. *J. Comput. Aided Mol. Des.* **2008**, *22* (2), 105-109.
52. Tyndall J. A.; Nall, T.; Fairlie, D. P., Proteases Universally Recognize Beta Strands In Their Active Sites. *Chem. Rev.* **2005**, *105* (3), 973-1000.
53. Stawiski, E. W.; Baucom, A. E.; Scott, S. C.; Gregoret, L. M., Predicting protein function from structure: Unique structural features of proteases. *Proc. Natl. Acad. Sci. U.S.A* **1999**, *97* (8), 3954-3958.
54. Tyndall, D. A.; Nall, T.; Fairlie, D. P., Proteases Universally Recognize Beta Strands In Their Active Sites. *Chem. Rev.* **2005**, *105* (3), 973-999.
55. Tyndall, J. A.; Fairlie, D. P., Conformational homogeneity in molecular recognition by proteolytic enzymes. *J. Mol. Recognit.* **1999**, *12*, 363-370.
56. Vasiljeva, O.; Reinheckel, T.; Peters, C.; Turk, D.; Turk, V.; Turk, B., Emerging roles of cysteine cathepsins in disease and their potential as drug targets. *Curr. Pharm. Des.* **2007**, *13* (4), 387-403.
57. Tan, G. J.; Peng, Z. K.; Lu, J. P.; Tang, F. Q., Cathepsins mediate tumor metastasis. *World J. Biol. Chem.* **2013**, *4* (4), 91-101.
58. Czapinska, H.; Otlewski, J., Structural and energetic determinants of the S1-site specificity in serine proteases. *Eur. J. Biochem.* **1999**, *260* (3), 571-595.
59. Mackman, R. L.; Katz, B. A.; Breitenbucher, J. G.; Hui, H. C.; Verner, E.; Luong, C.; Liu, L.; Sprengeler, P. A., Exploiting Subsite S1 of Trypsin-Like Serine Proteases for Selectivity: Potent and Selective Inhibitors of Urokinase-Type Plasminogen Activator. *J. Med. Chem.* **2001**, *44* (23), 3856-3871.
60. Schellenberger, V.; Braune, K.; Hofmann, H. J.; Jakubke, H. D., The specificity of chymotrypsin. A statistical analysis of hydrolysis data. *Eur. J. Biochem.* **1991**, *199* (1991), 623-636.
61. Perona, J. J.; Craik, C. S., Evolutionary Divergence of Substrate Specificity within the Chymotrypsin-like Serine Protease Fold. *J. Bio. Chem.* **1997**, *272*, 29987-29990.
62. Bose, K., *Proteases in Apoptosis: Pathways, Protocols and Translational Advances*. Springer: 2015.
63. Hardegger, L. A.; Kuhn, B.; Spinnler, B.; Anselm, L.; Ecabert, R.; Stihle, M.; Gsell, B.; Thoma, R.; Diez, J.; Benz, J.; Plancher, J. M.; Hartmann, G.; Banner, D. W.; Haap, W.; Diederich, F., Systematic investigation of halogen bonding in protein-ligand interactions. *Angew. Chem. Int. Ed. Engl.* **2011**, *50* (1), 314-318.
64. Choe, Y.; Leonetti, F.; Greenbaum, D. C.; Lecaille, F.; Bogyo, M.; Bromme, D.; Ellman, J. A.; Craik, C. S., Substrate profiling of cysteine proteases using a combinatorial peptide library identifies functionally unique specificities. *J. Bio. Chem.* **2006**, *281* (18), 12824-12832.
65. Irie, O.; Ehara, T.; Iwasaki, A.; Yokokawa, F.; Sakaki, J.; Hirao, H.; Kanazawa, T.; Teno, N.; Horiuchi, M.; Umemura, I.; Gunji, H.; Masuya, K.; Hitomi, Y.; Iwasaki, G.; Nonomura, K.; Tanabe, K.; Fukaya, H.; Kosaka, T.; Snell, C. R.;

- Hallett, A., Discovery of selective and nonpeptidic cathepsin S inhibitors. *Bioorg. Med. Chem. Lett.* **2008**, *18* (14), 3959-3962.
66. Lecaille, F.; Chowdhury, S.; Purisima, E.; Bromme, D.; Lalmanach, G., The S2 subsites of cathepsins K and L and their contribution to collagen degradation. *Protein Sci.* **2007**, *16* (4), 662-670.
67. Maignan, M.; Guilloteau, J. P.; Pouzieux, S.; Choi-Sledeski, Y. M.; Becker, M. R.; Klein, S. I.; Ewing, W. R.; Pauls, H. W.; Spada, A. P.; Mikol, V., Crystal Structures of Human Factor Xa Complexed with Potent Inhibitors. *J. Med. Chem.* **2000**, *43*, 3226-3232.
68. Smith, A. B.; Hirschmann, R.; Pasternak, A.; Guzman, M. C.; Yokoyama, A.; Sprengeler, P. A.; Darke, P. L.; Emini, E. A.; Schleif, W. A., Pyrrolinone-Based HIV Protease Inhibitors. Design, Synthesis, and Antiviral Activity: Evidence for Improved Transport. *J. Am. Chem. Soc.* **1995**, *117* (45), 11113-11123.
69. Smith, A. B.; Hirschmann, R.; Pasternak, A.; Akaishi, R.; Guzman, R.; Jones, D. R.; Keenan, T. P.; Sprengeler, P. A.; Darke, P. L., Design and synthesis of peptidomimetic inhibitors of HIV-1 protease and renin. Evidence for improved transport. *J. Med. Chem.* **1994**, *37* (2), 215-218.
70. Scholtz, J. M.; Baldwin, R. L., The mechanism of alpha-helix formation by peptides. *Annu. Rev. Biophys. Biomol. Struct.* **1992**, *21*, 95-118.
71. Loughlin, W. A.; Tyndall, J. D.; Glenn, M. P.; Fairlie, D. P., Beta-Strand Mimetics. *Chem. Rev.* **2004**, *104* (12), 6085-6117.
72. Jones, M. A.; Morton, J. D.; Coxon, J. M.; McNabb, S. B.; Lee, H. Y.-Y.; Aitken, S. G.; Mehrtens, J. M.; Robertson, L. J. G.; Neffe, A. T.; Miyamoto, S.; Bickerstaffe, R.; Gately, K.; Woodb, J. M.; Abell, A. D., Synthesis, biological evaluation and molecular modelling of N-heterocyclic dipeptide aldehydes as selective calpain inhibitors. *Bioorg. Med. Chem. Lett.* **2008**, *16*, 6911-6923.
73. Roussel, A.; Mathieu, M.; Dobbs, A.; Luu, B.; Cambillau, C.; Kellenberger, C., Complexation of two proteic insect inhibitors to the active site of chymotrypsin suggests decoupled roles for binding and selectivity. *J. Bio. Chem.* **2001**, *276* (42), 38893-38898.
74. Tully, D. C.; Liu, H.; Chatterjee, A. K.; Alper, P. B.; Epple, R.; Williams, J. A.; Roberts, M. J.; Woodmansee, D. H.; Masick, B. T.; Tumanut, C.; Li, J.; Spraggon, G.; Hornsby, M.; Chang, J.; Tuntland, T.; Hollenbeck, T.; Gordon, P.; Harris, J. L.; Karanewsky, D. S., Synthesis and SAR of arylaminoethyl amides as noncovalent inhibitors of cathepsin S: P3 cyclic ethers. *Bioorg. Med. Chem. Lett.* **2006**, *16* (19), 5112-5117.
75. Nam, D. H.; Lee, K. S.; Kim, S. H.; Kim, S. M.; Jung, S. Y.; Chung, S. H.; Kim, H. J.; Kim, N. D.; Jin, C.; Lee, Y. S., Design and synthesis of 4-quinolinone 2-carboxamides as calpain inhibitors. *Bioorg. Med. Chem. Lett.* **2008**, *18* (1), 205-209.
76. Abell, A. D.; Foulds, G. J., Synthesis of a cis-conformationally restricted peptide bond isostere and its application to the inhibition of the HIV-1 protease. *J. Chem. Soc. Perkin Trans.* **1997**, *0*, 2475-2482.
77. W, D.; Hartung, J.; Hahn, T.; Ulber, R.; Stumpf, T.; Fecher-Trost, C., Vanadate(V)-dependent bromoperoxidase immobilized on magnetic beads as reusable catalyst for oxidative bromination. *Green Chem.* **2011**, *13*, 102-108.

78. Vilsmeier, A.; Haack, A., Über die Einwirkung von Halogenphosphor auf Alkyl-formanilide. Eine neue Methode zur Darstellung sekundärer und tertiärer p-Alkylamino-benzaldehyde. *Ber. Dtsch. Chem. Ges.* **1927**, *60*, 119-122.
79. Lindegren, B. O.; Nilsson, T., Preparation of Carboxylic Acids from Aldehydes (Including Hydroxylated Benzaldehydes) by Oxidation with Chlorite. *Acta Chem. Scand.* **1973**, *27*, 888-890.
80. Sainsbury, M., *Heterocyclic Chemistry*. Wiley: 2001.
81. Tsanaktsis, V.; Bikiaris, D. N.; Guigo, N.; Exarhopoulos, S.; Papageorgiou, D. G.; Sbirrazzuoli, N.; Papageorgiou, G. Z., Synthesis, properties and thermal behavior of poly(decylene-2,5-furanoate): a biobased polyester from 2,5-furan dicarboxylic acid. *RSC Adv.* **2015**, *5* (91), 74592-74604.
82. Jewa, S.-s.; Park, B.-s.; Lim, D.-y.; Kim, M. G.; Chung, I. K.; Kim, J. H.; Hong, C. H.; Kim, J.-k.; Park, H.-j.; Lee, J.-h.; Park, H.-g., Synthesis of 6-formyl-pyridine-2-carboxylate derivatives and their telomerase inhibitory activities. *Bioorg. Med. Chem. Lett.* **2003**, *13* (4), 609-612.
83. Kurashige, N.; Fuchida, H.; Tabata, S.; Uchinomiya, S.; Ojida, A., Discovery of highly reactive peptide tag by ELISA-type screening for specific cysteine conjugation. *Bioorg. Med. Chem. Lett.* **2017**, *27* (15), 3486-3489.
84. Carpino, L. A.; El-Fahama, A.; Albericio, F., Racemization studies during solid-phase peptide synthesis using azabenzotriazole-based coupling reagents. *Tet. Lett.* **1994**, *35* (15), 2279-2282.
85. Nicolaou, K. C.; Baran, P. S.; Zhong, Y.-L.; Sugita, K., Iodine(V) Reagents in Organic Synthesis. Part 1. Synthesis of Polycyclic Heterocycles via Dess-Martin Periodinane-Mediated Cascade Cyclization: Generality, Scope, and Mechanism of the Reaction. *J. Am. Chem. Soc.* **2002**, *124* (10), 2212-2220.
86. Dess, D. B.; Martin, J. C., A useful 12-I-5 triacetoxyperiodinane (the Dess-Martin periodinane) for the selective oxidation of primary or secondary alcohols and a variety of related 12-I-5 species. *J. Am. Chem. Soc.* **1991**, *113* (19), 7277-7287.
87. Myers, A. G.; Zhong, B.; Movassaghi, M.; Kung, D. W.; Lanman, B. A.; Kwon, S., Synthesis of highly epimerizable N-protected α -amino aldehydes of high enantiomeric excess. *Tet. Lett.* **2000**, *41* (9), 1359-1362.
88. Ganneau, C.; Moulin, A.; Demange, L.; Martinez, J.; Fehrentz, J. A., The epimerization of peptide aldehydes--a systematic study. *J. Pept. Sci.* **2006**, *12* (7), 497-501.
89. Carulla, N.; Woodward, C.; Barany, G., BetaCore, a designed water soluble four-stranded antiparallel beta-sheet protein. *Protein Sci.* **2002**, *11* (6), 1539-1551.
90. Batra, J.; Szabo, A.; Caulfield, T. R.; Soares, A. S.; Sahin-Toth, M.; Radisky, E. S., Long-range electrostatic complementarity governs substrate recognition by human chymotrypsin C, a key regulator of digestive enzyme activation. *J. Biol. Chem.* **2013**, *288* (14), 9848-9859.
91. Knowles, J. R., Enzyme specificity: α -chymotrypsin. *J. Theor. Biol.* **1965**, *9* (2), 213-228.
92. Ma, W.; Tang, C.; Lai, L., Specificity of trypsin and chymotrypsin: loop-motion-controlled dynamic correlation as a determinant. *Biophys. J.* **2005**, *89* (2), 1183-1193.

93. Coombs, G. S.; Rao, M. S.; Olson, A. J.; Dawson, P. E.; Madison, E. L., Revisiting Catalysis by Chymotrypsin Family Serine Proteases Using Peptide Substrates and Inhibitors with Unnatural Main Chains. *J. Biol. Chem.* **1999**, *274* (34), 24074-24079.
94. Tyndall, J.; Fairlie, D. P., Macrocycles Mimic The Extended Peptide Conformation Recognized By Aspartic, Serine, Cysteine and Metallo Proteases. *Curr. Med. Chem.* **2001**, *8* (8), 893-907.
95. Kolb, H. C.; Finn, M. G.; Sharpless, K. B., Click Chemistry: Diverse Chemical Function from a Few Good Reactions. *Angew. Chem. Int. Ed.* **2001**, *40*, 2004-2021.
96. de Araujo, A. D.; Hoang, H. N.; Kok, W. M.; Diness, F.; Gupta, P.; Hill, T. A.; Driver, R. W.; Price, D. A.; Liras, S.; Fairlie, D. P., Comparative alpha-helicity of cyclic pentapeptides in water. *Angew. Chem. Int. Ed.* **2014**, *53* (27), 6965-6969.
97. Monfette, S.; Fogg, D. E., Equilibrium Ring-Closing Metathesis. *Chem. Rev.* **2009**, *109* (8), 3783-3816.
98. Fujishima, A.; Imai, Y.; Nomura, T.; Fujisawa, Y.; Yamamoto, Y.; Sugawara, T., The crystal structure of human cathepsin L complexed with E-64. *FEBS Letters* **1997**, *407* (1), 47-50.
99. Hoffmann, M.; Nowosielski, M., DFT study on hydroxy acid-lactone interconversion of statins: the case of atorvastatin. *Org. Biomol. Chem* **2008**, *6* (19), 3527-31.
100. Zhao, H.; Lee, C.; Sai, P.; Choe, Y. H.; Boro, M.; Pendri, A.; Guan, S.; Greenwald, R. B., 20-O-Acylcamptothecin Derivatives: Evidence for Lactone Stabilization. *J. Org. Chem.* **2000**, *65* (15), 4601-4606.
101. Roberts, K. S.; Sampson, N. S., Increased Polymer Length of Oligopeptide-Substituted Polynorbornenes with LiCl. *J. Org. Chem.* **2003**, *68* (5), 2020-2023.
102. Muthusamy, S.; Azhagan, D., Titanium Isopropoxide Promoted Tandem Self-Cross and Ring-Closing Metathesis Approach for the Synthesis of Macrotetralides. *Eur. J. Org. Chem.* **2014**, *2014* (2), 363-370.
103. Theodorou, V.; Skobridis, K.; Tzakos, A. G.; Ragoussis, V., A simple method for the alkaline hydrolysis of esters. *Tet. Lett.* **2007**, *48* (46), 8230-8233.
104. Pieters, J., Mycobacterium tuberculosis and the macrophage: maintaining a balance. *Cell Host & Microbe* **2008**, *3* (6), 399-407.
105. Russell, D. G., *Mycobacterium tuberculosis*: here today, and here tomorrow. *Nat. Rev. Mol. Cell Biol.* *2*, 569-586.
106. Ehrt, S.; Schnappinger, D., Mycobacterial survival strategies in the phagosome: defence against host stresses. *Cell Microbiol.* **2009**, *11* (8), 1170-1178.
107. Madan-Lala, R.; Sia, J. K.; King, R.; Adekambi, T.; Monin, L.; Khader, S. A.; Pulendran, B.; Rengarajan, J., Mycobacterium tuberculosis impairs dendritic cell functions through the serine hydrolase Hip1. *J. Immunol.* **2014**, *192* (9), 4263-4272.
108. Madan-Lala, R.; Peixoto, K. V.; Re, F.; Rengarajan, J., Mycobacterium tuberculosis Hip1 dampens macrophage proinflammatory responses by limiting toll-like receptor 2 activation. *Infect. Immun.* **2011**, *79* (12), 4828-4838.

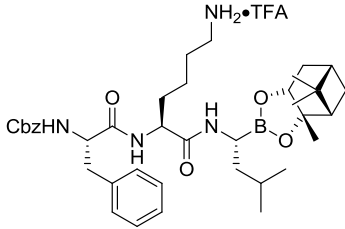
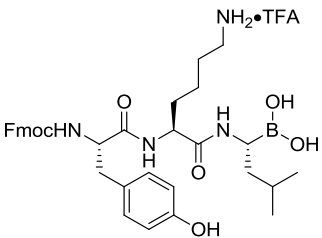
109. Rengarajan, J.; Murphy, E.; Park, A.; Krone, C. L.; Hett, E. C.; Bloom, B. R.; Glimcher, L. H.; Rubin, E. J., Mycobacterium tuberculosis Rv2224c modulates innate immune responses. *Proc. Natl. Acad. Sci. U.S.A* **2007**, *105* (1), 264-269.
110. Stewart, G. R.; Wernisch, L.; Stabler, R.; Mangan, J. A.; Hinds, J.; Laing, K. G.; Young, D. B.; Butcher, P. D., Dissection of the heat-shock response in Mycobacterium tuberculosis using mutants and microarrays. *Microbiology* **2002**, *148* (10), 3129-3138.
111. Zügel, U.; Kaufmann, S. H., Role of Heat Shock Proteins in Protection from and Pathogenesis of Infectious Diseases. *Clin. Microbiol. Rev.* **1999**, *12* (1), 19-39.
112. Naffin-Olivos, J. L.; Daab, A.; White, A.; Goldfarb, N. E.; Milne, A. C.; Liu, D.; Baikovitz, J.; Dunn, B. M.; Rengarajan, J.; Petsko, G. A.; Ringe, D., Structure Determination of Mycobacterium tuberculosis Serine Protease Hip1 (Rv2224c). *Biochem.* **2017**, *56* (17), 2304-2314.
113. Naffin-Olivos, J. L.; Georgieva, M.; Goldfarb, N.; Madan-Lala, R.; Dong, L.; Bizzell, E.; Valinetz, E.; Brandt, G. S.; Yu, S.; Shabashvili, D. E.; Ringe, D.; Dunn, B. M.; Petsko, G. A.; Rengarajan, J., Mycobacterium tuberculosis Hip1 modulates macrophage responses through proteolysis of GroEL2. *PLoS Pathog.* **2014**, *10* (5), e1004132.
114. Lentz, C. S.; Ordonez, A. A.; Kasperkiewicz, P.; La Greca, F.; O'Donoghue, A. J.; Schulze, C. J.; Powers, J. C.; Craik, C. S.; Drag, M.; Jain, S. K.; Bogyo, M., Design of Selective Substrates and Activity-Based Probes for Hydrolase Important for Pathogenesis 1 (HIP1) from Mycobacterium tuberculosis. *ACS Infect. Dis.* **2016**, *2* (11), 807-815.
115. CA, K.; AB, S., Inhibition of the serine proteases leukocyte elastase, pancreatic elastase, cathepsin G, and chymotrypsin by peptide boronic acids. *J. Bio. Chem.* **1984**, *259* (24), 15106-15114.
116. Hall, D. G., *Boronic Acids: Preparation and Applications in Organic Synthesis, Medicine and Materials*. Wiley: 2011.
117. Edwards, P. D.; Jr., E. F. M.; Vijayalakshmi, J.; Tuthill, P. A.; Andisik, D. A.; Gomes, B.; Strimpler, A., Design, synthesis, and kinetic evaluation of a unique class of elastase inhibitors, the peptidyl .alpha.-ketobenzoxazoles, and the x-ray crystal structure of the covalent complex between porcine pancreatic elastase and Ac-Ala-Pro-Val-2-benzoxazole. *J. Am. Chem. Soc.* **1992**, *114* (5), 1854-1863.
118. Matthews, J. H.; Krishnan, R.; Costanzo, M. J.; Maryanoff, B. E.; Tulinsky, A., Crystal structures of thrombin with thiazole-containing inhibitors: probes of the S1' binding site. *Biophys. J.* **1996**, *71* (5), 2830-2839.
119. Recacha, R.; Carson, M.; Costanzo, M. J.; Maryanoff, B.; DeLucas, L. J., Structure of the RWJ-51084-bovine pancreatic β -trypsin complex at 1.8 Å. *Acta Crystallogr.* **1995**, *55*, 1785-1791.
120. De Luca, L.; Giacomelli, G.; Taddei, M., An easy and convenient synthesis of Weinreb amides and hydroxamates. *J. Org. Chem.* **2001**, *66* (7), 2534-2537.
121. Nahm, S.; Weinreb, S. M., N-methoxy-n-methylamides as effective acylating agents. *Tet. Lett.* **1981**, *22* (39), 3815-3818.
122. Costanzo, M. J.; Harold R. Almond, J.; Hecker, L. R.; Schott, M. R.; Yabut, S. C.; Zhang, H.-C.; Andrade-Gordon, P.; Corcoran, T. W.; Giardino, E. C.; Kauffman, J. A.; Lewis, J. M.; Garavilla, L. d.; Haertlein, B. J.; Maryanoff, B. E., In-Depth Study of Tripeptide-Based α -Ketoheterocycles as Inhibitors of Thrombin.

Effective Utilization of the S1' Subsite and Its Implications to Structure-Based Drug Design. *J. Med. Chem.* **2005**, *48* (6), 1984-2008.

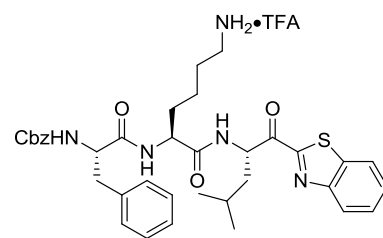
123. Routier, S.; Saugé, L.; Ayerbe, N.; Coudert, G.; Mérour, J., A mild and selective method for N-Boc deprotection. *Tet. Lett.* **2002**, *43* (4), 589-591.
124. Parisi, M., F.; Gattuso, G.; Notti, A.; Raymo, F., M.; Abeles, R., H., Conversion of alpha-keto esters into beta,beta-difluoro-alpha-keto esters and corresponding acids: a simple route to a novel class of serine protease inhibitor. *J. Org. Chem.* **1995**, *60* (16), 5174-5179.
125. Li, Z.; Patil, G. S.; Golubski, Z. E.; Hori, H.; Tehrani, K.; Foreman, J. E.; Eveleth, D. D.; Bartus, R. T.; Powers, J. C., Peptide .alpha.-keto ester, .alpha.-keto amide, and .alpha.-keto acid inhibitors of calpains and other cysteine proteases. *J. Med. Chem.* **1993**, *36*, 3472-3480.
126. Kazuyuki, O.; Kazuhito, K. Oxadiazole derivative compounds and drugs containing these compounds as the active ingredient. 2004.
127. Parikh, J. R.; Doering, W. V. E., Sulfur trioxide in the oxidation of alcohols by dimethyl sulfoxide. *J. Am. Chem. Soc.* **1967**, *89* (21), 5505-5507.
128. Zhang, X.; Heng, S.; Abell, A. D., Photoregulation of alpha-Chymotrypsin Activity by Spiropyran-Based Inhibitors in Solution and Attached to an Optical Fiber. *Chem. Eur. J.* **2015**, *21* (30), 10703-10713.
129. Citron, C. A.; Rabe, P.; Dickschat, J. S., The Scent of Bacteria: Headspace Analysis for the Discovery of Natural Products. *J. Nat. Prod.* **2012**, *75* (10), 1765-1776.
130. Ranganath, M. J. R.; Madhavan, G. R.; Shanmugam, P. Spiro-Substituted Oxindole Derivatives Having AMPK Activity. 2016.
131. Khusnutdinov, R. I.; Shchadneva, N. A.; Baiguzina, A. R.; Mukminov, R. R.; Mayakova, Y. Y.; Smirnov, A. A.; Dzhemilev, U. M., Synthesis of 2-thiophenecarboxylic and 2,5-thiophenedicarboxylic acid esters via the reaction of thiophenes with the CCl₄-ROH reagent in the presence of vanadium, iron, and molybdenum catalysts. *Pet. Chem.* **2008**, *48* (6), 471-478.
132. Goddard, C. J., 5-Heteroaryl-2-thiophenecarboxylic acids: Oxazoles and oxadiazoles. *J. Heterocyclic Chem.* **1991**, *28*, 17-28.
133. Wu, J.; An, G.; Lin, S.; Xie, J.; Zhou, W.; Sun, H.; Pan, Y.; Li, G., Solution-phase-peptide synthesis via the group-assisted purification (GAP) chemistry without using chromatography and recrystallization. *Chem. Comm.* **2014**, *50* (10), 1259-1261.
134. Vitaku, E.; Smith, D. T.; Njardarson, J. T., Metal-Free Synthesis of Fluorinated Indoles Enabled by Oxidative Dearomatization. *Angew. Chem. Int. Ed.* **2016**, *55* (6), 2243-2247.
135. Boyle, T. P.; Bremner, J. B.; Coates, J.; Deadman, J.; Keller, P. A.; Pyne, S. G.; Rhodes, D. I., New cyclic peptides via ring-closing metathesis reactions and their anti-bacterial activities. *Tetrahedron* **2008**, *64* (49), 11270-11290.
136. Johnsona, E. P.; Hubiekia, P. M.; Combsb, A. P.; Teleha, C. A., Preparation of α -Hydroxy- β -Fmoc Amino Acids from N-Boc Amino Acids. *Synthesis* **2011**, *24*, 4023-4026.

APPENDIX

Appendix 1: Inhibition constants, K_i , of Hip₁ inhibitors

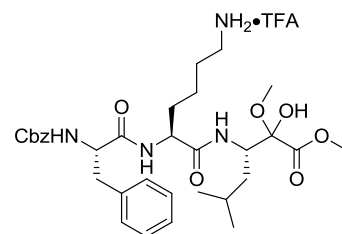
Entry	Structure	K _i (Hip ₁) (pM)
3.23		16000
3.36		7000

3.44



178

3.58



309